THE GEOLOGY AND PRELIMINARY SOIL GEOCHEMICAL INVESTIGATION OF POSSIBLEGOLD-BEARING FEAT URES IN THE TSARETA-TUNGAN KUDAKU AREA, NEAR ANKA (SOKOTO STATE)

BY

AKILA DUTSE BUNGWOM

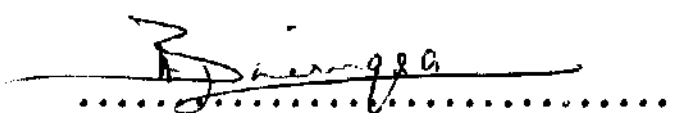
A Thesis submitted to the PostGraduate School,
Ahmadu Bello University, Zaria, in partial fulfilment
of the requirements for the degree of
Master of Science

Department of Geology
Faculty of Science
AHMADU BELLO UNIVERSITY, ZARIA

October, 1983

DECLARATION

I declare that this thesis is my own work and has not been submitted in any other form for another degree or diploma at any other University or Institution. Information derived from the published and unpublished work of others has been acknowledged in the text.



Signature of Candidate

October, 1983

ACKNOWLEDGEMENTS

This work was made possible through a paid Study Fellowship granted by the College of Advanced Studies, Zaria. I am greatly indebted to the Director and the Academic Board of the College for granting me the privilege.

I would like to express my indebtedness to the following staff of the Department of Geology, Ahmadu Bello University, Zaria:-

a. - the Head of Department, Dr. D. Osijuk, for allowing me the use of field mapping and laboratory facilities of the Department.

b. - Mr. M. Woakes, who directed this project, for his selflessness, guidance and constructive criticisms, suggestions and discussions throughout the research.

c. - Dr. C. Okujeni, who supervised the geochemistry section, also for his selflessness and willingness to assist at all times.

d. - Dr. A. C. Ajibade, who critically read through the project and made very useful suggestions.

e. - Dr. R. Glaeser, for cross-checking the petrographic description.

f. - Mallam Yahaya and Mallam Bawa for preparing the thin-sections, and Mr. Emmanuel for assisting me during the geochemical analysis.

My thanks and gratitude are also due to the Head of Department of Geology and Mining, University of Jos, Dr. Jan Pastor, for allowing me the use of the Departmental Atomic Absorption Spectrometer. I am also grateful to Dr. Matheis Gunter for assistance and discussions during part of the geochemical analysis.

Mrs. Gabby Anjorin of the Iya Abubakar Computer Centre, A. B. U., Zaria assisted me with the correlation analysis. I am grateful to her.

I thank the authorities of the Federal Survey of Nigeria with Headquarters at Gusau for allowing me to stay in their field houses at Anka.

I am grateful to two of my younger brothers, Haruna and Zakariya, for assisting me during part of the geochemical sampling.

All other persons who, directly or indirectly contributed to the completion of this project, which space would not allow me to mention them by names, are hereby adcnowledged with full thanks.

Bungwon, A. D.
1983.

DEDICATED

TO

My wife, Hawa

my daughter, Tabitha

and all the younger members of the BUNGWON family.

ABSTRACT

The Tsareta-Tungan Kudaku area, located about 7½ km south of Anka Town, Sokoto State, is part of the Anka Metasedimentary belt which lies within the Pan-African mobile belt.

Mapping, at a scale of 1:25,000, has shown that the three major rock units of the Nigerian basement are represented in the area. These, in order of decreasing age are:-

a) Granite-gneiss which forms a basement.

b) Low-grade metasediments associated with basic metavolcanics and banded-iron-formation overlie the basement.

c) Biotite-granite of probable Pan African age is intrusive both to the granite-gneiss and the metasediments.

Intruding the metasediments also is a large NNE-SSW trending serpentinite body which contains some chromite concentrations. The serpentinite body has in turn been intruded by diorites, trachyandesite and Lamprophyre.

Field and petrographic evidence indicate that the metasediments and the associated metavolcanics have been deformed at least twice.

The mapping has shown that old gold workings are spatially associated with shear zones which are thought to be part of the fault-silicified crush-ridge system mapped by McCurry (1978) which has been folded and is pre-granite in age. The regional pattern is discussed.

A preliminary geochemical soil survey has shown that most of the anomalous values of Ag, Pb, Zn and Cu fall into a NE-SW trending zone which approximately coincides with the fault-silicified crush ridge system mentioned above.

The soil survey has also shown that the element association, Cr-Ni-Co-Mg can be used to delimit the mafic and ultramafic rocks, while the Fe-Mn-Co association distinguishes the phyllites. Biotite-granite can be distinguished by relatively high magnesium values (not as high as in the mafic and ultramafic rocks) and also relatively high calcium values. Granite-gneiss is characterized by generally low content of all the elements.

The potential for gold, chromite and asbestos mineralization in this geologic setting is evaluated and it is concluded that more work is needed to ascertain whether they occur in commercial quantities. It is suggested that the search for gold should be focused on the shear zones. The occurence of chromite concentrations and the size of the serpentinite body is encouraging.

TABLE OF CONTENTS

		Page
	List of Tables	x
	List of Figures	xi
	List of Plates	xiii
	CHAPTER 1 - INTRODUCTION	
1.1	General Introduction	1
1.2	Objectives and Programme of Work ...	1
1.3	Accessibility	3
1.4	Climate, Vegetation and Soils ...	4
1.5	Topography and Drainage	5
1.6	Previous Work	6
	CHAPTER 2 - GEOLOGY	
2.1	Introduction	8
2.2	Granite-Gneiss-Basement	8
2.2.1	Granite-Gneiss	8
2.2.2	Granite-Gneiss/Biotite-Granite Contact Rock	11
2.2.3	Amphibolite	13
2.2.4	Epidote-Quartz-Rock	14
2.2.5	Quartz-breccia	15
2.3	Metasedimentary and Metavolcanic Rocks	16
2.3.1	Phyllites	17
2.3.2	Slates	18
2.3.3	Schists	19
2.3.4	Metaconglomerate and Psammitic facies	19
2.3.5	Quartzpods, veins and ridges ...	21
2.3.6	Dumi Cataclastic Rocks	22

		Page
2.3.7	Metavolcanics (or Amphibole Schist)	24
2.3.8	Banded-Iron-Formation	26
2.4	Serpentinite	27
2.5	Older-Granite Suite	30
2.5.1	Deformed Diorites	30
2.5.2	Undeformed Diorites	31
2.5.3	Trachyandesite (Latite) ...	33
2.5.4	Hornblende-Lamprophyre	33
2.5.5	Biotite-Granite	36
	CHAPTER 3 - GEOLOGIC HISTORY	
3.1	Structures	40
3.1.1	Foliation	40
3.1.2	Lineation	41
3.1.3	Minor Folds	42
3.1.4	Large Scale Structures	43
3.2	Metamorphism	45
3.3	Evolution of the area	46
3.3.1	Granite-Gneiss	47
3.3.2	Metasediments and Metavolcanics ...	49
3.3.3	Serpentinite	51
3.3.4	Diorites, Trachyandesite, Lamprophyre and Biotite-Granite	54
	CHAPTER 4 - MINERALIZATION	
4.1	Introduction	57
4.2	Geology	58

		Page
4.2.1	Gold	58
4.2.2	Chromite	60
4.2.3	Asbestos	60
4.3	Origin	61
4.3.1	Gold	61
4.3.2	Chromite	63
4.3.3	Asbestos	64
	CHAPTER 5 - PRELIMNARY SOIL GEOCHEMICAL INVESTIGATION	
5.1	Sampling and Analytical Methods ...	66
5.1.1	Sampling	66
5.1.2	Sample Preparation	69
5.1.3	Extraction Methods	69
5.1.4	Chemical Analysis of the Samples ...	70
5.2	Evaluation of Geochemical Data ...	71
5.2.1	Patterns of Distribution of Elements: Geochemical Maps	74
5.2.2	Element Association	93
	CHAPTER 6 - SUMMARY AND CONCLUSIONS	99
	REFERENCES	105
	APPENDIX	109

LIST OF TABLES

		Page
3:1	Mineral Assemblages and metamorphic facies of the rocks.	46
3:2	Radiometric dates of some older granite rocks in the Nigerian basement.	56
5:1	The range and mean of the elements in the Soil Samples.	72
5.2	Geochemical Parameters.	74
5.3	Correlation Matrix.	94
5.4	Element association and relative contrast of values in relation to bedrock.	98

LIST OF FIGURES

		Page
1.	Map of North-western Nigeria with location of the mapped area.	3b
2.	Geology map of Tsareta-Tungan Kudaku area.	
3.	Sketch of quartz breccia in thin section.	16b
4.	Sketch of quartz-pods and veins in phyllite.	21b
5.	Sketch of biotite-granite in thin section with corrosion of biotite by felsic minerals. Alteration also to opaques.	39b
6.	Regional fault/shear pattern in north-western Nigeria.	43b
7.	Sampling plan for geochemical soil survey.	67
8.	Distribution pattern of Silver.	75
9.	Distribution pattern of Lead.	77
10.	Distribution pattern of Zinc.	79
11.	Distribution pattern of Copper.	80
12.	Distribution pattern of Chromium.	82
13.	Distribution pattern of Nickel.	83b
14.	Distribution pattern of Cobalt.	84
15.	Distribution pattern of Manganese.	85
16.	Distribution pattern of Iron.	89
17.	Distribution pattern of Magnesium.	91
18.	Distribution pattern of Calcium.	92

LIST OF PLATES

		Page
i	Granite-gneiss showing folds.	10
ii	Photomicrograph of granite-gneiss: Mineralogy and texture.	11
iii	Photomicrograph of Amphibotite: Mineralogy and texture.	11
iv	Photomicrograph of phyllite showing crenulation	20
v	A granite clast in metaconglomerate.	20
vi	Dumi Cataclasitic rock showing rodding lineation.	23
vii	Dragfolds in Dumi Cataclastic rock.	23
viii	Folds in metavolcanic rocks.	25
ix	Honey-comb Structure in Serpentinite.	29
x	Photomicrograph of serpentinite showing prismatic crystals of anthophyllite.	29
xi	Mineralogy and texture of undeformed diorite.	32
xii	Photomicrograph of zoned and twinned plagioclase in trachy-andesite	34
xiii	Porphyritic texture of trachy-andesite	34
xiv	Photomicrograph of simple and cross-shaped twins of hornblende in Hornblende-lamprophyre.	35
xv	Spheroidal weathering core in biotite-granite.	35
xvi	Contact rock between granite-gneiss and biotite-granite.	38
xvii	Cross-fibre asbestos in amphibole-rich rock.	62

CHAPTER 1

INTRODUCTION

1.1 General Introduction

The Tsareta-Tungan Kudaku area in Anka Local Government Area of Sokoto State, Nigeria, lies within the Pan African mobile belt between the West African and Congo Cratons (Kennedy 1964, and Clifford 1970). The Pre-Cambrian to early Paleozoic rocks of the belt fall into three major groups:-

a) a migmatite-gneiss complex

b) north-south trending schist belts

c) a suite of largely granitic rocks of Pan-African age known in Nigeria as the "Older Granites"; they intrude both 'a' and 'b' above.

The mapped area falls in the southern part of the Anka belt (figure 1) one of the schist belts and has been intruded by granite. Several gold vein workings occur in the area and also a large previously unmapped serpentinite body with some chromite concentration.

1.2 Objectives and Programme of Work

The Tsareta-Tungan Kudaku area described in this work is about 7½ km. south of Anka town.

Reconaisance survey had indicated that a linear array of gold showings in the region was coincident in part with a NNE-SSW trending regional

structure mapped by McCurry (1978) (sheet 75) from air photographs as a fault-silicified crush ridge. The characteristics of this feature and its possible genetic relationship with the gold mineralization was the reason for the initial interest in the area.

The objectives of the project were to:-

a) undertake geologic mapping of the area and
   i) in particular, investigate the NNE-SSW trending structure
   ii) carry out a preliminary investigation of the areal extent and structural relationships of the large NNE-SSW serpentinite body within the mapped area,
b) carry out a preliminary soil geochemical survey to investigate the reflection of bedrock type and the mineralized structures.

The geologic mapping covers an area of about 130 km^2 which lies within the two 1:250,000 sheets, sheet 7 and 19. It is bounded by longitudes 5^{o} 57'E and 6^{o} 00'E and by latitudes 11^{o} 54'N and 12^{o} 02' 40"

Mapping was done on a scale of 1:25,000 during several visits between October, 1982 and February, 1983, and was concentrated mainly along stream valleys where good exposures, especially of phyllites, occur. Away from the valleys, only the more competent rocks have good exposures.

Thin sections of selected rock samples were prepared and described. The mode of the rocks in thin section was determined by visual estimation only.

Air-photographs on a scale of about 1:40,000 were very useful in supplementing the 1:25,000 basemap used for mapping and which was prepared from a direct blow up of the 1:100,000 topographic sheets. The air-photographs were also useful as guides in the general interpretation of features and structures. Landsat imagery on 1:500,000 was available towards the end of the project but did not contribute any additional useful information. The aeromagnetic maps reflect the occurrence of the serpertinite as a linear high.

Geochemical soil sampling was carried out during the rainy season using a hand anger. Details of sampling and analytical procedures are given in chapter 5.

1.3 Accessibility

Anka town lies on the main road linking Gusau and Zuru. From Anka to the mapped area, accessibility is good. Traversing the area are a number of minor roads. Two of them run north-south, while three run east-west. All these are motorable throughout the year except the Tsareta-New Project road which is rendered impassable (with a motor-vehicle) during the rainy season because of a culvert-washout located in

MAP OF N.W. NIGERIA WITH LOCATION OF MAPPED AREA



Fig. 1.

- Cretaceous - Basement unconformity
- Volcanics amphibolites basics and ultrabasics
- Pan- African Granites
- Metasediment (and metavolcanic) belts
- Basement gneiss migmatite e.t.c.
- Regional linears and fault-zones

After Woakes 1981

a "fadama"* area. Apart from these, there are many dry season roads used mainly by fire-wood collectors. In addition, there is a good net-work of foot-paths and cattle tracks. Traversing by compass bearing or along drainage channels is generally possible.

1.4 Climate, Vegetation and Soils

The Tsareta area lies within the zone of tropical continental climate with an average annual temperature range of 18.3°C and characterized by two distinct seasons: the wet and the dry seasons. The wet season is relatively short and starts in mid May and ends in the second or third week of September. The highest amount of rain (227 mm) falls in August while the average annual rainfall is 871 mm. Most of the rains are shortlived and torrential. The remaining part of the year constitutes the dry season during which there is little or no rain. From about mid October to January or February is the harmattan period which is characterized by lower temperature (18 - 21°C) and haze caused by dust particles transported from the Sahara Desert. The months of March and April constitute a short hot period during which the daily maximum temperatures range between 37°C and 40.5°C. It preceeds the wet season.

The vegetation is a function of the climate. It consists of shrubs, thorn trees, a few boabab trees

* "Fadama" is the Hausa term for swamp or marsh.

and low grass with occassional bare ground. During the wet season, the vegetation is full, but with the coming of the dry season, trees shed their leaves while the grasses dry up. Rock exposure at this time is good.

Different soil types have developed in this area. Generally, the serpentinite and "fadama" areas are characterized by dark-grey soils of high clay content. In the other areas there is considerable colour variation of the soils. These include reddish-brown, light-grey and light-brown. A few indurated laterite patches were encountered in areas underlain by phyllites.

1.5 Topography and Drainage

The area consists of fairly level plains approximately 300 m above sea-level. These are interrupted in places by quartz and granite-gneiss ridges. The highest of these ridges is the Tsareta-ridge composed of granite-gneiss and has a relief of about 50 m and is aligned in a NNW-SSE direction. The area has also been cut by many gullies and stream valleys, and has a general gentle slope towards the north-west and north-east.

Drainage is accomplished by two sets of streams. One set flows generally to the west and north-west, while the other flows to the east and north-east.

However, all these eventually flow into the River Zamfara located to the north (outside the mapped area). The divide coincides approximately with the NNE-SSW trending serpentinite body.

Most of the streams have developed "fadama" (flood plain) consisting of transported alluvium along their valleys and they are water-logged during the wet-season. In the dry season, both the streams and their "fadama" are completely dry.

The drainage pattern is generally dendritic in nature and across the structural grain of the bedrock, as a result, some irregularities are probably due to the influence of the jointing and foliation. On the "fadama" areas, the streams are often winding due to low gradient.

1.6 Previous Work

The earliest geologic work in the Anka belt is reported in geologic and economic mineral reports including those of Falconer (1911), and Russ (1932 and 1957). Russ reports that early local gold prospectors obtained some alluvial gold from the Zamfara River and its tributaries. Small amounts were also gained from quartz-veins

Systematic geologic accounts of the general area are given for sheet 52 by Fargher (1961) and for sheet 75 by McCurry (1978). McCurry's work was based mainly

on photo-interpretation. A review of the geology of North-Western Nigeria has also been given by McCurry (1976).

Ogezi (1977) undertook some detailed geologic, geochemical and geochronological studies in several small selected areas with particular attention to the ultramafic intrusions of the region, but these did not include the serpentinite of the Tsaroto area which is part of the present mapped area. More recently, Holt (1982) carried out a detailed structural study of the Anka Belt basing such a study mainly on evidence gathered from three areas: Sauna, Anka, and Bunkasau, all north of the present study area.

CHAPTER 2

GEOLOGY

2.1 Introduction

The area mapped is underlain by igneous and metamorphic rocks of Pre-Cambrian to Lower Paleozoic age. The dominant rock types are metapelites, granite-gneiss, biotite-granite, serpentinite, metavolcanics and diorites. Other rock types occuring are amphibolite, epidote-quartz rock, quartz-fault breccia, banded-iron-formation, cataclastic rocks, lamprophyre, and trachyandesite (latite).

In this chapter, the rocks are described and the geologic history of the area is discussed in chapter 3.

2.2 Granite-Gneiss Basement

The main rock type of the basement is granite-gneiss but other varieties are observed at the contacts.

2.2.1 Granite-Gneiss

The granite-gneiss in this area is restricted to the north-western corner where it underlies an area of about 15 km^2. Outcrops occur either as hills or as pavement exposures. The largest hill is the Tsareta ridge with a relief of about 50 m and is aligned in a NNW-SSE direction.

Typically, the granitic-gneiss is a fine-to medium-grained streaky, hornblende gneiss with a well developed foliation The foliation is due mainly to the

parallel alignment of hornblende. The dominant strike of the foliation is NW, but it has different and often complex strike directions. Minor folds with dominant NNE-SSW trending axial planes are superimposed on the foliation (plate i). Parts of the granite-gneiss are banded due to segregation of minerals into mafic and felsic layers. Frequently portions of the rock possess a granitic texture.

In thin section, DB 51, the rock is seen to be composed of microcline, quartz, oligoclase and hornblende. Biotite, sphene, and opaques occurr in accessory amounts (plate ii).

Microcline is the dominant mineral and it makes up to 35% of the rock. It occurs as large anhedral to subhedral porphyroblasts sometimes showing cross-hatch-twinning. Crystals of quartz and plagioclase are enclosed in these porphyroblasts giving a poikiloblastic texture.

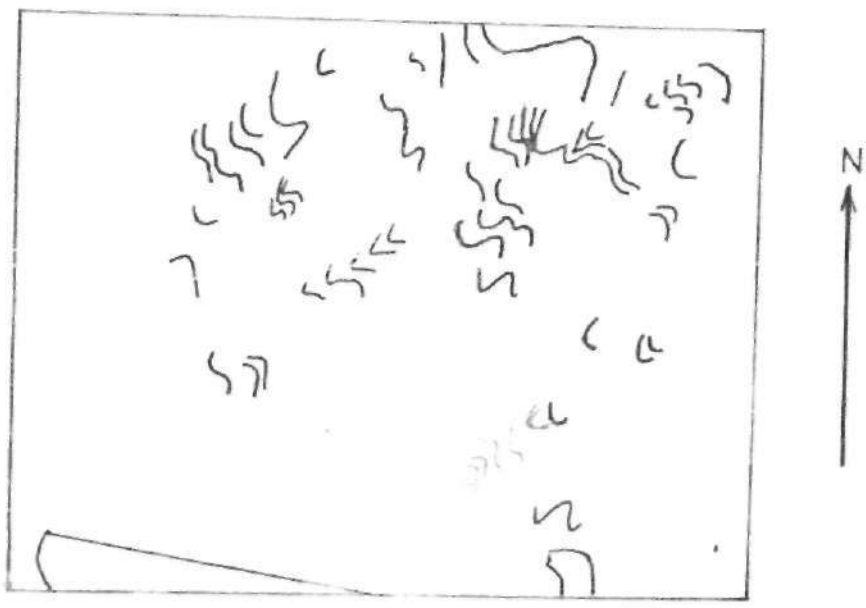
Quartz occurs at least in two generations. Smaller (early) rounded quartz crystals form inclusions in microcline, oligoclase, and hornblende, and also occur at the interstitial boundaries of these minerals. A later generation forms larger anhedral crystals. They appear to be imposed on the general fabric of the rock. Both types show undulatory extinction.

Oligoclase, An_{12} (maximum extinction angle = 10^{o}) occurs as anhedral to subhedral laths showing albite and sometimes paricline twinning. Sericitization has



Plate i

Granite-Gneiss with deformed foliation



Sketch of Plate i above showing the folds.

affected most of the crystals and this together with numerous tiny inclusions gives it a cloudy appearance.

Green honblende occurs as anhedral crystals in various sizes. It is replaced by opaques especially along the cleavage.

Biotite also occurs as anhedral crystals. It is pleochroic from yellow to dark-greenish brown. Some plates have bent cleavages and therefore show a wavy extinction. It is replaced by chlorite (light-green) and opaques especially along the cleavage planes.

Sphene occurs mostly as anhedral crystals. A few crystals are exhedral with the characteristic diamond shape. Other accessories include zarcon, allanite and many grains of apatite.

2.2.2 Granite-gneiss/Biotite-granite Contact Rock

The contact between the granite-gneiss and biotite-granite is marked by a 10-20 m wide rock which crops out at the south-eastern end of Tsareta ridge.

This contact rock is a variety of the granite-gneiss and its contact with the granite-gneiss is gradational.

In hand specimen, it is a medium-grained equigranular (massive) rock with a brownish appearance.

In thin section (DB 7) it is seen to be composed of microcline, orthoclase, plagioclase, quartz and minor chlorite.



Plate ii

Photomicrograph of granite-gneiss. It shows the mineralogy and a granitic texture. Crossed polarizers. x 2·5.

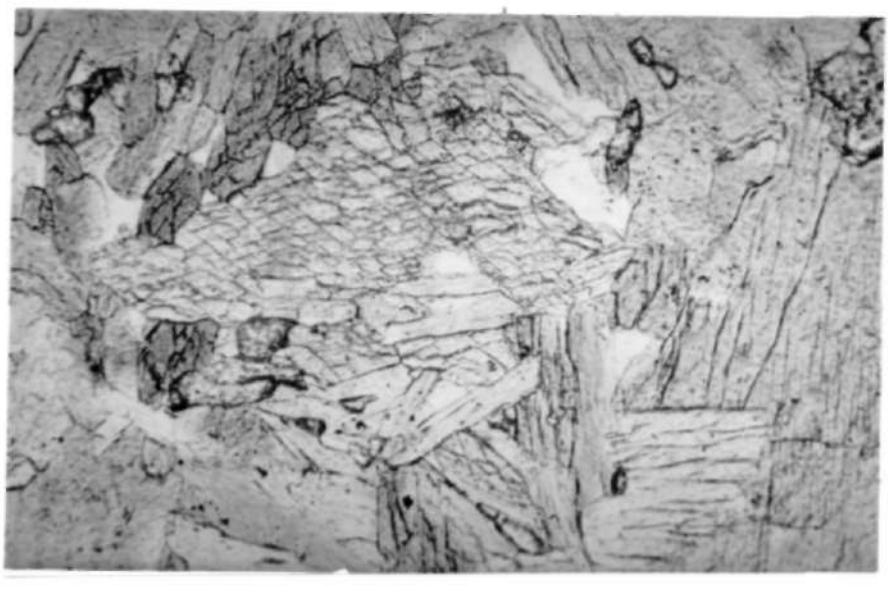


Plate iii

Photomicrograph of Amphibotite with granoblastic texture. One Polarizer x 16

Microcline forms about 35% of the rock. and also occurs as anhedral crystals. It is often altered to kaolin (?).

Oligoclase, An_{28} (maximum extinction angle = 8^{o}) forms about 10% of the rock. It occurs as anhedral to subhedral laths showing albite-twinning. It has a cloudy appearance due to alteration and the presence of tiny inclusions.

Quartz is about 25% of the rock. It occurs as anhedral crystals and shows undulatory extinction.

Minor amounts of chlorite occur as green anhedral crystals which are occassionally associated with biotite.

Biotite, sphene, and opaques constitute the accessory minerals.

2.2.3 Amphibolite

Amphibolite occurs as large (up to 5 m) xenolithic blocks within the serpentinite and is probably a more mafic component of the basement complex. It is dark, shiny-green, massive and coarse-grained. It is occassionally covered by a dark-brown ferruginous crust.

In thin section (DB 107 and DB 119) it has a granoblastic texture (plate iii) with hornblende making up about 80 to 85% of the mineral assemblage. This occurs generally as randomly oriented ragged

plates. Basal sections show the two characteristic cleavages intersecting at 124° and 56°. The maximum extinction angle, C/γ , in longitudinal section is 28°. The pleochroic scheme is as follows:

α = yellow or pale yellow brown

β = green

γ = blue-green

Present also is clinozoisite which in thin section (DB 119) makes up to 10% of the rock. It is colourless to pale-yellow with weak pleochroism, high relief (higher than bornblende) and shows anomalous interference colours. It is zoned.

A light-coloured mineral, plagioclase (?), occuring as tiny veinlets, together with sphene, constitute about 5% of the rock.

2.2.4 Epidote-Quartz Rock

This rock was found in only one locality about 6 km south-west of Tsareta ridge, in the western part of the mapped area. It occurs in a fault zone (indicated by the presence of a fault-breccia close by) which, is located close to the contact between the granite-gneiss and biotite-granite (figure 2).

The rock outcrops as a low blocky ridge about 3 m high and extends for about 350 m in a NNE direction.

In hand specimen, it is a hard, light-green and medium-grained rock with an even-grained texture. Thin section study (DB 19) shows that it is composed of quartz and epidote.

Quartz makes up to 70% of the rock and occurs as large anhedral crystals showing undulatory extinction. Some crystals contain tiny opaque inclusions and may be cracked.

Large epidote crystals have been subgrained giving several small crystals. The epidote is biaxial negative and has a 2V angle of 80° . It is weakly pleochroic from colourless to pale-yellow. Zoning is common especially in the large crystals and is indicated by different interference colours within the same crystal.

2,2,5 Quartz-Breccia

This rock occurs about 200 m south-east of the epidote-quartz rock described in the previous section (2.2.4). It occurs as boulder float over a zone 3 m by 250 m aligned in a 030° direction.

Weathered surfaces are reddish-brown. Fresh samples however reveal white angular fragments of quartz set in a very fine-grained matrix of quartz.

Thin section study (DB 92) shows a highly brecciated rock consisting almost entirely of quartz.

Quartz clasts have been broken up (figure 3). These contain numerous opaque inclusions.

Chlorite, plagioclase and zircon occur as accessory minerals.

2.3 Metasedimentary and Metavolcanic Rocks

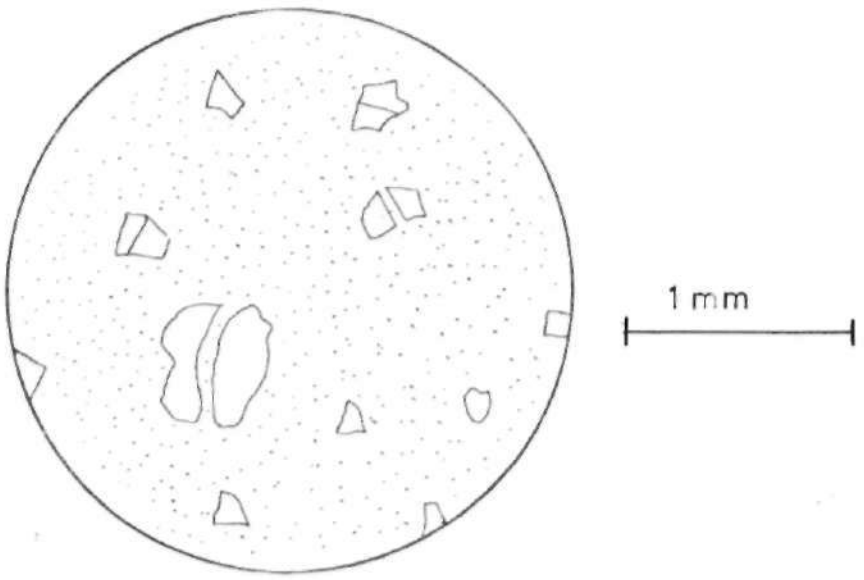
Low-grade metasediments are known to occur in essentially N-S to NNE-SSW trending belts in North-Western Nigeria (figure 1). In the present area which forms part of the Anka belt, metasediments underlie about 90 km^2 or about 70% of the total area mapped.

The dominant rocks are phyllites. Small areas however are underlain by slate, schist and meta-conglomerate. These minor rock types could not be mapped as separate units and they are grouped or mapped with phyllites on the geological map, but they will be described separately in the text.

Described in this section also (and shown on the geological map- figure 2) are the Dumi Cataclastic rocks, metavolcanics, and the banded-iron formation.

Compared with other rock types, the rocks described in this section are among the most susceptible to weathering. With the exception of the metavolcanic and the banded-iron formation, most outcrops are found along stream valleys, gullies and road cuttings. Away from these areas, they are mostly

QUARTZ - BRECCIA



Angular fragments of quartz set in a fine-grained matrix of quartz
Sketch from thin-section DB 92

Fig 3

hidden beneath the surficial soils. When they do outcrop however, it is due to their partial induration by the introduction of siliceous material. A few other outcrops are preserved by the association of abundant quartz in phyllites.

2.3.1 Phyllites

These are fine-grained and highly-fissile rocks. There is a prominent steeply dipping foliation (with dips east or west) which strikes in a NNW-NNE range.

The phyllites show a wide colour variation from grey to greenish or yellowish-grey or reddish to purplish-brown. When fresh, they have a sheen.

Many samples have compositional banding. The bands range in size from a few millimetres to 2 cm. Essentially, they are made up of alternating dark and light, pelitic and psammitic or micaceous and less micaceous bands.

In thin section (DB 95, DB 122) the phyllites have a lepidoblastic texture and are composed essentially of muscovite and quartz. Chlorite may make up to 5% of the rock. Calcite, plagioclase (albite ?) and opaques constitute the accessory minerals.

A sample, DB 122, from the north-eastern part of the mapped area contains disseminated crystals of pyrite. The thin section of the same sample shows that opaques constitute about 10% of the rock.

The foliation is defined by the alignment of mica and quartz crystals. This has further been emphasized in many places by the compositional banding described above. About 2½ km west of Tungan Kudaku village, at a river confluence, sample DB 95 indicates that the phyllite has been crenulated by a later deformation (plate iv).

East of the south-eastern corner of the Tsareta ridge is an area (less than ½ km^2) underlain by silicified phyllite. This is located approximately at a granite/phyllite contact. This rock is fine-grained, massive and hard with essentially the same foliation as the normal phyllites. It is light grey to grey in colour.

2.3.2 Slates

Slates underlie two small areas. One area lies about 1 km north of River MaiTalba. The other is about 1½ km east of the Tsareta-Tungan Kudaku road along the Zurzurfa River. They are dull-grey and very fine-grained with good cleavage. They are relatively harder and more resistant to weathering than the phyllites. Weathering especially along the cleavage has produced prevalently 010° trending and steeply dipping outcrops.

2.3.3 Schists

These occur in a pit located 500 m west of the Tsareta-New Project road junction, and also along the river valley west of Dumi I.

The rocks are highly weathered. Alignment of coarse muscovite flakes gives a distinct schistosity.

2.3.4 Metaconglomerates and Psammitic facies

Poorly sorted oligomictic metaconglomerates outcrop 2 km east of the Tungan-Kudaku-New Project road junction.

The matrix is phyllitic and the strike of the foliation is comformable with that of the surrounding phyllites.

The clasts range in size from fine sandy grains to up to 10 cm in their long axes (plate v). They are well rounded and generally have a low sphericity. They occur with their long axes aligned parallel to the foliation of the matrix.

In a thin section (DB 106) of the largest clast found, a granitic mineral assemblage is observed. In it, plagioclase is the dominant feldspar and has been highly altered mainly to sericite. Some of the large crystals enclose quartz grains giving poikiloblastic texture.

Orthclase occurs as large pophyroblasts which have been highly altered to sericite. The other K-feldspar is microcline which is less altered and is microperthitic.

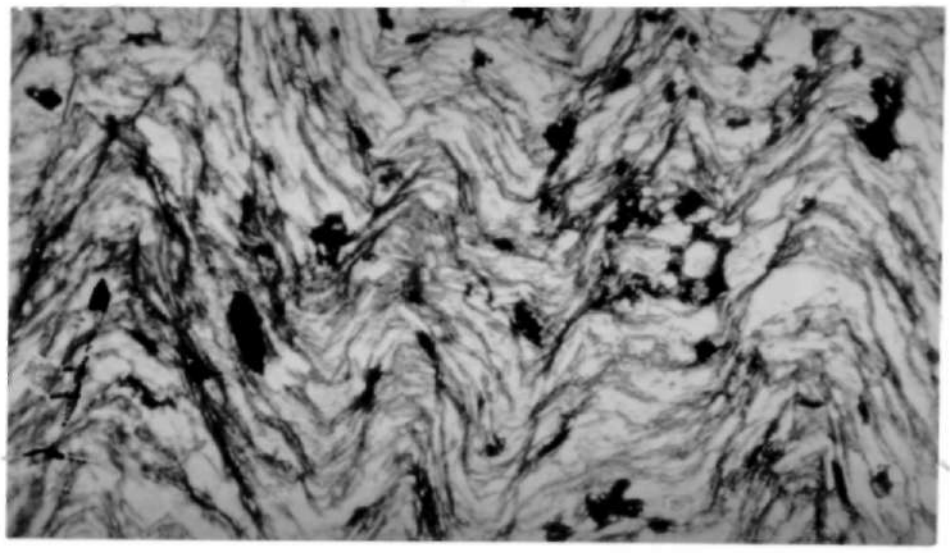


Plate iv
Photomicrograph of phyllite crenulations.
One polarizer. x 6·3

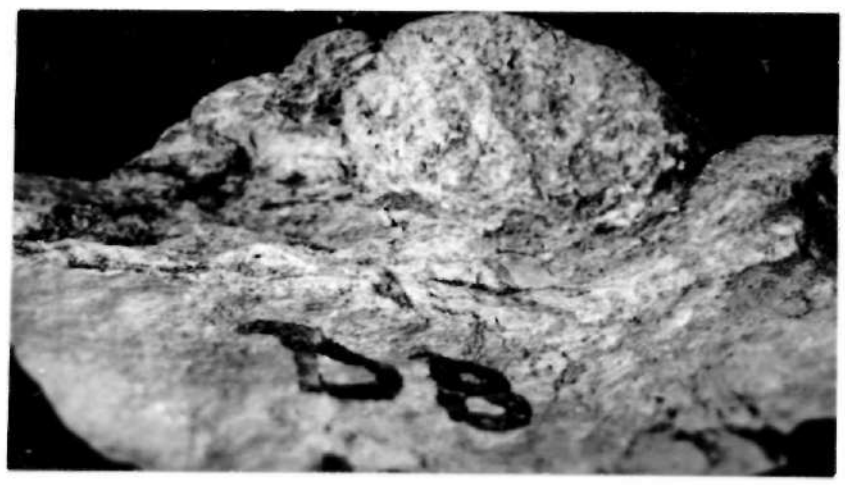


Plate v
A granite-clast in metaconglomerate

There are two generations of quartz. One consists of small crystals which are mostly enclosed in the feldspars or occur interstitially along the boundaries of the large quartz crystals which belong to the younger generation. The larger quartz crystals are craked and show undulatory extinction.

Muscovite is common and occurs along grain boundaries of the minerals, and to a limited extent, as an alteration product of plagioclase.

Chlorite, biotite, sphene, and opaque minerals occur as accessories.

Towards the south, about 300 m, the metaconglomerate grades laterally into an area of essentially psammitic facies. The rock, in hand specimen, is seen to be composed of quartz and feldspar grains which, at first sight, gives the appearance of a foliated granite.

2.3.5 Quartz pods, veins and ridges

Quartz occurs within the metasediments mainly as concordant pods (figure 4) veins and ridges. Quartz pods have a near vertical long axis and on the surface, they measure up to 25 cm in the long dimension.

Quartz veins are often continuous with the quartz pods along the planes of foliation of the phyllites. A few veins however cut across the foliation.

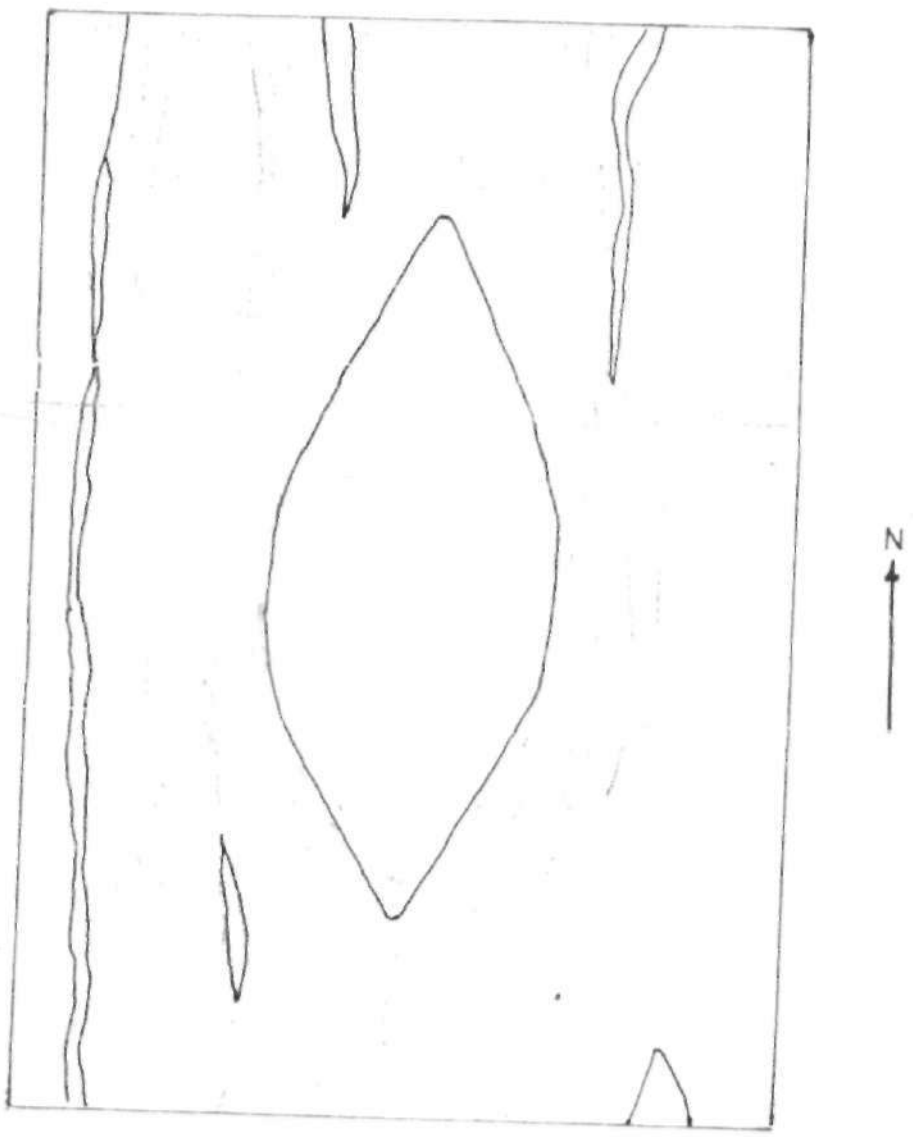


Fig. 4.

SKETCH OF QUARTZ PODS AND VEINS IN PHYLLITE

Quartz ridges form distinct topographic features (up to 600 m long and about 30 - 40 m high). Some of these ridges are associated with phyllite.

Quartz-float is ubiquitous over most of the metasedimentary areas having been released from the phyllite because of the great disparity in their susceptibility to weathering.

Fresh quartz is milky-white and occassionally contains disseminated anhedral to cubic crystals of pyrite (brass yellow). Quite often however, it is stained reddish-brown with limonitic material on the surface, along joint planes and in cavities. Small euhedral crystals of quartz occassionally occur in tabular vugs.

2.3.6 Dumi Cataclasitic Rocks

A group of cataclastic rocks occur over a zone about 150 m wide around Dumi I. It is thought to be part of a regional shear zone mapped by McCurry (1978) as a fault-silicified crush ridge (see 1.2).

In the field, the cataclastic rocks are medium to coarse-grained with a gneissic aspect. The foliation is defined by the alignment of elongated grains of quartz and feldspar (plate vi).

Small drag folds of quartzveins with horizontal fold axes occur in a few vertical sections (plate vii).



Plate VI

Rodding lineation in Dumi Cataclastic rocks



Plate vii

Drag-folds in Dumi Cataclastic rocks

The contact of these rocks with the surrounding phyllites and schists are gradational.

2.3.7 Metavolcanics (or Amphibole schist)

Metavolcanics occur in subparallel to parallel discontinuous lenses interbedded with phyllites in the eastern part of the mapped area (figure 2). In the field, they occur generally as low-lying outcrops, but a few outcrops composed largly of boulders attain a height of about 5 m. The largest outcrop located about 500 m south of the eastern Tungan Kudaku junction, is a north-south trending ridge about 100 m long. The metavolcanics are fine to medium-grained, dark-green to greyish-green and well foliated rocks. When weathered, they have a dull appearance and are friable. The foliation is comformable with the essentially north-south striking phyllites with which they are intercalated.

Folds with steeply dipping axes (plate viii) are well preserved in several outcrops. They range from tight to open, and harmonic to disharmonic folds of various sizes. Quartzveins lying parallel to the foliation have also been folded with the metavolcanics. In one location, portions of the metavolcanics are ovoid-shaped and are coarse-grained.

In thin section (DB 24, DB 35, DB 41 and DB 124) the rocks are composed of amphibole (60 - 80%) with variable amounts of calcite, quartz, andesine, An_{32} (extinction angle = 15^{o}), epidote, and opaques.



Plate viii(a)

Folds in metavolcanic rocks. Foliation of rocks is east-west.



Plate viii(b)

Tight folds in metavolcanic rocks. Foliation is north-south.

The amphibole consists of bladed and acicular crystals of actinolite which are aligned to give the rock foliation. It is pleochroic from green to pale-brownish-green.

Calcite occurs in two sets of veins with granoblastic texture. One set lies parallel while the other cuts across the foliation. The proportion of calcite varies from place to place and within the same sample. For example, in DB 35 there is no calcite, but in DB 24 it makes up about 30% of the rock.

Quartz and andesine are partially segregated from the mafic minerals to give a microbanding. The bands are not persistent and several of them pinch out or are transected by wider bands. A few leucocratic veins cut across the foliation. Quartz shows undulatory extinction.

Epidote granules are present in many sections. Generally, they are colourless, but yellow (iron rich) patches sometimes occur in the same crystal. Under cross-nicols, they exhibit variable interference colours. Actinolite laths occassionally wrap round a single crystal of epidote.

2.3.8 Banded-Iron Formation

Outcrops of this rock occur as north-south trending lenses interbedded with phyllites and metavolcanics in the eastern part of the mapped

area. They lie within the area defined by the two limbs of the metavolcanics described in the previous section.

In hand specimen, they are fine to medium-grained dark-grey to dark-reddish-brown and weakly foliated or massive rocks. One sample has a minor fold which appears to be sheared out. They are composed of quartz (70%) magnetite and/or hematite. These minerals have been sheared and their alignment imposes the foliation. Weak banding is shown by the partial separation of quartz from the iron-minerals (opaques). Late quartz occurs in veins cutting across the foliation.

2.4 Serpentinite

In the Tsareta area, serpentinite occurs within a NNE-SSW trending zone about 15 km long and up to 1 km in the widest part. McCurry (1978) had, from air-photo-interpretation, mapped the serpentinite body as a granite. In July 1981, it was first identified during reconaissance fieldwork (Woakes, personal communication).

In the field, outcrops are generally low-lying, but may locally attain a height of 10 m. They may be bouldery or consist of elongated bodies which are essentially parallel to the regional trend of the surrounding phyllites.

When fresh, the serpentinite is a dense, dark-green rock. Most outcrops are weathered to a light green or greyish-green colour. A few outcrops have been silicified on the surface and are consequently hard and less susceptible to weathering. They are dark-grey or orange-brown.

The serpentinite is commonly transected by asbestos veins and a later generation of chalcedonic quartzveins. These veins weather more slowly than the serpentinite to produce the characteristic honey-comb structure on the surface of the rock (plate ix).

In a few parts some boulders of the serpentinite show a foliation. On one outcrop, the strike of the foliation was measured as 020° with a dip of 75°E.

The contact between serpentinite and phyllite was nowhere observed, but phyllites closeby show no contact metamorphic effects. The contact is thought to be sharp without alteration.

Large xenolithic blocks of coarse-grained massive amphibolite occur within the serpentinite body (see section 2.2.3).

Diorites and trachyandesite have intruded the serpentinite body. They are described in section 2.5.



Plate ix
Honey-comb structure in serpentinite



Plate x
Photomicrograph of prismatic crystals of anthophyllite in serpentinite.
Cross-polarizers. x 63

Several massive lenses or pods (about 2 m long) consisting predominantly of chromite and some magnetite and ilmenite occur in the serpentinite. Partially formed layers of chromite were observed.

Thin section study (DB 12, DB 12a) shows that the mineral assemblage consists essentially of antigorite, 75-80% and anthophyllite, 20 - 25%. Antigorite occurs as fine lamelae forming a matrix in which the anthophyllite is set. Anthophyllite occurs as yellow prismatic crystals (plate x). It shows straight extinction and anomalous birefringence colours. Along the edges and cross-fractures, it is studded with opaque-grains, probably of magnetite.

2.5 Older Granite Suite

This is a group of intrusive rocks in this area which, apart from some local structures, are largely undeformed. They are regarded to be the youngest rocks in the area.

2.5.1 Deformed Diorites

These occur in the central part of the serpentinite body in a zone extending for about 1½ km long in a north-south direction. They are weathered and consist of low-lying outcrops. In hand specimen, they are medium-to coarse-grained with dark-green and light-coloured minerals (most probably amphiboles and feldspars respectively) aligned to give a distinct north-south linear fabric.

2.5.2 Undeformed Diorites

These are more wide-spread and more abundant than the deformed diorites. They are medium-to coarse-grained variegated green to grey-green rocks with an equigranular texture. They occassionally occur as rounded boulders due to spheroidal weathering.

In thin section (DB 13) they are seen to have a subhedral-granular texture and are composed of hornblende, endesine, orthoclase and quartz, while opaque minerals and epidote occur as accessories (plate xi).

Hornblende makes up to 60% of the rock and occurs as anhedral crystals. It has the following pleochroic scheme:-

α = green

β = brownish-green

γ = brown

The hornblende is occassionally altered to epidote and to opaque minerals especially along the cleavage.

Andesine, An_{46} (maximum extinction angle = 25^{o}) constitutes between 25% and 30% of the rock and is the dominant feldspar. It occurs as anhedral to subhedral laths showing characteristic albite twinning. It is often altered to sericite and contains several tiny opaques.



Plate xi

Photomicrograph of undeformed diorite with subhedral granular texture.

Crossed-polarizers. x 63

Orthoclase is less than 10% of the rock. It is anhedral and altered, especially at the marginal areas, to kaolin (?).

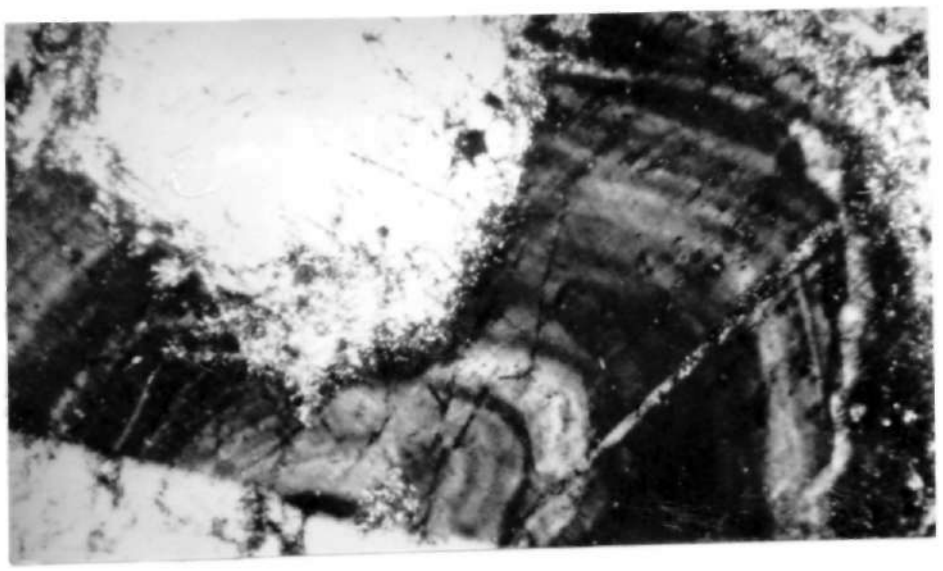
2.5.3 Trachyandesite (Latite)

This usually occurs as loose boulders. In one locality, about 2½ km east of Zurzurfa I and along the southern major tributary of the River Zurzurfa, it occurs as a dyke cutting through the undeformed diorite. The rock is usally grey-green and porphyritic.

In thin section (DB 96) it consists of phenocrysts of sanidine and rhythmically zoned and twinned plagioclase (plate xii) set in a fine-grained matrix (plate xiii). The sanidine has cracks and shows undulatory extinction. It can be mistaken for quartz, but conoscopic examination proves that it is biaxial negative. All the phenocrysts have a dense rim of mafic minerals. The main mafic mineral in the matrix is amphibole. Chlorite is also present, but as an accessory. The light coloured minerals in the matrix are probable feldspars.

2.5.4 Hornblende Lamprophyre

This rock occurs in this area as loose boulders (up to 50 cm) within a 2 m wide by 30 m long zone. Its field occurence indicates that it is a dyke

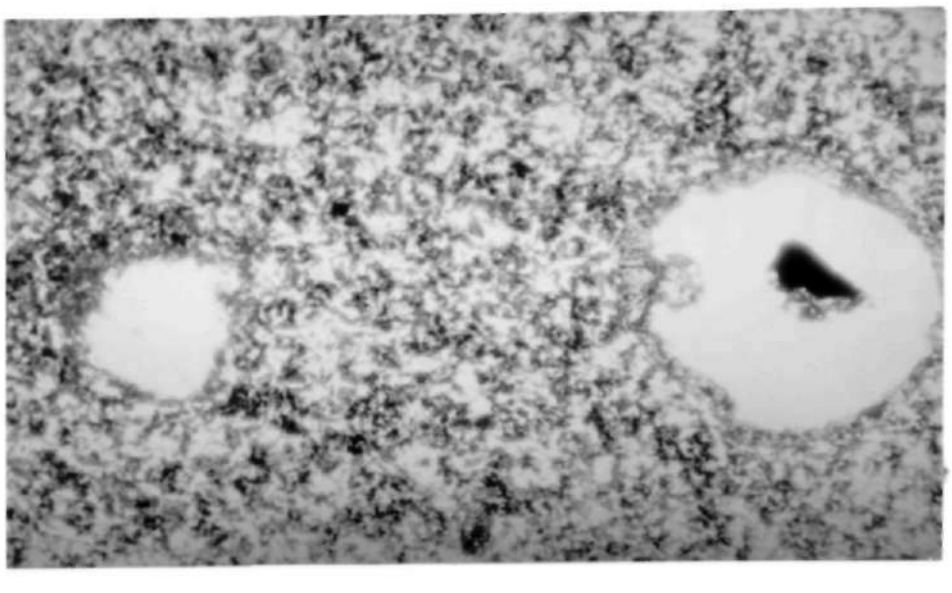


0·25mm

Plate xii

Photomicrograph of rhythmic zoning and twining of plagioclase in trachyandesite.

Crossed polarizers. x 6·3



1mm

Plate xiii

Photomicrograph of trachyandesite showing porphyritic texture. The phenocrysts are sanidine crystals. One polarizer x 25



Plate xiv
Photomicrograph of cross-shaped twining of hornblende in Hornblende-Lamprophyre. Crossed-polarizers x 6·3

cutting serpentinite. Its northern end is bordered by an undeformed diorite intrusion (figure 2).

In hand specimen, it is a dark-grey, fine-grained, porphyritic rock. The phenocrysts consist of randomly oriented needles.

In thin section, the rock is seen to be composed of idiomorphic phenocrysts of green hornblende set in a fine-grained matrix. The hornblende commonly shows zoning indicated by the occurence of different birefringence colours between the outer and central parts in the same crystal. Twinning is also common. See plate xiv for simple and cross-shaped twins.

The matrix is composed of amphibole, clinozoisite, and feldspars. The feldspars have simple twins, but the laths are too fine to enable a specific identification. A hornblende-plagioclase lamprophyre is known as spessartite, while that containing K-feldspar is known as vogesite (Hatch et al 1972 and Nockolds et al. 1978).

2.5.5 Biotite-Granite

Biotite-granite underlies an area about 4 km^2 between the granite-gneiss to the west and the phyllites to the east. This rock occurs as bouldery outcrops or as pavements mostly along stream channels. In some places e.g. along the

Zurzurfa river channel, the rocks are strongly weathered. Spheroidal weathering is active (plate xv).

The rock is typically coarse-grained with an equigranular texture. It occassionally contains dark, fine-grained, biotite-rich xenolithic inclusions. In one locality, the contact with granite-gneiss is exposed. It is a typical example of a chilled intrusive margin. Here, the biotite-granite is characterized by:-

a) abundant xenoliths of granite-gneiss in various stages of assimilation (plate xvi)
b) a finer-grained texture
c) a higher percentage of biotite (up to 25%).

The major component minerals of this rock are microcline and/or orthoclase (30 - 35%), quartz (25 - 30%), plagioclase (15 - 20%) and biotite (about 10%). Accessories include hornblende, sphene, epidote, apatite, zircon, sericite and opaque minerals.

In a thin section (DB 49) made from a sample obtained from the contact zone between the biotite-granite and granite-gneiss, microcline is absent, and the only K-feldspar is orthoclase. In other areas the two feldspars occur together, with microcline being the more abundant. Microcline usually occurs as large crystals up to 3 mm in



Plate xv
Spheroidal weathering in biotite-granite



Plate xvi
Contact rock between granite-gneiss and biotite-granite. Several xenoliths of granite-gneiss at various stages assimilation can be seen.

size and shows the characteristic cross-hatch twinning. Orthoclase also occurs as large crystals and shows incipient alteration to clay minerals.

The plagioclase is oligoclase, An_{28} (maximum extinction angle = 14^{o}) and shows fine polysynthetic albite twinning. Plagioclase occurs in all sections examined.

Quartz occurs as anhedral crystals which are either enclosed in feldspars or as single large late crystals. Both show undulous extinction.

Biotite is usually the dominant mafic mineral and occurs as anhedral laths which are quite often replaced by quartz, plagioclase, chlorite (light-green) and opaque minerals. The opaques can be seen studded along the edges and the cleavage (figure 5). Biotite is pleochroic from brown to brownish-green and is corroded by the felsic minerals.

A few ragged crystals of hornblende occur associated with biotite. It is pleochroic from dark-green to pale-brownish-green.

BIOTITE – GRANITE

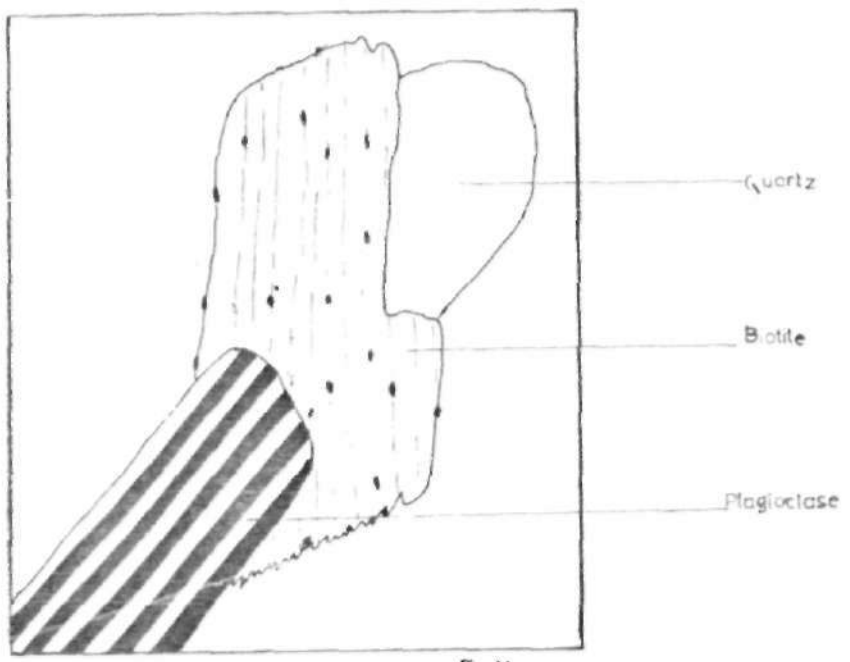


Fig. 5

Biotite being corroded by quartz and plagioclase.
Biotite is also altered to opaque minerals.
Sketched from thin section DB. 49.

CHAPTER 3

GEOLOGIC HISTORY

3.1 Structures

The metamorphic rocks in the area mapped are well-foliated with a distinct north-south regional trend in conformity with the structural grain of the country. The north-south trend is considered to represent the imprint of the Pan-African event which is the last major tectonic event to affect the Nigerian Basement.

In the field, several generations of small-scale structures (foliation, folds and lineations) were observed, but no detailed investigation of them was made. Some of the structural elements are described below.

3.1.1 Foliation

A well developed foliation is preserved in the metasediments, metavolcanics, and granite-gneiss. This foliation is defined by the parallel alignment of platy minerals (micas), quartz, and feldspars. In the metaconglomerate, the granite-clasts are elongated and aligned parallel to the same foliation. A foliation is also developed in the banded-iron formation. Parts of the serpentinite body show a foliation. The Dumi cataclastic rocks are characterized by a strong foliation which makes the rocks look flaggy.

The foliation in the different rock types strike NNW-SSW with subvertical dips. This foliation is locally seen to be deformed by later movements.

A compositional banding occurs in several places in the metapelites, especially the phyllites. It is not clear whether this banding represents primary layering or metamorphic differentiation. Shandelmeyer (personal communication, 1983) suggested that it is often primary layering which is parallel to the metamorphic foliation. In one locality, along a stream (flowing from east to west) in the most norther part of the mapped area, the metamorphic foliation was seen to be oblique to the banding indicating that the observed banding is most probably primary layering. Transposition of bedding may have been important in producing some of the banding seen in some of the rocks (Egbuniwe, 1982).

Lying parallel and along the foliation planes of both the metasediments and metavolcanics are quartz veins which are often impersistent. The quartz veins are probably the product of metamorphic sweating (Boyle, 1979).

3.1.2 Lineation

Crenulation lineation is common on the foliation surfaces of the phyllites. It plunges moderately, up to a maximum of 030°, to the north or south.

The crenulation is due to a later deformation.

In the cataclastic rocks, a strong rodding lineation is present (plate vi).

Mineral lineation is shown by the deformed diorite (section 2.5.1) due to alignment of hornblende crystals. It has a north-south trend which is parallel with the foliation observed in the metasediments.

3.1.3 Minor Folds

Folds are observed in the metavolcanics and not in the phyllites with which they are interbedded. The folds have steeply plunging fold axes. The various geometric froms (some shown in plate viii) include tight to open folds, isoclinial to assymetric folds and cherron folds.

These folds are considered to have resulted from a later and less intense deformation than that which produced the commonly observed north-south regional foliation of the area. The absence of these folds in the phyllites, can be attributed to the difference in competence between the two rocks i.e. whereas, the folds were formed in the more competent metavolcanics, the same did not form in the phyllites with relatively lower competence.

Folds are also observed in the granite-gneiss (plate i). These are considered to have formed after the foliation observed in the granite-gneiss.

Dragfolds with horizontal fold axes are present in the Dumi cataclasitic rocks (plate vii). They were probably produced by shearing.

3.1.4 Large Scale Structures

A large-scale linear shear zone traversing the area in a NNE-SSW direction was recognized by McCurry (1978) from air-photo-interpretation. In this work, air-photographs were also examined and the shear zone mapped. Though McCurry, at a scale of 1:250,000, mapped the zone as a straight line, the present mapping, at a scale of 1:25,000, shows that the zone which is marked by discontinuous quartz ridges and the Dumi Cataclastic rocks, is folded. Some of these ridges have an intricate network of a second generation of vein-quartz considered to have been emplaced after shearing.

The quartz ridges appear to have been folded by the intrusion of the biotite-granite body immediately west of the shear zone. One of the quartz ridges can be traced through an arc of 320° to 020°. Two others have trends of 315° and 045°. This implies that the shear zone is older than the biotite-granite body considered to be of Pan African age. However, further north, outside the mapped area (figure 6) a parallel shear zone perhaps of the same system, cuts the Pan African Maiinchi granoclorites dated as 680 m.y. (Ogezi 1977).

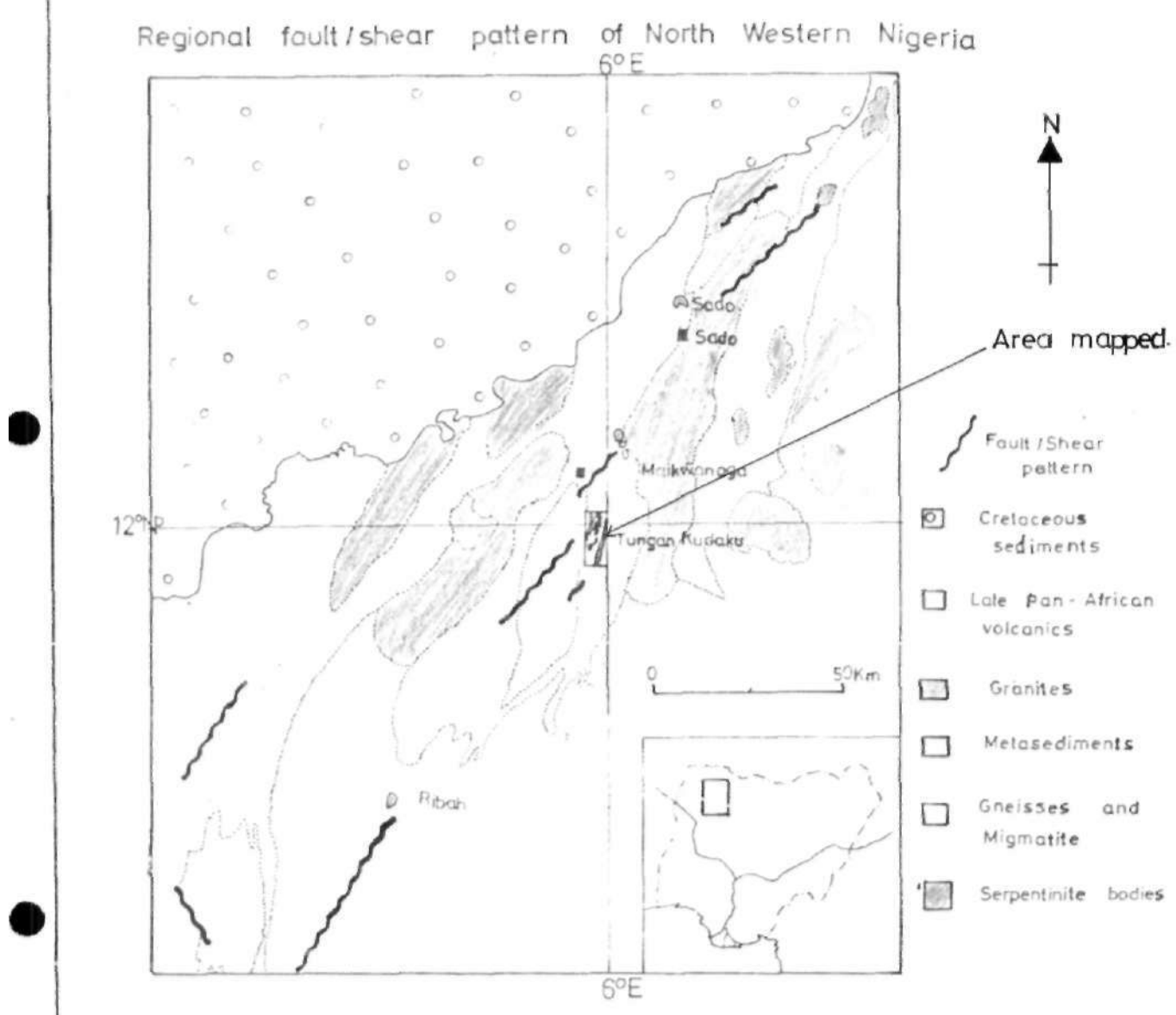


Fig. 6

After McCurry and Wright 1977

This suggests that the shear zone represents an ancient linearment along which movements re-occurred in late or post Pan African times.

In a later section (3.3.3) evidence for the emplacement of serpentinite by tectonic processes is discussed both for the mapped area and on a regional basis.

In the western part of the mapped area, about 6 km south-west of Tsareta ridge, a fault zone, indicated by the occurrence of quartz breccia (2.2.5) is located just east of the granite-gneiss outcrops. Though no phyllite crops out, the fault appears, from the field mapping, to mark the contact between the granite-gneiss and the phyllites.

Large scale forms recognized in air-photographs and later verified by ground mapping are the NNW-SSE trending Tsareta ridge, formed by granite-gneiss, and quartz-phyllite ridges with trends varying little from north-south.

Also from the air-photographs, large-scale folds are observed in the phyllites both east and west of the serpentinite body in the southern half of the map. However, due to lack of good exposure and distinct marker horizons, these folds could not be defined in the field.

The generally parallel north-south trending lens-shaped metavolcanic bodies occuring east of the serpentinite body probably represent the two limbs of a fold with a surface interlimb distance of up to 500 meters. From the map, figure 2, probable fold closures occur in at least two places: one is located about 500 meters east of the Tsareta-New-Project road junction, and the other about 4.5 km south of the junction.

3.2 Metamorphism

Apart from the biotite-granite, the undeformed diorite, trachyandesite and lamprophyre, all other rock units are metamorphic rocks. Index minerals are unfortunately lacking. Therefore, the mineral assemblages are compared to those of the Barrovian region (Harker 1932). From this, it is concluded that the granite-gneiss has been metamorphosed to the amphibolite facies, while the metamorphic grade of the metasedimentary and metavolcanic rocks is the green schist facies (Table 1).

Table 3:1 Mineral assemblages and metamorphic facies of the rocks

Rock	Mineral Assemblage	Metamorphic facies
Granite-Gneiss	Microcline, oligoclase, quartz, green-horn blende	Amphibolite
Phyllite	Quartz, muscovite, albite (?) and pyrite	Greenschist
Metavolcanic	Actinolite, calcite, epidote, quartz andesine	Greenschist

The sharp difference in the metamorphic grade between the granite-gneiss (amphibolite facies) and the metasedimentary/metavolcanic rocks (green-schist facies) provides evidence that metamorphism in the Tsareta-Tungan Kudaku area is polycyclic.

Evidence of rock flowage indicates that the temperature during the high grade metamorphism of the granite-gneiss was high.

3.3 Evolution of the Area

Field relations and metamorphism indicate that the rocks in the area mapped are of widely different ages. Like in other parts of the Nigerian Basement, the granite-gneiss is considered to be the oldest rock which is overlain by the metasediments. Both the granite-gneiss and the metasediments have been cut by biotite-granite considered to be of Pan-African age. In the central part of the mapped

area, a NNE-SSW trending serpentinite body cuts the metasediments and has in turn been intruded by diorites and a lamprophyre dyke - figure 2.

3.3.1 Granite-Gneiss

The contact between the granite-gneiss and the phyllites is nowhere observed. The contact has largely been intruded by biotite-granite and in an area, about 6 kilometers south-west of Tsareta ridge, the contact appears to be marked by a fault - figure 2. The nature of the contact between the migmatite-gneiss complex and the low-grade metasediments of the Nigerian Basement has been extensively discussed by many authors. Truswell and Cope (1963) mapped the 1:250,000 sheet 31, and on finding no evidence for an unconformity, proposed that the rocks in the area , and possibly in the whole of North-Western Nigeria and beyond, belong to what they termed the Gwarian, Complex formed during a single orogenic cycle. However, many authors (e.g. Russ 1957, McCurry 1976 and Ajibade 1980) now favour the view that the metasediments lie unconformably on the migmatite-complex. Ajibade (1980) has, during the study of the Zungeru region, stated that the unconformity has been obliterated by deformation to form the Zungeru Mylonites.

In the Tsareta-Tungan Kudaku area, the granite-gneiss has been metamosphosed to the amphibolite facies, while the metasediments attain only greenschist facies. It is suggested that the metamorphism of the metasediments occurred after the higher-grade metamorphism of the granite-gneiss which is a regional phenomena and is the older rock.

Radiometric age determinations were not carried out during the present work, but data from other areas of the Nigerian Basement show that gneisses are as old as the Archean, 2.1b.y. or older (Grant 1970 and Ogezi 1977), while younger dates are interpreted as representing later orogenic events (Grant et al, 1972).

McCurry (1976) has proposed that gneisses in the Nigerian Lasement Complex were derived from ancient metasediments, referred to in the literature as the Older Metasediments of probable Birrimian age.

Gneiss and amphibolite xenolithic blocks found in serpentinite are considered to have been stoped from the granite-gneiss basement.

At the south-eastern end of Tsareta ridge the granite-gneiss grades into a massive equigranular felsic material near the contact with brotite-granite. This maybe due to thermal recrystallization (contact metamorphism).

3.3.2 Metasediments and Metavolcanics

Fine-grained pelitic rocks constitute the predominant metasediments in the Tsareta-Tungan Kudaku area and are indicative of deposition in a moderate to deep and quiet water environment.

The metaconglomerate and the psammitic facies probably represent shallow-water sediments. The well-rounded granite-clasts in the metaconglomerate indicate long distance transportation, or long period of reworking.

The metavolcanics in this area are considered to have been emplaced at the same time with the metasediments. They are 50 - 100 meters thick, but the contacts are not exposed and it is not clear whether they were emplaced as sills, flows or pyroclastics. Some ovoid structures found south of the Tungan-Kudaku junction are interpreted as possible submarine pillows. Bar (1982) and Egbuniwe (1982) have reported the occurence of pillows from the Maru Belt which is adjacent to this area. The mineral composition of the metavolcanics is actinolite, calcite, epidote, quartz and andesine. This suggests that the original rock has a composition in the basic - intermediate or basalt - andesite range.

The banded-iron formation has a close spatial relationship with the metavolcanic rocks and suggests that it is a submarine volcanogenic exhalative laid down on a basin floor of predominantly pelitic sediments.

Quartz veins, pods and ridges in phyllite and metavolcanics often represent excess silica produced during the low-grade metamorphism of the area.

The major controversy surrounding the schist belts is the age of deposition of the original sediments and deformation. McCurry (1976) suggested that deposition occured during the Katangan (100 - 800 m.y.) and metamorphism during the early stage of the Pan-African event, about 850 - 650 m.y. ago. However, an isotopic date in the phyllite of 1090 m.y., obtained by Ogezi (1977) from Maru area indicates that the meta-sediments are as old as the Kibaran. Younger ages in the phyllites are interpreted as representing cooling dates of the Pan African event (Ajibade 1980).

The granite-clasts in the metaconglomerates indicate pre-Pan African granites in the basement.

The metasediments, commonly referred to in the literature as the "Younger Metasediments" were formerly thought to be relicts of a once

continuous supracrustal cover laid down on the basement and later infolded and metamorphosed along with it (Russ 1957 and McCurry 1976). However, lithologic and structural differences between the metasedimentary belts introduces the possibility that the metasediments may have been deposited in separate basins (Ajibade 1980).

3.3 Serpentinite

The age of emplacement of Mallam Tanko serpentinite, about 150 km east-south-east of the present area, has been discussed by Bar and Glaeser (1981) and they concluded that the body is younger than the Pan-African granites. This conclusion rests on two lines of evidence:-

a) the occurence in the serpentinite of undeformed granite xenoliths purported to be of Pan African age.

b) the reported absence of north-south Pan-African deformation structures in the serpentinite.

In the Tsareta-Tungan Kudaku area where the granite, of assumed Pan African age, is also undeformed, the serpentinite is deformed locally by north-south structures. Furthermore, the intrusion of the biotite-granite in the area appears to have deformed the fault/shear zone system of which the serpentinite is part.

Therefore, it is suggested that the serpentinite in this area is older than the biotite-granite.

The physical state of serpentinite at the time of emplacement has been extensively discussed by other writers (Krauskofp 1967, Bar and Glaeser 1982, Nockols 1978 and Hatch et al 1972). The occurrence of massive and partially layered bodies of primary chromite in this serpentinite shows that the parent material once existed as a true magma which allowed for gravity settling of the cummulates. Experimental studies in the system $MgO-SiO_2-H_2O$ by Hess (1955) and cited by Hatch et al (1972) show that forsterite and enstatite (main constituents of peridotite) remain crystalline at temperatures above 1,000°C. This means that a magma of dunite or peridotite exists at extremely high temperatures and when intruded into crusted rocks should produce intense contact metamorphic effects. These features are not exhibited in the Tungan Kudaku area.

Hatch et al (1972) further pointed out that olivine remains stable down to a temperature of 500°C in the presence of any amount of water before it is altered to serpentinite. Serpentinization is essentially a hydration reaction leading to increase in volume. Coleman (1971) citing

Nicholas (1969) states that the volume increase during serpentinization can be up to 58% in dunites. This volume increase coupled with the low density of the rock may have ensured upward displacement. This was facilitated by the incompetence and therefore lubricating nature of the serpentinite at its contact with the surrounding phyllites. Stress generated by movements at the contact were not easily transmitted into the main body of the serpentinite which therefore remained largely undeformed. The occurence of a few clearly deformed parts of the serpentinite can be attributed to movement along local planes which have cut through parts of the serpentinite body.

The increase of volume accompanying the serpentinization necessarily led to the development of internal expansive stresses. As the serpentinite body rose up, lithostatic pressure diminished and at a certain level the expansive force became the greater force which resulted in free expansion. This led to the formation of dilatant fractures which have been infilled by asbestos. Fracturing occured in two stages. The later fractures were infilled by chalcedonic quartz. This is an indication that the serpentinization was not just a simple hydration, but also involved the mobilization of some silica. It further indicates that the process was not completed at depth, but was

continuous right through to the final emplacement of the serpentinite body at the present upper levels.

One sample of the serpentinite examined in thin section (DB 115) shows that hornblende is the dominant mineral. The same sample has cross-fib asbestos. The rock was possibly also formed by hydration (Wyllie 1970).

From the foregoing discussion, it is suggested that the serpentinite body in this area was emplaced as a relatively cold intrusion with the serpentinization having started at lower levels. This implies that the serpentinite was tectonically emplaced and that there was a structural weakness along which movement took place. Furthermore, the regional distribution of the Sado, Maikwanoga, Tungan-Kudaku and Ribah serpentinite bodies (fig. 6) suggests a system of faults. Williams and Williams (1977) have suggested that similar faults are the continental extensions of trans-Atlantic transform faults.

3.4.4 Diorites, Trachyandesite, Lamprophyre and Biotite-Granite

The rocks discussed in this section are intrusives and are thought to be representatives of the Older Granite suite of Pan African age.

The diorites in this area have been mapped as intruding the serpentinite. The occurence of north-south structures in certain parts of both of these rock types can be attributed to local deformation.

The lamprophyre dyke (2.5.4) is intrusive to the serpentinite and at its northern end, it runs into or is terminated by a diorite intrusion. According to Hatch et al (1972) lamprophyres represent highly specialized magma fractions of diorite.

The biotite-granite in this area is clearly an intrusive body. Its contact with the granite-gneiss described in section 2.5.5 shows features of a chilled margin. However the contact of biotite-granite and the other rock types discussed in this section was nowhere observed.

Isotopic data from other parts of the Nigerian basement has shown that rocks of the older-granite suite are undoubtedly Pan African in age (Table 2).

Table 3:2

Radiometric dates of some older Granite rocks in the Nigerian basement

Location	Material analysed	Method	Age	Author
Minna	Granodiorite	K-Ar	505 ± 15	Ajibade, 1980
Zaria	Porphyroblastic Granite	Rb -Sr	794 ± 73	Ogezi, 1977
Maiinchi	Granodiorite	Rb -Sr	697 ± 65	Ogezi, 1977
Dan Garamfa	Granite	Rb -Sr	740 ± 5.6	Holt, 1982

CHAPTER 4

MINERALIZATION

4.1 Introduction

The area investigated is included in the former gold producing areas of north-western Nigeria. During this work three types of economic minerals were noted. These include gold, chromite, and asbestos. However, no detailed investigation of the mineralization has been carried out.

The total recorded gold production in Nigeria since 1914 amounts to 12,000kg (Annual reports of the Department of Mines, 1922-1968). Most of this came from the Kazai-Beni, Birnin-Gwari, Malendo and the River Zamfara areas of North-western Nigeria (R ss 1957). Records of gold production before 1914 have not been found, and this perhaps is indicative of insignificant or total lack of local gold mining prior to this date.

In the Tsareta area, old gold workings were first shown to A.B.U. staff by the local people and this is one of the reasons for the initial interest in the area. Local history and tradition gives some guidance regarding mining activity in the area, but this must be interpreted with caution.

Up to date no chromite and asbestos of sufficient quantity to be of commercial value have been reported

in Nigeria. A small occurence of iron-rich chromite has been reported from the Mallam Tanko serpentinite by Ogezi (1977) and Bar and Glaeser (1981). Anthophyllite asbestos in phyllite has been reported from Karau-Karau by McCurry (1973).

The geology and mineralization of the Tsareta area are discussed below.

4.2 Geology

4.2.1 Gold

In the area mapped, primary gold mineralization occurs in quartz-veins associated with shear zones. Old gold workings found include Dumi I and II, and Zurzurfa I and II (figure 2). The workings consist of elongate open pits aligned generally in a north-south direction. This indicates that the mined auriferous quartz-veins were also aligned in a north-south direction and conformable with the surrounding phyllites and are vertical or very steeply dipping.

The old gold miners probably followed the quartz-veins until they became too deep and uneconomic to work. Gold was obtained by handcrushing and washing the quartz-vein material. The gold-bearing quartz-veins are thought to be covered now by thick debris from the sidewalls of the pits.

The size of the gold workings is a rough indication of whether gold was obtained in appreciable amounts or not. For example, the small Zurzurfa I working appears to have been tested and found barren and therefore abandoned almost immediately. On the other hand Zurzurfa II measures about 25m long, 2m wide at the bottom and 4m deep with a large dump around it. It is very unlikely that the old miners would have gone so deep had they found nothing. Dumi II is the largest gold working found. It measures about 35m long, 5m wide and 6m deep also with a large dump. From the dump around Dumi I, a gold grain was seen in a fragment of quartz.

A few rock pieces in the dump around the gold workings contain sulphides. At Dumi I, galena occurs in quartz. At Zurzurfa II, pyrite, chalcopyrite and energite occur as inclusions in galena (Polished section DB 86). The galena is altered to cerrusite with colloform banding. This structure is considered to be a product of periodic changes in weathering conditions, for example, changes in the pH - Eh regimes (Ramdohr, 1975). Pyrite is replaced by limonite.

Outside the mapped area, other gold-workings are known to occur. The abandoned Kuba (Cooper?) and Monsur mines to the north-north-east were visited. The Kuba mine consists of underground and open pit workings which indicate that gold was contained in a

complex and extensive system of quartzveins. To the south-south-west is the Magyelma mine also now abandoned (J.Y Gominah, personal communication, 1982). On a regional scale, these workings together with those within the mapped area plot on or close to the fault-silicified-crush-ridge structure mapped by McCurry (1978) and its extension to the north-north-east.

4.2.2 Chromite

The chromite occurrence in the serpentinite of this area is an example of podiform chromite. The largest occurence is exposed in a area about 1km east of Tungan Kudaku village.

The chromite occurs mainly as disseminated fine to coarse-grains, up to 1cm, sometimes with a nodular appearance. Pods, about 2m long, of massive chromite occur. Examination of a polished section shows that they are high in magnetite and ilmenite.

4.2.3 Asbestos

Anthophyllite occurs mainly as slip-fibre asbestos in veins cutting serpentinite. It has a dark-grey appearance and is brittle due to weathering. It weathers more slowly than the serpentinite and is partly the cause for the development of the honey-comb structure in the serpentinite.

In one locality, fresh, silky, cross-fibre asbestos occurs in veins cutting a rock composed

predominantly of hornblende (Plate XVII). The largest fibres found measure 2½ cm.

The asbestos is usually associated in the serpentinite with an unidentified pale-yellowish-green amorphous material.

4.3 Origin

4.3.1 Gold

The occurrence of the old gold workings in this area along shear zones suggests that mineralization was structurally controlled. It is suggested that the mechanism of gold transport and deposition is related to metamorphic processes (Keays, 1978; Boyle, 1979; and Koln 1982). It is speculated that the gold, in the Tsareta area, was leached from the metavolcanic rocks during metamorphism and migrated to structurally favourable depositional sites. It is recalled that several authors (e.g Read and Watson, 1975; and Boyle 1979) have drawn attention to the relatively high gold content of basic volcanic rocks and consequently the metavolcanic rocks in this area may well be the main source of the gold.

In the alternative, the gold may have been derived from the reworking of Birrimian rocks which according to McCurry (1976) have largely been converted to gneisses and migmatites. In the West African Craton

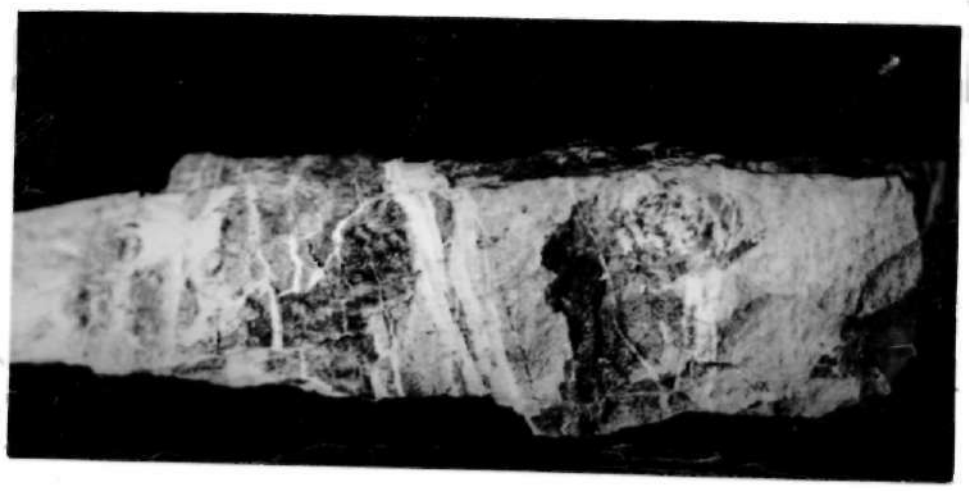


Plate xvii

Cross-fibre asbestos in an amphibole-rich rock.
Length of rock = 13 cm.

(West of Nigeria) the Birrimian sediments together with granites intruding them contain gold (Read and Watson 1975; and Agyakwa 1979).

Granites in general contain low gold (Boyle 1979). In north-western Nigeria, the Pan-African granites are characterized by an almost total lack of mineralization (Russ 1957) and similar potassium granites in Zimbabwe are reported to be rarely associated with gold deposits (Mann1982). The folding of the quartz ridges in the shear zones in this area indicates that the granite emplacement is post mineralization. There seems no genetic link between the gold mineralization and the granite though it is possible that heat from the intrusion mobilized mineralizing solutions.

Gold production in this area ceased long ago and the story is virtually the same for the whole country. The search however has been continued by the Nigerian Mining Corporation. It is suggested that exploration work in this area should focus on shear zones, which, from this study, appear to control the distribution of the mineralization.

4.3.2 Chromite

All economic primary deposits of chromite occur either stratiform or alpine type ultrabasic rocks and their serpentinized derivatives (Mikami 1979 and Evans 1980). In the Tsareta map area, podiform chromite occurs in a NNE-SSW trending serpentinite body.

already been discussed in section 3.3.3. It is envisaged that the open fractures provided avenues for the movement of mineralizing solutions originating from the main ultrabasic body undergoing serpentinization.

The pale-green amorphous material almost invariably associated with the anthophyllite in the serpentinite may be an intermediate product in the formation or breakdown of the anthophyllite. Onyeagocha (1979) has also pointed to the restricted stability field of anthophyllite as a reason for it being unlikely to occur in commercial quantities.

CHAPTER 5

PRELIMNARY SOIL GEOCHEMICAL INVESTIGATION

5.1 Sampling and Analytical Methods

The sampling was carried out during the rainy season, in the months of July and August, when the soils were still relatively soft.

The aim of the geochemical soil survey is to define some structures which would be related to gold mineralization and also investigate the reflection of the overlying bedrock by the chemical composition of their weathered products (soils). The reflection of the underlying bedrock by the chemical composition of the soils can be used as an indirect geologic mapping method. This is of particular importance in the project area where most parts of the rock units are overlain by soils and alluvium. The boundaries and extent of these rock units are therefore difficult to define.

5.1.1 Sampling

East-West traverses on a besemap of 1:25,000 were used to plot the distribution of the sample points with a spacing of one sample per kilometer. This was however reduced to 500m and 250m in areas of suspected gold related structures especially in the phyllites.

The choice of the sampling plan with east-west traverses (figure 7) was based on:-

SAMPLING PLAN FOR GEOCHEMICAL SOIL SURVEY

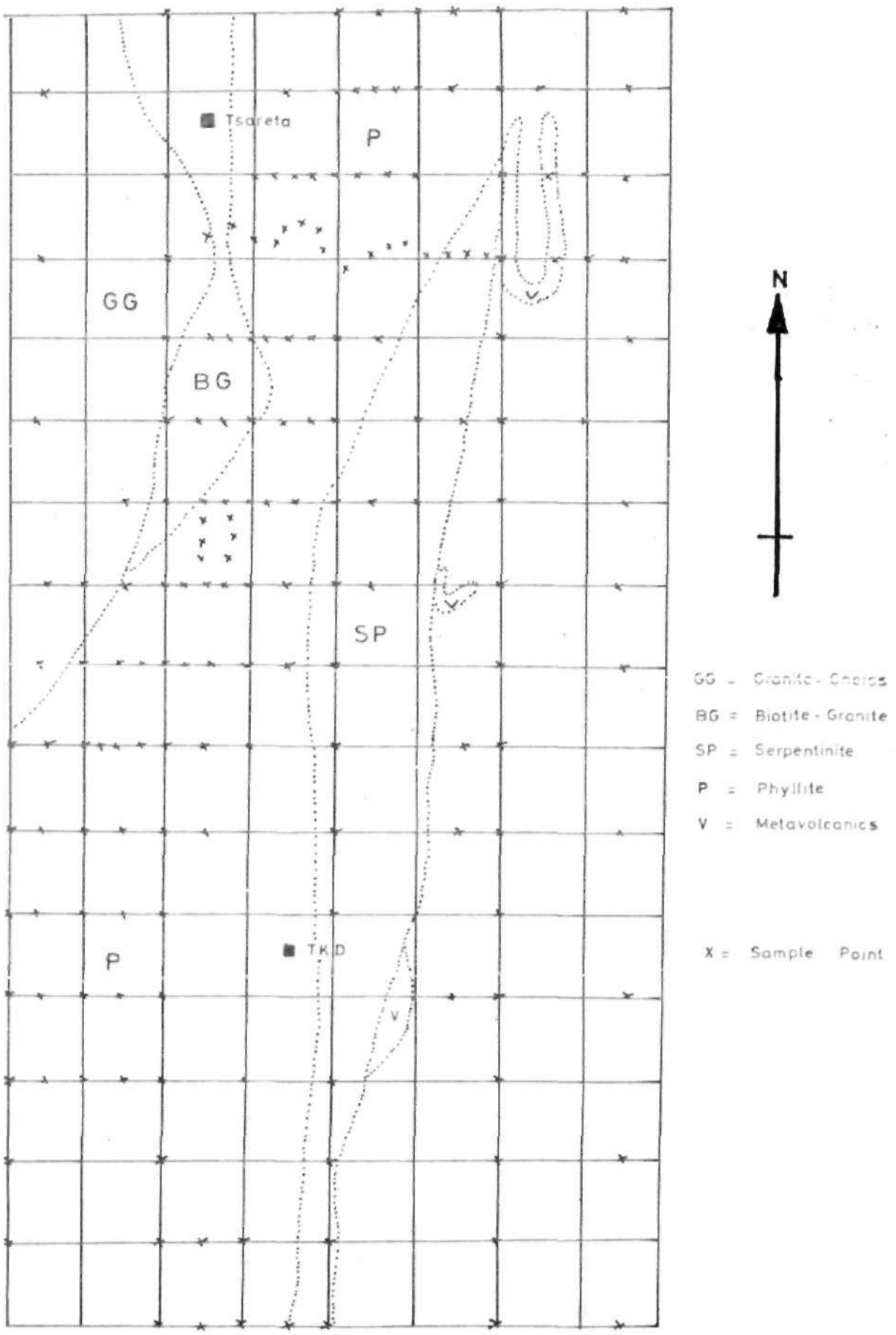


Fig. 7

(a) previous mining which indicated that gold is associated with quartz veins which are located in the phyllites. Their trend of emplacement coincides with a NNE-SSW trending regional linearment (Shearzone) recognized first by McCurry (1978) and

(b) the pattern of emplacement of the variety of rock types in the project area which also coincides with the plus or minus north-south regional trend.

Prior to the sampling, a soil orientation survey was carried out during which two horizons of the soil profile were be recognized: the A and the B horizons. The A horizon is porous, dark grey to light-grey and has a high content of organic matter. The B-horizon is reddish-brown, massive and maybe concretionary. The depth of occurence of the B-horizon varies with lithology and topography. This could be distinguished clearly from the A-horizon mostly in areas underlain by phyllites. However, this was not always the case in soils overlying serpentinite and along "fadama." This maybe due to its greater depth of occurence. The B-horizon, whenever present, was always the target for sampling whereas areas covered by "Fadama" were not sampled.

A hand auger with a core length of 100cm was used both for the orientation survey and the detailed

sampling. This was driven down to a depth of at least 60cm and the B-horizon, wherever present, was separated from the A and preserved in a polythene bag. The lower part of the soil collected with the auger was sampled in places where the soil was dark throughout and the B-horizon not clearly recognized.

A total of 182 samples were collected including the 23 samples from the orientation survey. More than $\frac{2}{3}$ of the samples are located in the phyllites as shown in the sampling plan in figure 7 .

5.1.2 Sample Preparation

Most of the samples collected were wet and some existed in the form of lumps. They were therefore dried at a temperature of about 105°C in an oven. These were then disaggregated in a porcelain mortar with a pestle. They were then sieved through a brass screen of 200 mesh (75μ). The - 75μ fraction was preserved in glass and plastic sample bottles for further treatment (extraction and analysis).

5.1.3 Extraction Methods

Two methods were used to extract the elements from the samples: Cold extraction, Cx, and hot extraction, Hx. The aim of the cold extraction was to study the variation of the loosely adsorbed elements in the soils.

(a) Cold Extraction

The extraction procedure was carried out in accordance with the extraction method described in the Perkin Elmer manual for atomic absorption determination for loosely adsorbed cations in soils.

The extraction solution consisted of 1 molar HCl and molar H_2SO_4 mixed in a ratio of 2:1.

2 grams of the minus 200 mesh fraction was weighed into a conical flask and 20ml of extraction solution added and shaken mechanically for one hour. This was filtered through a Whatman filter paper and the extract made up to 50ml with the extraction solution and stored in a platic bottle.

(b) Hot Extraction

In this method the extraction solution was made by mixing one part of concentrated hydrochloric acid with ten parts of distilled water.

As in the cold extraction, 2 grams of the minus 200 mesh fraction was weighed into a conical flask and 20ml of the extraction solution added. This was then heated in a sandbath for one hour. The solution was then filtered and the extract made up to 50ml and stored also in plastic bottles.

5.1.4 Chemical Analysis of the Samples

A Perkin Elmer atomic absorption spectrometer was used for the analysis of the samples in the Department of Geology, A.B.U., Zaria.

The reliability of the results was cross-checked by repeating the analysis for selected elements using another Perkin Elmer A.A.S. (model 410) at the University of Jos. Samples were analysed for eleven elements: Ca, Fe, Mg, Mn and Zn from the cold extraction, and Ag, Co, Cr, Cu, Ni, and Pb from the hot extraction.

An air-acetylene flame was used for all analyses. The elements content in the samples was estimated by comparing the absorbance with that of a standard prepared from a stock solution of known concentration.

Distilled water was used as reference with a zero absorbance. Routine checks, using the standard, were carried out after every 10 samples so that background variation (noise) could be controlled.

Aliquots from the hot extraction method generally gave higher element values than for the cold extraction method, but their relative contents remained essentially similar.

5.2 EVALUATION OF GEOCHEMICAL DATA

The analytical data are tabulated and presented in Appendix 1. A summary of the range, and average values of the elements distribution in the soil samples is given in Table 5:1.

Table 5:1 Range and Mean of the Elements in the Soil Samples

Element	Range in ppm	Mean in ppm
Silver	1.2 - 30.0	1.1
Lead	3.3 - 64.2	3.6
Zinc	2.8 - 31.3	5.3
Copper	1.7 - 100.0	10.0
Chromium	4.0 - 314.0	18.0
Nickel	2.9 - 326.6	8.6
Cobalt	3.7 - 175.0	15.0
Manganese	5.7 -1543.0	120.0
Iron	120.0 -3161.0	620.0
Magnesium	12.5 -2625.0	200.0
Calcium	4.8 - 833.0	72.0

The relatively low average values for Fe, Mg, and Ca are due to the cold extraction method used. This does not affect their relative content in the samples. However Ag, Co, Cr, Cu, Ni, Pb and Zn still show a lower average value than Fe, Mg, Mn and Ca.

Histograms and cummulative frequencies were plotted to enable a clearer understanding of the pattern

of variation and distribution of the elements. These are presented in Appendix 2 and 3.

The histograms, Appendix 2, show that the low values of the elements dominate i.e they have a higher frequency. They therefore do not show a normal distribution and are positively skewed to the right. Their cummulative curves, Appendix 3, on a logarithmic scale show straight lines for the distribution of Fe, Co, Pb, and Ni and two or more populations for the other elements. The Cr, Mn, Ca, Ag, and Mg cummulative curves show two population whereas that of Cu has a mixed population character i.e three different curves (see 5.3.1).

Certain parameters were extracted from the cummulative curves. These include the geometrical mean, $\bar{X}$, at the 50th percentile, and the standard deviation at the 84th percentile. These parameters were used for the selection of the background, the threshold and the anomalous element content in the soil samples. According to Siegel (1974), it is common in geochemical prospecting to select as the background the value that corresponds to $\bar{X} + 1S$, the threshold the values that fall between $\bar{X} + 1S$ and $\bar{X} + 2S$, while all values $> \bar{X} + 2S$ are anomalous. With exception of silver, chromium and nickel (see 5.3) this criteria was applied with the values rounded up for all the other elements.

A brief summary of the parameters for each specific element is presented in Table 5.2. These parameters were used for plotting distribution pattern of the elements in the maps Figures 6 to 13.

Table 5·2 Geochemical Parameters

Element	X + 1S	X + 2S	Back ground	Threshold or Subanomalous	Anomalous
Silver	3.6	10.5	3.6	3.6 - 10.0	10*
Lead	13.5	60.0	13.0	13 - 60	60
Zinc	10.0	15.2	10	10 - 15	15
Copper	19.0	41.0	19	19 - 40	40
Chromium	33.0	55.0	60	60 - 79	79*
Nickel	25.5	52.0	50	50 - 70	70*
Cobalt	38.0	69.0	38	38 - 69	69
Manganese	290.0	620.0	300	300 -600	600
Iron	1030.0	1680.0	1000	1000 -1500	1500
Magnesium	460.0	820.0	450	450 - 800	800
Calcium	220.0	370.0	200	200 -350	350

*Criteria used to select anomaly is different from other elements.

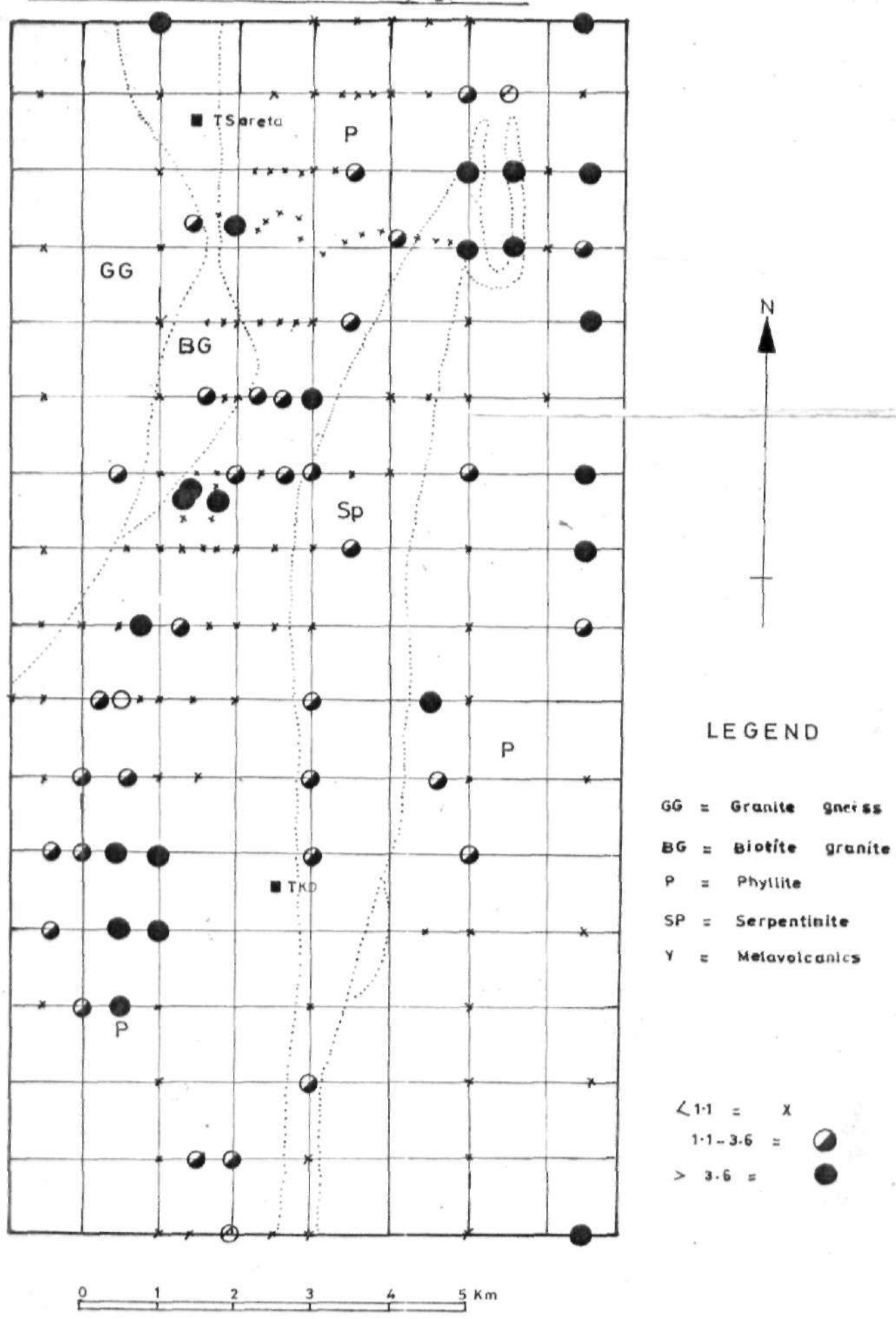
5.2.1 Patterns of Distribution of Elements: Geochemical Maps

(a) Silver (Ag). See Figure 8

Anomalous silver content, with 3.6ppm and above, exist over areas underlain by phyllites, about 1km West of Tungan Kudaku village and also around the old Zurgurfa II working pit.

Another area of anomalous silver content exists over the metavolcanic body in the north-eastern part of the area.

DISTRIBUTION OF SILVER (Ag)/ Hx



LEGEND

GG = Granite gneiss

BG = Biotite granite

P = Phyllite

SP = Serpentinite

Y = Metavolcanics

< 1·1 = X

1·1 – 3·6 =

> 3·6 =

Fig. 8

The volcanic rocks maybe the source of the silver in the soil. A few threshold (subanomalous) to anomalous values are randomly distributed in the north-west and south-east area.

Generally, the area underlain by granite-gneiss, biotite-granite and serpentinite are characterized by low silver values.

Considering the area as a whole, the anomalous silver content appears to be aligned in a NE - SW direction.

(b) Lead (Pb) - See Figure 9

All the threshold and anomalous values, with 13 - 60 ppm and above 60ppm respectively, occur only in areas underlain by phyllites and granite-gneiss. In the phyllites, they occur both to the east and to the west of the serpentinite body.

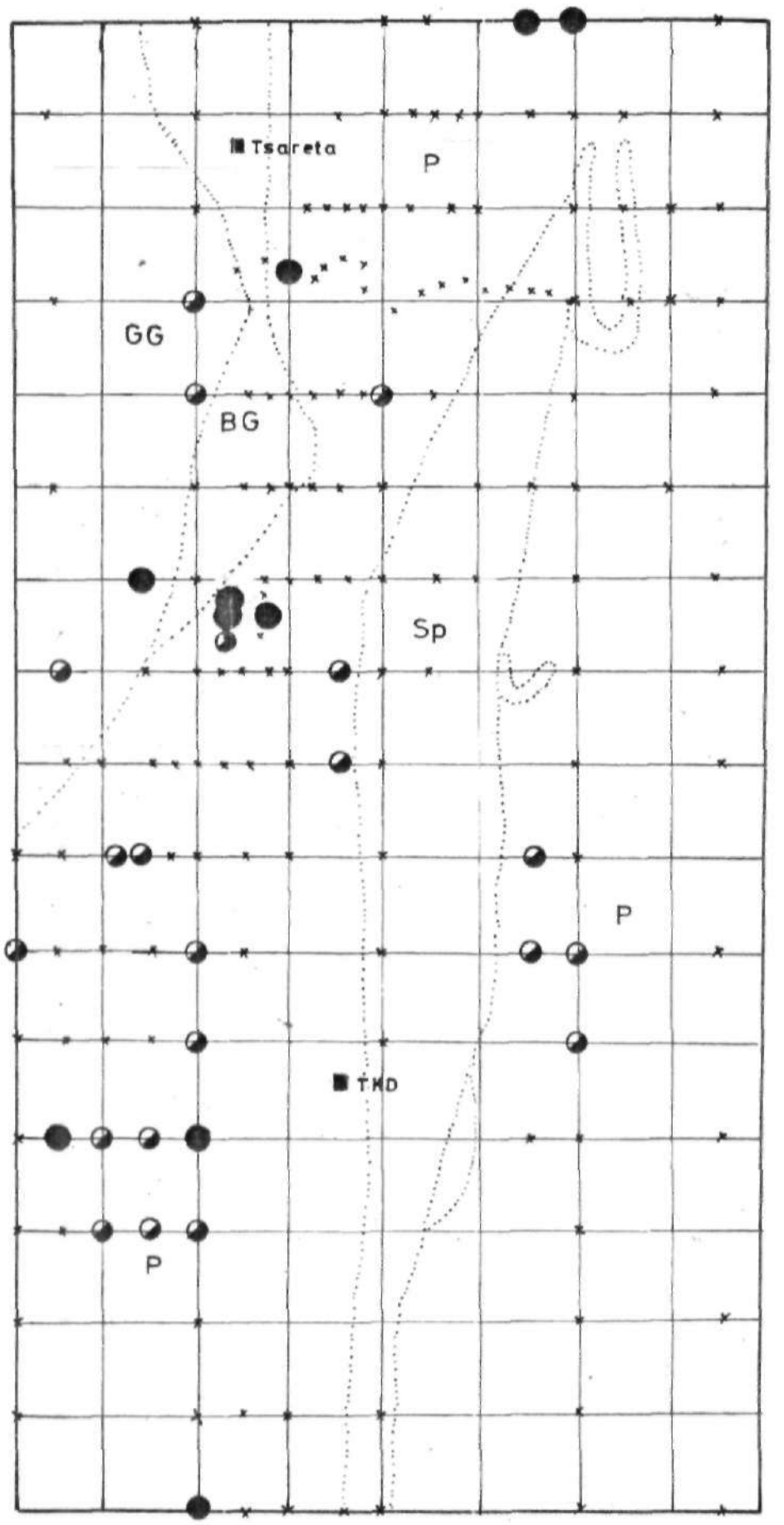
The presence of lead anomalies can be related to the occurence of visible galena at the old gold workings in Dumi I and Zurzurfa II.

In the south-western part of the area, the geochemical anomaly for lead coincides with that of silver.

There are no anomalous lead values in the biotite granite, metavolvanic and the serpentinite body.

The general pattern of distribution of the lead anomalies coincides with that of silver with a N-S to NE-SW direction or trend.

DISTRIBUTION OF LEAD (Pb) / Hx



LEGEND

GG = Granite gneiss

BG = Biotite granite

P = Phyllite

SP = Serpentinite

V = Metavolcanics

< 13 = X

13 – 60 = ◪

> 60 = ●

Fig.9

(c) Zinc (Zn) - See Figure 10

Anomalous zinc values above 15ppm exist in the soils overlying the metavolvanic body in the north-eastern part of the area. Threshold values i.e values between 10 and 15 ppm and anomalous values are distributed in the other rock types. There are no anomalis in the serpentinite body.

Most of the threshold and anomalous values occur in the northern part of the mapped area. These anomalous zinc values coincide with those of silver especially in soils overlying the metavolvanics.

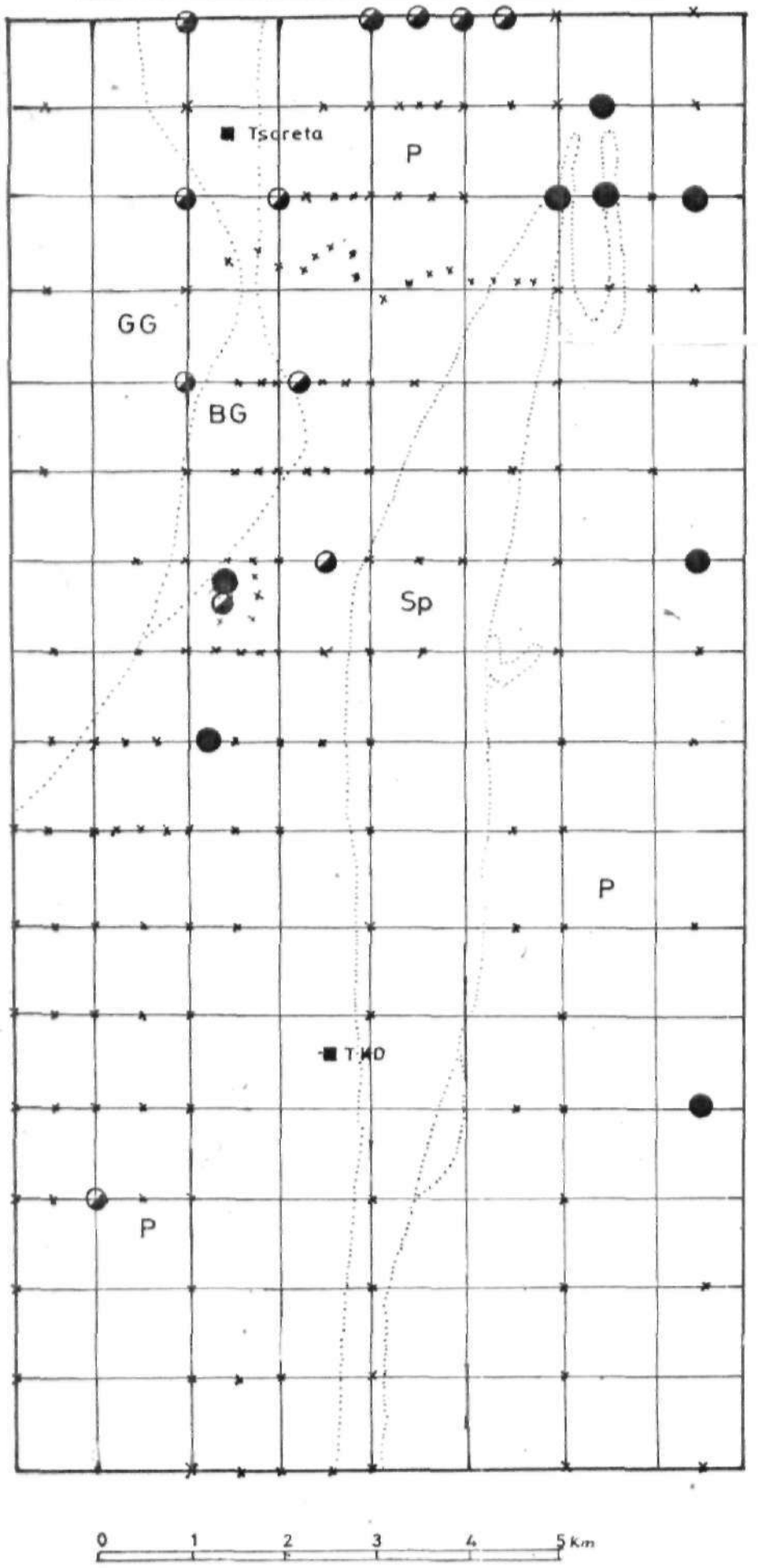
The general absence of anomalous zinc values in the south maybe related to its moderately high mobility along drainage. Most of the anomalous zinc values however fall within the NE-SW zone with high lead and silver values.

(d) Copper (Cu) - See Figure 11

Anomalous copper values above 40ppm have been registered mostly in the phyllites (east and west of the serpentinite body) and in the metavolvanics. These are absent in the granite-gneiss, biotite-granite, and in most parts of the serpentinite body.

The cummulative curve of copper shows three curves (lines) or mixed populations. The upper part of the curve could be attributed to the relatively very high copper values in soils overlying the

DISTRIBUTION OF ZINC (Zn) / Cx



LEGEND

GG = Granite gneiss

BG = Biotite granite

P = Phyllite

SP = Serpentinite

V = Metavolcanics

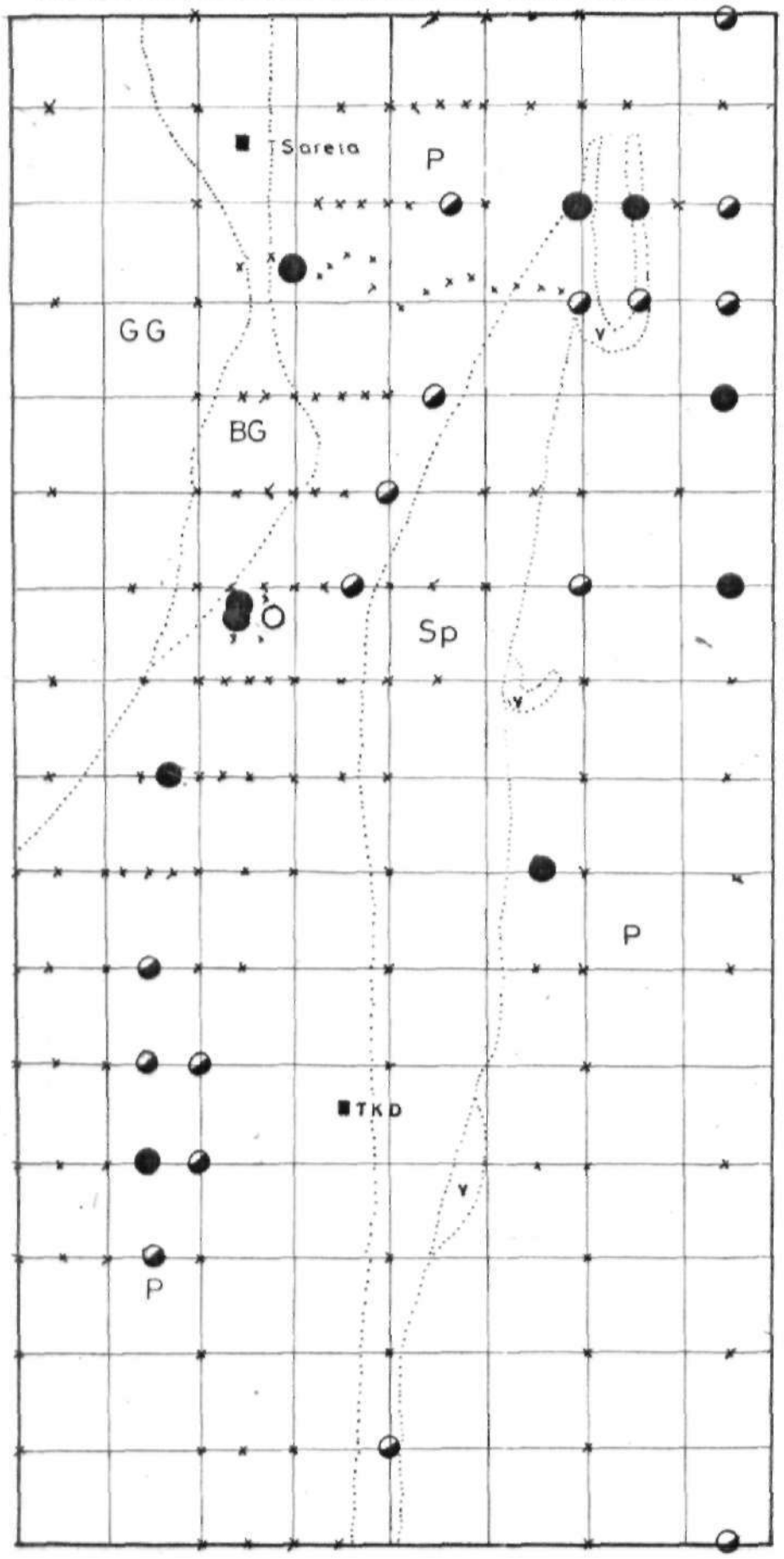
< 10 = X

10 - 15 =

> 15 =

Fig.10

DISTRIBUTION OF COPPER (Cu) / Hx





LEGEND

GG = Granite gneiss

BG = Biotite granite

P = Phyllite

SP = Serpentinite

V = Metavolcnics

< 19 = X

19 - 40 =

740 =

0 1 2 3 4 5 Km

Fig.11

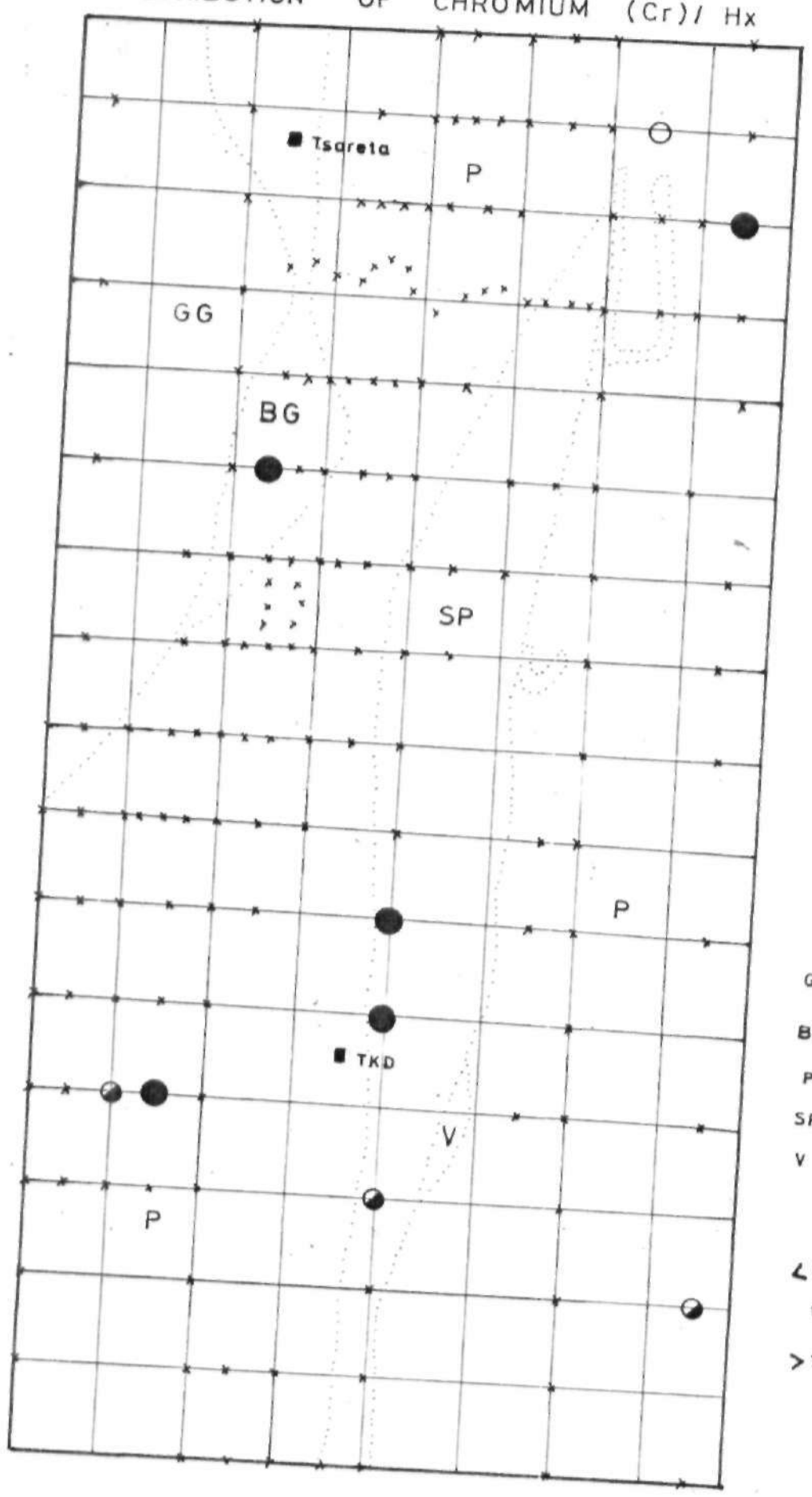
metavolvanics and the old gold working at Zurzurfa II. Dominant copper anomalies have been registered in those areas with copper values above 60 ppm. The lower part of the curve can be related to copper values in the phyllites and other rock types whereby the anomalous content originate solely in soil samples from areas underlain by phyllites.

The general distribution of the copper has a NE - SW trend with the serpentinite body cutting through the anomalous zone.

(e) Chromium (Cr) - See Figure 12

The distribution of chromium (see cummulative curve) shows a weak mixed population. The low density sampling in the ultramafic and mafic rocks compared to the phyllites could be responsible for the inability to clearly separate their respective chromium values statistically. A close examination of the analytical data however shows that there are few extremely high chromium values in the ultramafic rocks. This can actually be separated from the relatively high values in the phyllites if the minimum anomalous value is put at X + 3S i.e 79ppm. The use of this criteria to delimit the anomalous values shows that all the chromium anomalies are in the range of 79 - 314ppm (Figure 12) and occur only in the serpentinite and the biotite - granite.

DISTRIBUTION OF CHROMIUM (Cr)/ Hx





LEGEND

GG = Granite gneiss

BG = Biotite granite

P = Phyllite

SP = Serpentinite

V = Metavolcanis

< 60 =

60 79 =

> 79 =

Fig 12

These anomalous values only occur in soils close to serpentinite outcrops. The chromium values diminish rapidly with increasing overburden on the serpentinite.

The low chromium values north of the main serpentinite outcrops and those in the phyllites represent the 4 - 79 range.

The distribution of the chromium anomalies shows a north-south trend within the serpentinite.

(f) Nickel (Ni) - See Figure 13

An examination of the analytical data for nickel shows that all the extremely high values between 150 and 327 ppm occur in the serpentinite body. These could not clearly be separated from the lower values between 2.9 and 60 ppm which also occur in the serpentinite body with thick overburden and other rock types. The failure to do so could also be due to the low density sampling within the ultramafic and mafic rocks as was observed for chromium. The minimum anomalous nickel value was therefore read at the 97th percentile and is 70ppm.

All the anomalous values fall within the ultramafic body in soils not far from outcroping serpentinite. The other rock types are characterized by nickel values in the lower range (2.9 - 70ppm).

The distribution of the anomalous values show a north-south trend in the serpentinite body.

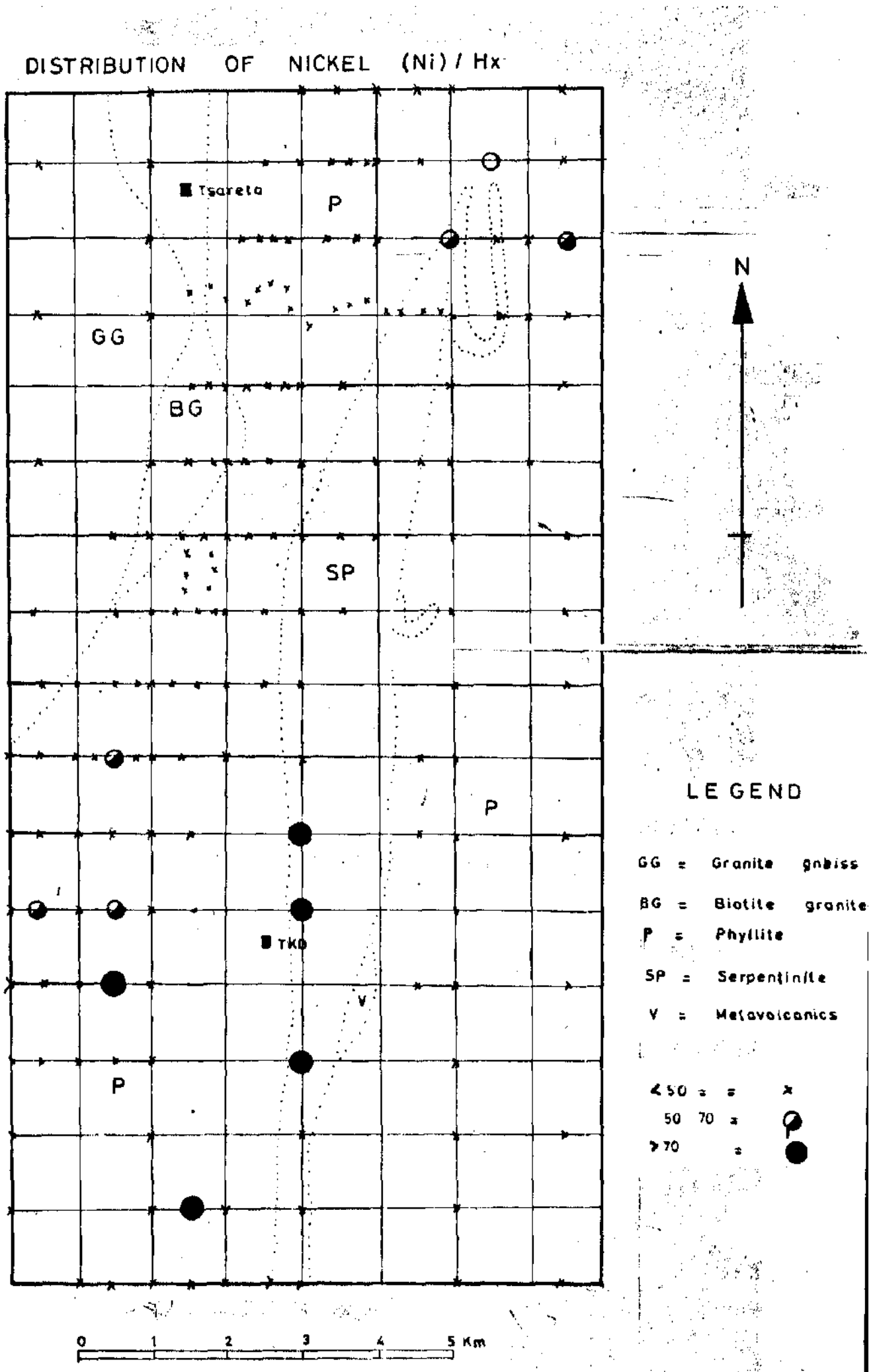

DISTRIBUTION OF NICKEL (Ni) / Hx
Tsareta
P
GG
BG
SP
P
TKB
V
P
N
0 1 2 3 4 5 Km
LE GEND
GG = Granite gneiss
BG = Biotite granite
P = Phyllite
SP = Serpentinite
V = Metavolcanics
< 50 = =
50 70 =
> 70 =

Fig. 13

(g) Cobalt (Co) - See Figure 14

Most of the anomalous cobalt values above 69ppm occur in the phyllites (east and west of the serpentinite body). A few subanomalous (threshold) to anomalous values occur in the metavolvanics and the serpentinite.

Low cobalt values occur in the south-east, north, and north-western part of the project area especially those underlain by granite-gneiss and biotite-granite.

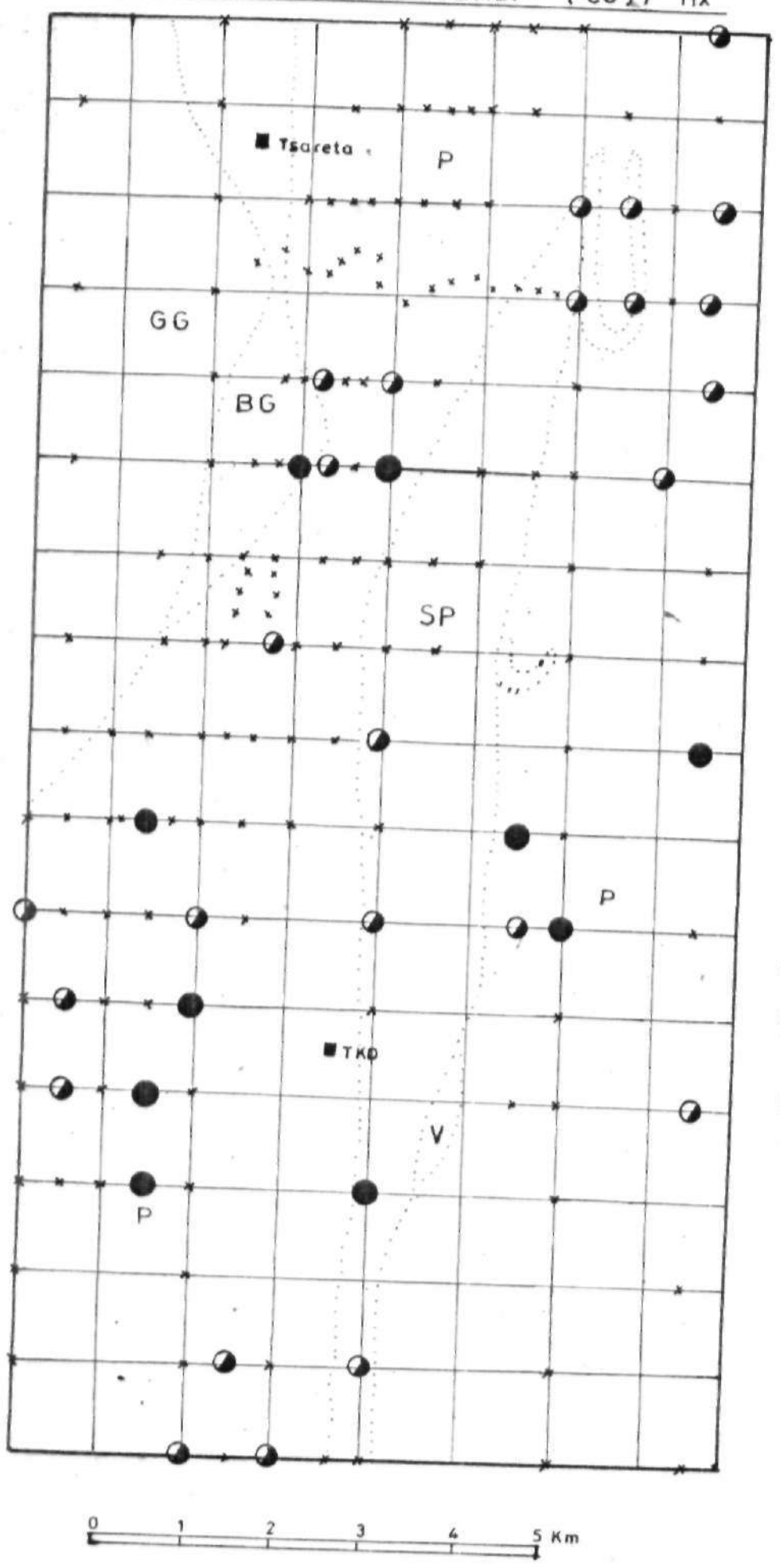
The distribution of the cobalt anomalies have a NE - SW trend which corresponds to that of silver and copper.

(h) Manganese (Mn) - See Figure 15

Most of the threshold and anomalous values of manganese (360- 600 ppm and above 600ppm respectively) occur in areas underlain by phyllites east and west of the serpentinite body, and in the biotite-granite. Most of the anomalies occur in a narrow zone consisting of phyllites east of the serpentinite body with a NE - SW trend.

The granite-gneiss, serpentinite and the metavolvanic body (in the north east) are characterized

DISTRIBUTION OF COBALT (Co) / Hx



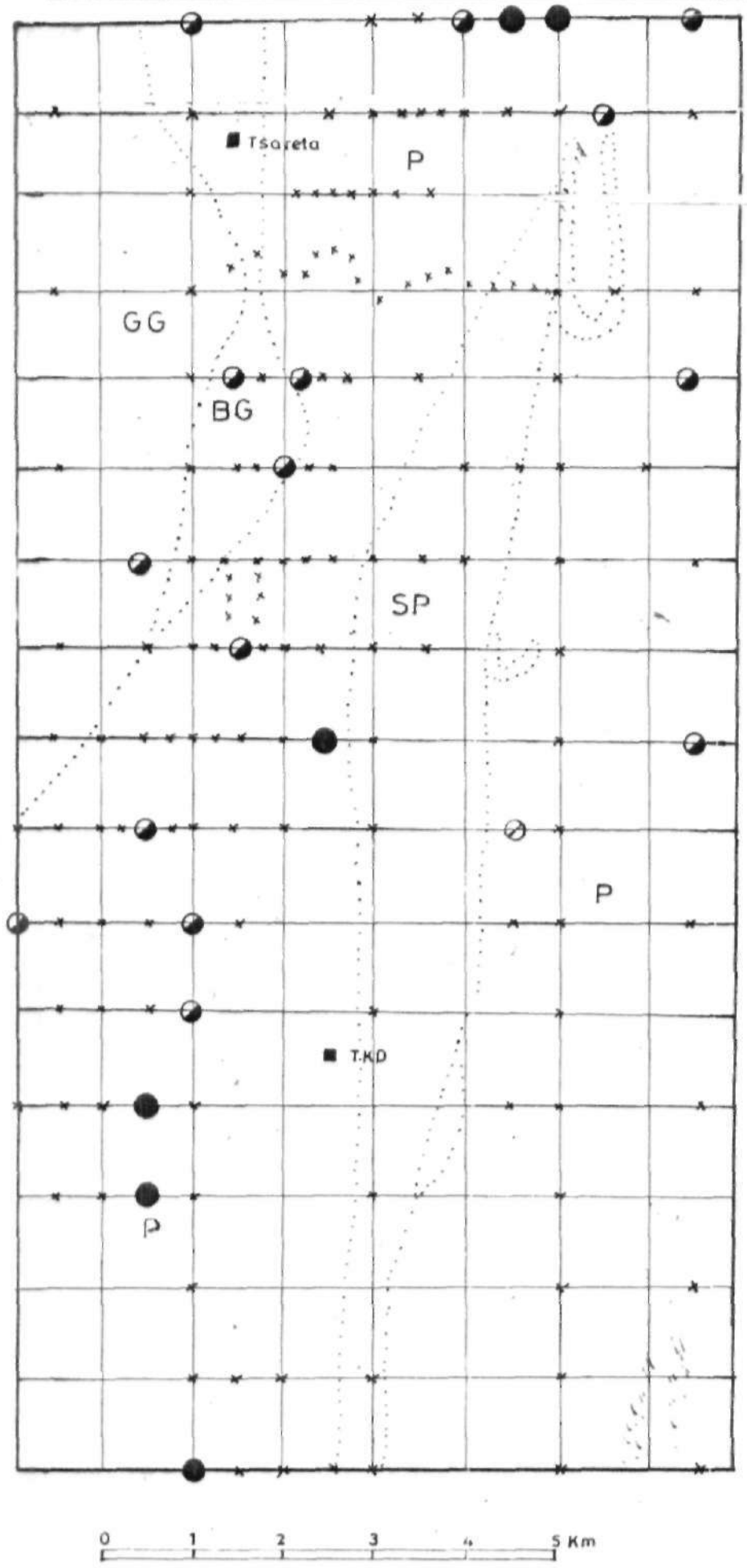
LEGEND

GG = Granite gneiss
BG = Biotite granite
P = Phyllite
SP = Serpentinite
V = Metavolcanics

< 38 = X
38 - 69 =
> 69 =

Fig.14

DISTRIBUTION OF MANGANESE (Mn) / Cx



LEGEND

GG = Granite gneiss

BG = Biotite granite

P = Phyllite

SP = Serpentinite

V = Metavolcanics

< 300 = X

300 – 600 =

> 600 =

Fig.15

by low manganese values.

The anomalous zone has a weak NE-SW trend.

(i) Iron (Fe) - See Figure 16

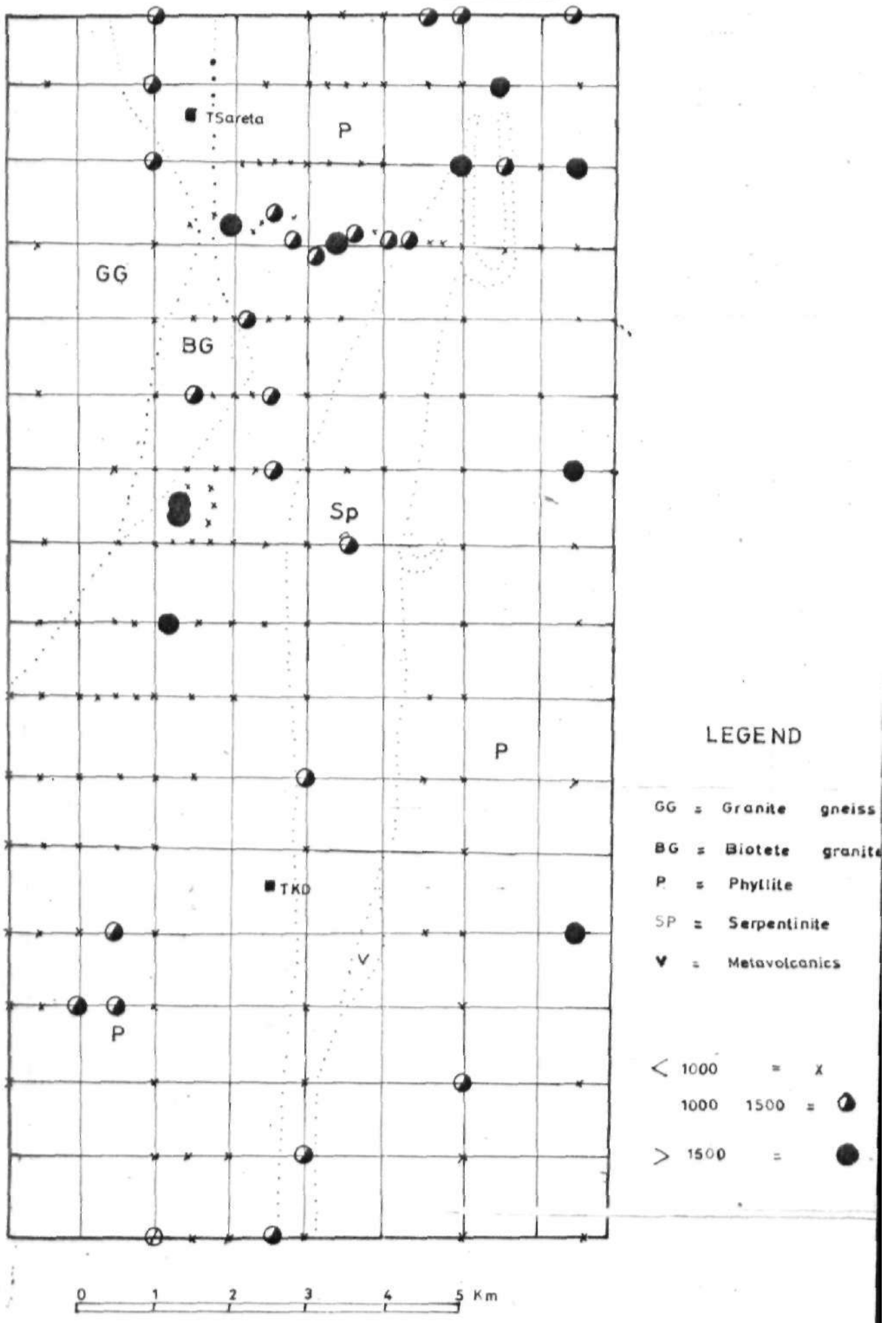
There is no clearly defined anomalous zone for iron in the project area. The only weakly discernable anomalous area occurs in the soils underlain by the metavolvanic body in the north-eastern part of the project area.

It is surprising that the serpentinite has low iron values. This is because ultramafic rocks are known to be rich in iron. Furthermore, in this area, visible chromite in the serpentinite is associated with magnetite and ilmenite.

A few subanomalous and anomalous values of iron are randomly distributed in the phyllites, granite-gneiss and biotite-granite. The highest value, 3161ppm, occurs in phyllites and this is considered to be due to concentration of iron near the surface.

The unexpectedly low iron values in the area may be related to a combination of sampling and analytical factors. Generally, areas underlain by serpentinite have deep and very dark soils which may be an indication that the iron-rich horizon of the soil was never reached by the hand auger.

DISTRIBUTION OF IRON (Fe) / Cx



Fig,16

(j) Magnesium (Mg) - See Figure 17

Anomalous magnesium values of 800ppm and above occur in soils overlying the serpentinite body, the metavolvanics and the phyllites whereby some of the anomalous values east of the serpentinite body could be as a result of buried metavolcanics. A few subanomalous values also occur with biotite-granite.

Most of the anomalous (above 800ppm) to subanomalous (between 450 and 800 ppm) magnesium values tend to conform with the N - NNE trend of the serpentinite body thus reflecting the high magnesium content of the ultramafic rocks.

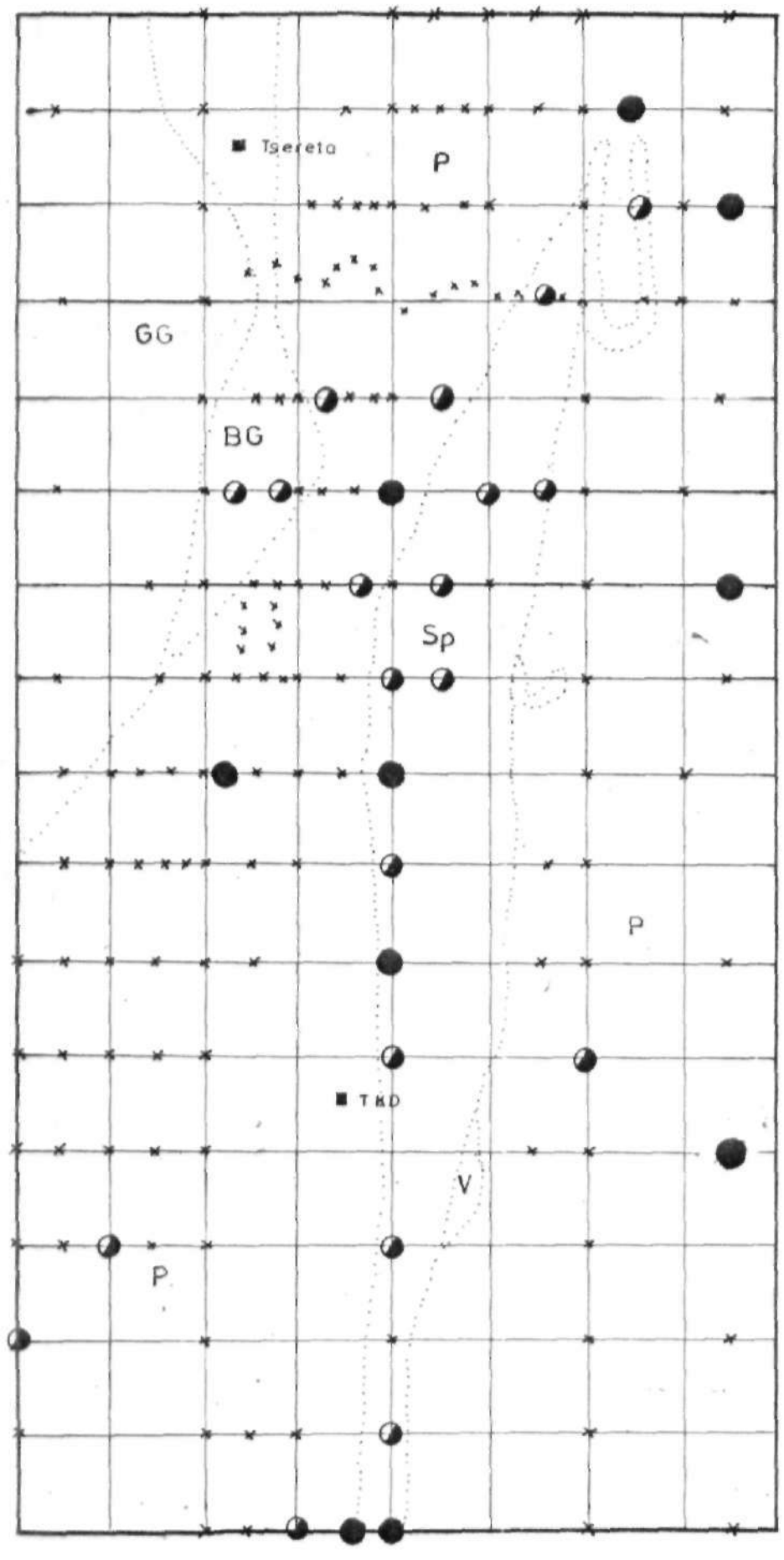
Low magnesium values were registered in the soils overlying the north-western part of the project area especially soils overlying the granite-gneiss.

(k) Calcium (Ca) - See Figure 18

Most of the subanomalous to anomalous calcium values, with 200 - 350 ppm and above 350 ppm respectively, occur in soils overlying the serpentinite, the metavolcanics and the biotite-granite mostly at the contact areas of these rock units. Thus the anomalous values can be grouped into two: those that conform with the serpentinite body and the second group with the biotite-granite.

Low calcium content occurs in the phyllites and in the granite-gneiss.

DISTRIBUTION OF MAGNESIUM (Mg) / Cx



GG = Granite gneiss

BG = Biotete granite

P = Phyllite

SP = Serpentinite

V = Metavolcanics

< 450 = X

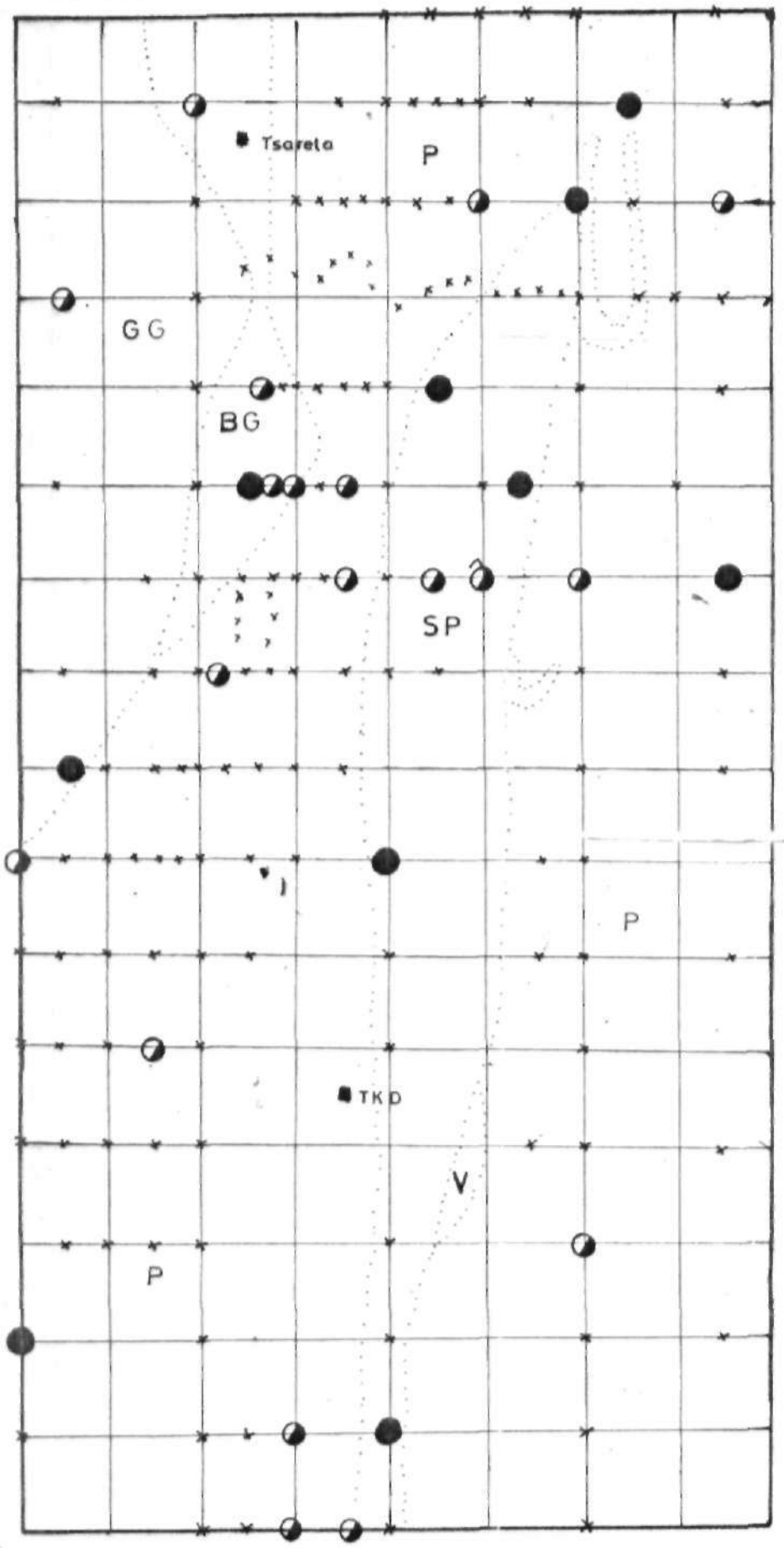
450 - 500 =

> 800 =

0 1 2 3 4 5 Km

Fig.17

DISTRIBUTION OF CALCIUM (Ca) Cx



LEGEND

GG = Granite gneiss

BG = Biotite granite

P = Phyllite

SP = Serpentinite

V = Metavolcanics

< 200 = X

200 - 350

> 350 =

Fig.18

5.2.2 Element Association

The geochemical maps show some variation in the element distribution. For example, the anomalous zones of some of the elements tends to conform into a NE - SW orientation, while others reflect the variation in the chemical composition of the bedrock.

In order to clearly group together those elements which are related to the NE - SW trend and those that can be associated to the variation of the chemical composition of the bedrock, a correlation analysis was carried out.

The Pearson Product Moment correlation analysis was put into use as described by Davis (1973) and Marshal (1970) using the SPSS package in the Iya Abubakar Computer Centre, A.B.U., Zaria. The degree of relationship between a pair of elements or two groups of values is denoted by the correlation coefficient, P.(Siegel 1974). The value of the coefficient ranges from -1, through 0 and up to +1 whereby lack of a relationship is indicated by zero. Perfect correlation has a value of +1, while a perfectly invariant relationship has a value of -1. The correlation matrix is presented in Table 5:3.

For the evaluation, the value of the correlation coefficient and its error of estimation were taken into consideration. The matrix shows that all the

CORRELATION MATRIX

		Ag	Ca	Co	Cr	Cu	Fe	Mg	Mn	Ni	Pb	Zn
Ag	P	1.000										
	S	0.001										
Ca	P	0.1084	1.000									
	S	0.073	0.001									
Co	P	0.3462	0.0106	1.000								
	S	0.001	0.444	0.001								
Cr	P	0.1479	0.0646	0.3679	1.000							
	S	0.023	0.193	0.001	0.001							
Cu	P	0.02374	0.0093	0.553	0.0142	1.000						
	S	0.001	0.450	0.229	0.424	0.001						
Fe	P	0.4392	0.2804	0.2760	0.1315	0.0234	1.000					
	S	0.001	0.001	0.001	0.038	0.377	0.001					
Mg	P	0.1114	0.4860	0.0933	0.3888	0.0469	0.5594	1.000				
	S	0.067	0.001	0.105	0.001	0.265	0.001	0.001				
Mn	P	0.2953	0.0410	0.4203	0.0266	-0.0045	0.5068	-0.0072	1.000			
	S	0.001	0.291	0.001	0.361	0.476	0.001	0.461	0.001			
Ni	P	0.1671	0.0573	0.4737	0.7011	0.0551	0.1815	0.3587	0.1043	1.000		
	S	0.012	0.221	0.001	0.001	0.0230	0.007	0.001	0.081	0.001		
Pb	P	0.6236	0.0365	0.0110	0.0402	0.1151	0.1983	-0.0575	0.3472	-0170	1.000	
	S	0.001	0.312	0.442	0.295	0.061	0.004	0.220	0.001	0.410	0.001	
Zn	P	0.3356	0.1635	0.0350	0.0242	0.226	0.3740	0.3345	0.0518	0.0493	0.4846	1.000
	S	0.001	0.014	0.230	0.373	0.381	0.001	0.001	0.244	0.254	0.001	0.001

Table 5:3 P = Correlation coefficient S = Error of estimation

coefficients above 0.3 have a significance above 99%. However, the coefficients with this high significance were evaluated as follows;

P ≥ + 0.7 as very good

P < + 0.7 to ≥ + 0.45 as good

P < + 0.45 to ≥ 0.3 as fairly good.

The same applies to the negative correlation coeffients.

On this basis, Cr and Ni show very good correlation. Good correlation is shown by the following element pairs: Pb - Ag, Ca - Mg, Co - Ni, Fe - Mg, Fe - Mn, Pb - Zn; while fairly good correlation exists in Co - Ag, Fe - Ag, Ag - Zn, Co - Cr, Co - Mn, Cr - Mg, Fe - Zn, Mg - Ni, Mg - Zn, and Mn - Pb. Copper shows only a weak correlation with Ag and Pb. This, the author believes, can be attributed to the majority of the Pb and Ag values falling below the detection limit.

The correlation further shows that there is a clear association between certain element groups; for example, between Ag, Pb and Zn with P > 0.45 Copper could still be linked with this group because it shows its closest association, P = 0.24 and 0.12, with Ag and Pb respectively.

Most of the anomalies of these elements are distributed in the granite-gneiss, biotite-granite, phyllites and metavolvanics. No anomalous Cu, Zn, Ag, and

Pb content was registered in the serpentinite and diorite (with the exception of a few anomalous values.

Within areas underlain by metasedimentary and metavolcanic rocks, the four elements conform to a NE-SW zone which has been cut through by the serpentinite bod y.

Another dominant element group is that of Cr-Ni-Co, whose association can be attributed to their occurrence in mafic and ultramafic rocks(e.g. diorite, metavolcanic rocks and serpentinite) and biotite -granite. The Cr-Ni-Co association furthermore has good to fairly good correlation with magnesium which can be used to distinguish the rocks mentioned above from phyllites.

Biotite -granite can be distinguished from the mafic and ultramafic rocks by its lower magnesium content and relatively high calcium content in the overlying soils. This explains the good correlation of calcium to magnesium and not to any other element.

The geochemical maps show that cobalt is associated with iron and manganese in areas underlain biotite-granite and phyllite. However, a Fe-Mn-Co association is not reflected in the correlation matrix. This could be due to the generally very low values of cobalt compared to the much higher values of iron and manganese.

A brief summary of the element association in relation to the different types of bedrocks is presented in Table 5:4. This table indicates for example, that soils overlying serpentinite, metavolcanics, and diorites are characterized by high values of Mg, Ca, Cr, and Ni.

Presented also in Table 5:4 are some relative values which help to contrast between the different types of bedrock. As an example, the relative values of magnesium in ultramafic and mafic rocks range between 1.2-4.8 times the values found in biotite-granite. A comparison between calcium and magnesium values in biotite-granite shows that calcium is usually 0.5 - 1 times the values of magnesium.

Table 5:4. Element Association and Relative Contrast of Values in Relation to Bedrock.

Bedrock	Element Association	Relative Contrast
Serpentinite Metavolcanic and Diorites	High Mg,Ca, Cr and Ni	(mg) 1.2-4.8 $\frac{UM}{BG}$ and $\frac{M}{BG}$ 1.2-4.8
Biotite-granite	High Ca and Mn Moderately high Mg	$\frac{Ca}{Mg}$ 0.5-1.0
Phyllites	High Mn and Co Low Mg and Ca	$\frac{Mn}{Ca}$ 1.8-3.0
Granite-Gneiss	Generally low element content	

UM = ULTRAMAFIC ROCK
M = BASIC ROCK
BG = BIOTITE-GRANITE

CHAPTER 6

SUMMARY AND CONCLUSIONS

In the preceeding chapters, the geology and a preliminary geochemical soil survey of the Tsareta-Tungan Kudaku area were described and discussed. In this chapter, a summary of the discriptions and deductions is given.

The area mapped covers an total area of about 130 km^2 and comprises four major rock groups:

a. a granite-gneiss basement
b. low-grade metasedimentary and metavolcanic rocks.
c. a large NNE-SSW trending serpentinite body
d. a suite of igneous intrusives of probable Pan African age and referred to in Nigeria as the "Older Granites".

The granite-gneiss basement occupies about 15 km^2 in the north-western part of the area mapped. The predominant rock unit is granite-gneiss. Others are the granite-gneiss/biotite-granite contact rock, amphibotite, epidote-quartz-rock, and quartz-breccia.

The granite-gneiss is typically a fine-to medium-grained rock with a well developed foliation. This foliation has been deformed giving rise to folds shown in plate i. The rock can be described as a hornblende-gneiss.

Outcroping i a 10 - 20 wide zone at the south-eastern end of Tsareta ridge, and marking the contact between the granite-gneiss and biotite-granite, is a medium-grained equigranular felsic rock.

The granite-gneiss has been metamorphosed under amphibotite facies conditions and it is considered to be the oldest rock in this area. It is suggested that the granite-gneiss/biotite-granite contact rock represents thermal recrystalization of contact material.

Xenolithic blocks of amphibotite found in serpentinite are considered to be stoped material from the granite-gneiss-basement.

Epidote-quartz rock and quartz-breccia represent fault material which appear to mark the boundary between granite-gneiss and the metasediments.

Metasedimentary and metavolcanic rocks occupy the greater part of the area mapped. Phyllites constitute the predominant rocks in this group. Schists, slates, metaconglomerate, Dumi cataclastic rocks, metavolcanics and banded-iron formation, each occupies relatively much smaller areas.

The fine-grained pelitic rocks are considered to have been deposited on a relatively quiet-water environment on the granite-gneiss basement and subsequently metamorphosed to the greenschist facies. Field relations of the

metaconglomerate, metavolcanics and banded-iron formation suggest that these rocks were emplaced with the phyllites and metamorphosed at the same time.

A NNE-SSW trending serpentinite body cuts the metasediments. It is inferred that it also cuts the granite-gneiss basement. The serpentinite is composed essentially of antigorite and anthophyllite and in parts contains small concentrations of chromite.

Based on experimental evidence and discussions by many authors (Krauskofp 1967, Bar and Glaeser 1982, Nockols 1978, Hatch et al 1972) and the regional distribution of the Sado, Maikwanogga, and the Ribah serpentinite bodies, it is suggested that the serpentinite body in this area was tectonically emplaced as a relatively cold intrusion along a fault.

The group of intrusive rocks observed in this area are diorites, trachyandesite, hornblende-lamprophyre and biotite-granite. They are consided to be members of the Older Granites suite of Nigeria generally held to be of Pan African age. They are also considered to be the youngest rocks in this area. This is based on the fact that the diorites, tranchyandesite and hornblende lamprophyre all intrude the serpentinite body which was described above as cutting the metasediments. It is also observed that the biotite-granite intrusion has deformed a system of shear-zones

with which the serpentinite body is thought to be associated.

In the area mapped, three types of economic-mineral occurences were noted and these are gold, chromite and asbestos.

The orientation of old gold workings at Dumi and Zurzurfu suggest that gold was mined from north-south, steeply dipping quartz veins. These veins are mostly associated with shear zones. It is therefore suggested that gold mineralization in this area was structurally controlled. It is envisaged that gold was leached from the surrounding rocks, particularly the metavolcanics, during metamorphism (Boyle 1979). In this area, the biotite-granite is considered an improbable source of the gold, because:

a) - granites in general and in north-western Nigeria in particular are characterized by a paucity or total lack of gold deposit

b) - the biotite-granite intrusion in the area is younger than the shear zones and consequently post-mineralization.

However, heat from the intrusion might have mobilized mineralizing fluids.

From the spatial distribution of the old gold workings with shear zones, it is suggested that exploration for gold should focus on the shear zones.

Chromite occurs in the serpentinite as lens-shaped pods, 2 - 3 m long, and as disseminated grains. The mineralization can best be explained by magmatic segregation through gravity settling.

The potential for chromite occurence in this area can only be speculative, but the occurence of some chromite concentration and the size of the serpentinite body is encouraging. More work is needed to evaluate this.

Anthophyllite asbestos occurs mainly as slip-fibre asbestos in veins cutting serpentinite. In one locality, it occurs as cross-fibre asbestos with lenghts up to 2½ cm.

The mineralization can be related to the fracturing of the serpentinite body during the late stages of serpentinization.

A preliminary geochemical soil survey was undertaken of the area in order to ascertain whether a regional fault-silicified-crush ridge feature, recognized by McCurry (1978) and which is associated with old gold showings in this area, could be traced. Also investigated was the reflection of the underlying bedrock by the chemical composition of their weathered products.

The geochemical soil survey has shown from maps of element distribution that most of the anomalous values of Ag, Pb, Zn and Cu fall into a NE-SW trending zone

which approximately coincides with the regional fault-silicified/crush ridge of McCurry (1975).

The soil survey has also shown that soils in this area do bear an imprint of the underlying bedrock and can therefore be used as an indirect geologic mapping method. Thus, the Cr-Ni-Co-Mg association can be used to delimit the mafic and ultramafic rocks while the Fe-Mn-Co association characterizes the phyllites. Biotite-gneiss can be distinguished by relatively high values of magnesium (though not as high as in the mafic and ultramafic rocks) and also by relatively high calcium values. The granite-gneiss is characterized generally by low content of all the elements.

REFERENCES

Agyakwa, N. Y. 1979. Relationships between gold and manganese mineralization in the Birrimian of Ghana, West Africa. Geol Magazine Vol. 116 No. 5, pp 345-352. Cambridge University Press.

Ajibade, A. C., Geotectonic evolution of the Zungeru region, Nigeria. Unpublished Ph.D. Thesis. University College of Wales, Aberystwyth, 1980.

Annual Reports of the Department of Mines, Nigeria 1922 - 1968.

Bar, H. P., 1982. Evidence of late Pre-Cambrian submarine volcanism in the metasedimentary belts of NW-Nigeria. In Abstracts of the 18th Annual Conference of NMGS, Kaduna, 1982 pp 41 -42.

Bar, H. P. and Glaeser, R. 1982. The Mallam Tanko Serpentinite Late-Orogenic Ultramafic Intrusion in Pan-African Basement Complex of NW-Nigeria. In Pre-Cambrian Symposium of Nigeria.

Boyle, R. W., 1979. The geochemistry of gold and its deposits. Geological Survey of Canada. pp 395 - 428.

Clifford, T. N. 1970. The Structural framework of Africa. In African magmatism and tectonics edited by T. N. Clifford and I. G. Gass. Oliver and Boyd. Edinburg

Coleman, G. R. 1971. Petrologic and Geophysical nature of Serpentinites. Geol. Soc. Ame. Bulettin. Vol. 82 pp 897-918.

Davies, C. J., 1973. Statistics and Data Analysis in Geology. John Wiley and Sons, Inc. New York.

de Swardt, A. M. J., 1953. The geology of the country around Ilesha. Geological Survey of Nigeria, Bulletin No. 23.

Evans, A. M., 1980. An introduction to Ore-geology. Blackwell Scientific Publications, Oxford. pp 77-85.

Falconer, J. D., 1911. The geology and geography of Northern Nigeria. Geological Survey of Nigeria. Bulettin No. 1.

Fargher, M. N., 1961. The Pre-Cambrian geology of the 1:100,000 sheet No. 52 (Anka), Sokoto Province. Report of the Geological Survey of Nigeria, No. 1324. (Unpublished)

Egbuniwe, I. G., 1982. Geotectonic evolution of Maru Belt, N.W. Nigeria. Unpublished Ph.D. Thesis University College of Wales, Aberystwyth, 1982.

Grant, N. K., 1970. Geochronology of Pre-Cambrian basement rocks from Ibadan, South-Western Nigeria. Earth and Plan. Sci. Lett. 10, pp 29-38.

Grant, N. K., Hickman, M., Burkholder, F. R. and Powel, S. L., 1972. Kibaran metamorphic belt in the Pan-African domain of W. Africa. Nature Physc. Science 238, pp 90 - 91.

Harker, A., 1932. Metamorphism. A study of the Transformations of Rock-Masses. London. Methuen.

Hatch, F. H., Wells, A. K., and Wells, M.K., 1972. Petrology of igneous rocks, xiii edition. Thomas Murby and Co. 40 Museum Street, London, W.C.I.

Hess, H. H., 1955.Serperntinites, orogeny and epirogeny. In Crust of the Earth Symposium. Geol. Soc. Amer. Special paper. 62 (1955)

Holt, R.W.,The Geotectonic evolution of the Anka belt in the Pre-Cambrian basement complex of N.W. Nigeria. Unpublished Ph.D Thesis, Department of Earth Sciences, The Open University, Walton Hall Milton Keyness, MK 6AA, England. 1982

Keays, L.R. and Glasson, M.J. 1978. Gold mobilization during cleavage development in sedimentary rocks from auriferous slate belt of Central Victoria, Australia. Some important boundary conditions. Econ. Geol. Vol.73, pp 496-511.

Kennedy, W.Q., 1964. The structural differentiation of Africa in the Pan African (± 500 m.y.) tectonic episode. Res. Inst. for African Geology. 8th Annual Report, pp 48-49

Koln, R.S., 1982. The primary origin of gold in epigenetic gold deposits. Geochemical-metallogenetic problem discussed on the example of the granite-greenstone gold province of South Africa. Fortschr. Miner. Vol. 60 No. 2. pp 235-258.

Krauskopf, K. B., 1967. Introduction to Geochemistry. McGraw Hill, New York. p. 456.

Mann, A. G., 1982. Gold in granite rocks in Zimbabwe. Gold '82. International Symposium. Abstracts. Geologic Society of Zimbabwe, Harare. pp 30 - 31.

Marshall, 1970. Geostastistics in mineral exploration review. In: Proceedings of the second seminar on

geochemical processes pp 314-340.

McCurry, P., 1973. Geology of degree sheet 21, Zaria, Nigeria. Overseas Geological and Mineral Resources. No. 45. H.M.S.O., London.

McCurry, P., 1976. The geology of the Pre-Cambrian to Lower Paleozoic rocks of Northern Nigeria - A Review. In, Geology of Nigeria edited by C.A. Kogbe. pp 15-40. Elizabethan Publishing Co., Lagos.

McCurry, P., 1978. Geology of Sheet 19 (Zuru)., 20(Ghafe) and part of 9(Katsina), Nigeria. Overseas Geological and Mineral Resources.No. 53, H.M.S.O.

McCurry, P., and Wright J.B. 1977. Geochemistry of Calc-Alkaline volcanics in N.W. Nigeria and a possible suture zone. Earth and Planetary Science letters. 37 (1977) pp 90-96

Mikami, H.M. 1979. Chromite. In, industrial minerals and rocks. ed. by Lefond, J.S. pp 501-518.

Nicolas, A., 1969. Serpentinization d'une lherzolite-Bilan Chemique implication tectonique. Bull. Volcanol., Vol. 32 No. 3 pp 499-508.

Nockolds, S. R., 1978. Igneous Rocks. In, Petrology for Students by S.R. Nockolds, R.W. O'B.Knox, G.A. Chinner. pp 145-148.

Ogezi, A.E.O., 1979. Geochemistry and geochronology of basement rocks from North-Western Nigeria. Unpblished Ph.D. Thesis. University of Leeds.

Onyeagocha; A.C., 1979. The Mallam Tanko Serpentinite. Petrology and economic implications. Journal of Mining and Geology. NMGS Vol. 16, No.1 pp37-40.

Ramdohr, P., 1975. The Ore minerals and their intergrowth Akademic - Verlag , Berlin. pp 156-173.

Read, H.H., and Watson, J. 1975. Introduction to geology. Vol.2: Earth history Part 1, Early Stages of earth history. The Macmillan Press Ltd., London pp 97-123.

Russ, W., 1932. The Birnin-Gwari Goldfield. Annual Report of Geological Survey (Nigeria) for 1931.

Russ, W., 1957. The geology of parts of Niger, Zaria and Sokoto Provinces, with special reference to the occurrance of gold. Geological Survey of Nigeria. Bulletin No. 27.

Siegel, F.R., 1974. Applied geochemistry. A Wiley-inter-science publication. John Wiley and Sons. New-York, p 217.

Truswell, J.F., and Cope, R.N., 1963. The geology of parts of Niger and Zaria Provinces, Northern Nigeria. Explanation of 1:250,000 sheet No. 31. Geological Survey of Nigeria. Bulletin No. 29.

William, H.R. and William, R.A., 1977. Kimberlites and plate tectonic in West Africa; Nature, Vol. 270, pp507-508.

Woakes, M. and Bafor, B.E. 1982. Primary gold mineralization in Nigeria. Proceedings of International Symposium. Gold 1982.

Woakes, M., 1981. Basement Metallogeny of North Western Nigeria - Symposium on Precambrian of Nigeria, Kaduna (Proceedings in press).

Wyllies, P.J., 1971. The dynamic earths. John Willey and Sons, Inc., Canada, p 121.

APPENDIX 1

ANALYTICAL DATA

SAMPLE No.	Ag Hx	Ca Cx	Co Hx	Cr Hx	Cu Hx	Fe Cx	Mg Cx	Mn Cx	Ni Hx	Pb Hx	Zn Cx
T1	4.6	0.0	0.0	4.5	4.3	400.0	50.0	105.5	0.0	0.0	9.0
T2	0	43.2	0.0	4.5	6.0	533.3	62.5	132.6	0.0	0.0	4.0
T3	24.7	60.1	26.8	13.6	60.3	1900.0	75.0	153.5	0.0	1516.7	7.3
T4	0	132.2	6.7	9.0	5.2	466.7	250.0	76.2	0.0	0.0	6.2
T5	0	91.3	0.0	9.0	5.2	366.7	315.5	32.0	0.0	0.0	7.4
T6	0	103.4	11.2	9.0	5.2	1166.7	287.5	304.3	0.0	0.0	6.3
T7	0	134.6	15.6	9.0	7.8	666.7	362.5	173.9	0.0	6.8	12.5
T8	0	443.2	2.2	6.8	4.3	1083.3	312.5	239.1	7.8	0.0	12.5
T9	0	9.6	8.9	9.0	6.9	1333.3	50.0	22.8	11.7	0.0	6.6
T10	2.3	0.0	29.0	9.0	10.3	1750.0	350.0	934.8	3.9	0.0	12.1
T11	0	74.5	6.7	4.5	6.9	1116.7	342.1	206.5	15.6	0.0	7.5
T12	0	96.2	0.0	4.5	6.0	950.0	118.4	195.6	0.0	0.0	7.5
T13	4.6	57.7	22.3	6.5	10.3	1333.4	157.7	532.6	0.0	0.0	8.1
T14	0	153.8	22.3	6.8	6.0	1333.4	289.5	478.3	0.0	0.0	8.8
T15	0	414.8	15.6	9.0	6.0	766.7	592.2	109.8	0.0	0.0	6.9
T16	0	221.2	0.0	11.5	4.3	466.7	381.6	50.3	0.0	0.0	7.1
T17	2.3	192.3	4.5	20.5	11.2	1000.0	421.0	71.6	0.0	0.0	8.8
Z1	13.8	158.7	0.0	9.2	65.6	666.7	263.2	97.6	31.2	1163.6	86.7
Z2	30.0	86.2	4.5	13.9	91.4	1716.7	184.2	184.7	0.0	991.7	14.7
Z3	0	4.8	6.7	32.4	5.2	1700.0	131.6	630.4	0.0	0.0	7.5
Z4	0	125.0	2.2	4.6	10.5	400.0	407.9	97.8	7.8	16.7	7.1
Z5	4.0	108.2	15.6	13.9	21.6	600.0	289.5	206.5	7.8	83.3	5.3
Z6	0	55.3	4.5	13.5	12.1	683.3	223.7	130.4	3.9	6.8	8.8

SAMPLE No.	Ag	Ca	Co	Cr	Cu	Fe	Mg	Mn	Ni	Pb6	Zn
1	4.4	306.3	22.3	10.4	12.5	1033.3	375.0	357.0	11.7	16.7	11.3
2	0.0	62.5	4.5	6.3	9.6	333.3	200.0	76.2	0.0	0.0	13.6
3	0.0	100.0	8.9	4.5	5.7	200.0	162.5	71.6	15.6	0.0	12.2
4	0.0	43.8	31.3	10.4	8.7	883.3	150.0	428.6	11.7	3.3	11.3
5	0.0	43.8	15.6	16.7	8.7	1266.7	100.0	666.7	7.8	23.3	10.2
6	0.0	25.0	13.4	12.6	11.4	1533.3	87.5	1261.9	7.8	23.3	9.7
7	4.4	100.0	53.6	14.6	24.0	1233.3	137.5	500.0	15.0	0.0	7.9
8	0.0	25.0	0.0	4.2	7.7	200.0	75.0	39.6	0.0	3.3	6.8
9	0.0	627.8	8.9	8.4	7.7	1033.3	262.5	190.5	0.0	0.0	8.5
10	0.0	18.8	4.5	8.4	9.6	466.7	100.0	70.1	0.0	0.0	9.9
11	0.0	118.8	0.0	10.4	6.7	433.3	387.5	121.9	0.0	0.0	9.3
12	0.0	112.5	0.0	8.4	7.7	333.3	150.0	35.1	0.0	0.0	6.8
13	0.0	75.0	13.4	6.3	9.6	150.0	125.0	46.9	11.7	0.0	8.8
14	0.0	125.0	6.7	10.4	7.7	583.3	162.5	115.6	7.8	0.0	6.5
15	0.0	162.5	17.9	16.7	8.7	583.3	337.5	175.0	7.8	0.0	7.9
16	0.0	0.0	22.3	14.6	9.6	733.3	100.0	129.7	11.7	3.3	9.3
17	2.2	31.3	0.0	4.2	4.8	200.0	37.5	29.7	0.0	0.0	5.9
18	2.2	425.0	22.3	68.8	18.3	2533.3	2625.0	312.5	39.1	0.0	29.5
19	0.0	25.0	0.0	8.4	3.8	266.7	50.0	26.1	0.0	0.0	8.5
20	0.0	75.0	0.0	4.2	6.7	1200.0	137.5	262.5	7.8	0.0	10.2
21	0.0	59.5	4.4	14.6	3.8	333.3	212.5	120.2	0.0	0.0	11.6
22	0.0	11.9	4.4	10.4	4.8	350.0	125.0	91.3	0.0	0.0	6.5
23	0.0	35.7	8.8	8.4	4.8	683.3	150.0	104.2	0.0	0.0	4.3
24	0.0	0.0	4.4	8.4	3.8	416.7	25.0	16.0	0.0	0.0	7.4

SAMPLE No.	Ag Hx	Ca Cx	Co Hx	Cr Hx	Cu Hx	Fe Cx	Mg Cx	Mn Cx	Ni Hx	Pb Hx	Zn Cx
25	0.0	29.8	8.8	12.6	6.7	350.0	37.3	52.9	0.0	0.0	4.5
26	0.0	29.8	8.8	25.2	10.6	633.3	100.0	128.2	7.8	0.0	3.9
27	3.4	0.0	11.0	45.8	21.2	900.0	200.0	202.4	46.8	3.4	4.5
28	0.0	273.8	8.8	25.2	11.5	916.7	350.0	225.0	15.6	0.0	8.5
29	24.9	470.2	57.0	31.3	110.0	2583.7	222.5	166.7	58.3	0.0	18.2
30	15.9	119.0	48.2	39.6	67.3	1650.0	615.5	144.2	26.3	0.0	15.1
31	0.0	0.0	15.4	10.4	8.7	241.4	0.0	26.6	0.0	0.0	4.4
32	4.5	215.9	43.9	79.2	28.8	2068.9	1842.0	238.0	62.4	0.0	16.3
33	0.0	204.5	0.0	10.4	7.7	413.8	223.7	37.5	0.0	0.0	5.0
34	0.0	45.5	13.2	10.4	7.7	500.0	118.4	178.6	7.8	20.3	6.3
35	5.7	79.5	48.2	45.8	36.7	224.1	52.6	62.6	23.4	0.0	5.0
36	7.9	34.1	39.5	20.8	38.5	241.4	78.9	117.2	23.4	0.0	6.9
37	0.0	181.8	13.2	12.6	11.5	568.9	263.0	118.8	7.8	0.0	5.0
38	2.3	22.7	52.6	27.1	19.7	534.5	52.6	51.6	23.4	6.7	5.0
39	0.0	68.2	10.9	12.6	11.5	551.7	144.7	202.4	0.0	13.3	10.6
40	0.0	375.0	17.5	18.8	11.5	758.6	460.5	309.5	11.7	0.0	4.0
41	0.0	156.3	4.0	10.4	9.6	483.3	197.4	48.7	0.0	0.0	4.4
42	0.0	193.8	14.1	16.8	13.5	832.3	236.0	125.0	15.5	0.0	6.3
43	0.0	112.5	44.4	27.1	15.4	1466.7	710.5	302.5	29.2	0.0	10.0
44	0.0	62.5	20.2	35.4	7.7	333.3	184.2	45.5	8.3	0.0	6.3
45	0.0	50.0	30.2	27.1	10.6	366.7	131.6	118.5	16.7	3.6	5.6
46	0.0	25.0	48.4	25.2	15.5	650.0	118.4	186.0	8.3	35.7	5.3
47	2.4	362.5	20.2	33.3	19.1	916.7	513.2	120.1	8.3	0.0	9.4
48	0.0	156.3	8.1	20.8	15.4	533.3	131.6	68.2	42	0.0	8.1

SAMPLE No.	Ag Hx	Ca Cx	Co Hx	Cr Hx	Cu Hx	Fe Cx	Mg Cx	Mn Cx	Ni Hx	Pb Hx	Zn Hx
49	9.4	56.3	52.4	25.2	46.0	600.0	92.1	306.5	15.5	0.0	8.1
50	0.0	100.0	8.1	12.6	11.5	800.0	197.4	112.0	0.0	3.6	8.8
51	0.0	136.9	22.2	12.6	8.9	800.0	225.0	225.0	0.0	0.0	8.1
52	2.4	392.9	20.2	83.3	17.8	1000.0	725.5	125.0	29.2	0.0	9.4
53	0.0	273.8	4.0	6.8	7.1	733.0	550.0	250.0	0.0	0.0	7.4
54	0.0	241.7	78.6	22.9	8.9	733.0	212.5	325.0	24.9	0.0	7.5
55	1.2	23.8	42.3	45.8	12.3	933.3	262.5	153.8	33.3	0.0	6.3
56	1.2	261.9	16.1	22.9	16.0	1000.0	312.5	225.0	8.3	0.0	7.8
57	4.8	214.3	26.2	29.2	25.0	616.7	900.0	129.8	20.8	0.0	9.4
58	0.0	202.4	24.2	20.8	8.9	666.7	558.5	150.0	8.3	0.0	6.3
59	0.0	833.3	22.2	20.8	13.4	766.7	612.3	162.5	8.3	0.0	6.3
60	0.0	154.8	12.1	20.8	14.2	350.0	325.0	67.3	4.2	0.0	5.5
61	0.0	11.9	38.6	8.9	8.9	281.3	37.5	158.3	0.0	0.0	5.9
62	2.4	178.6	33.[illegible]	40.2	17.8	718.8	237.5	341.5	17.0	58.6	8.8
63	0.0	160.7	0.0	17.9	9.8	312.5	325.0	16.2	4.3	0.0	8.2
64	0.0	29.8	18.4	22.3	15.1	93.8	237.5	112.2	8.6	0.0	5.9
65	0.0	41.7	7.4	17.9	8.9	484.4	125.0	146.1	0.0	0.0	5.3
66	0.0	154.8	18.4	37.9	10.7	234.4	162.5	90.9	21.6	0.0	7.9
67	0.0	0.0	0.0	17.9	9.8	515.6	12.5	27.6	0.0	0.0	5.1
68	2.4	279.8	11.0	11.2	20.5	1406.3	550.0	81.2	12.9	0.0	14.4
69	2.4	23.8	14.8	15.6	16.0	296.9	175.0	79.5	12.9	0.0	4.5
70	0.0	303.6	18.4	13.4	11.6	578.1	450.0	219.5	4.3	0.0	5.7
71	0.0	250.0	20.2	24.6	13.4	578.1	412.5	135.7	8.6	0.0	5.7
72	3.5	285.7	14.7	26.8	21.4	500.0	187.5	108.9	4.3	0.0	3.9

SAMPLE No.	Ag	Ca	Co	Cr	Cu	Fe	Mg	Mn	Ni	Pb	Zn
73	11.8	369.0	23.9	31.3	51.8	3161.8	2625.0	215.9	25.9	0.0	31.3
74	0.0	101.2	12.9	13.4	8.0	640.6	150.0	181.8	0.0	23.3	5.4
75	0.0	142.9	0.0	11.2	4.5	468.8	175.0	42.2	0.0	0.0	3.4
76	0.0	202.4	3.7	15.6	6.2	466.7	337.5	105.4	4.3	0.0	2.8
77	0.0	315.5	12.9	20.1	7.1	343.8	337.5	35.7	8.6	0.0	4.5
78	0.0	172.6	29.4	15.6	8.9	812.5	237.3	306.8	4.3	6.7	3.9
79	0.0	23.8	51.5	26.8	10.7	500.0	200.0	150.0	21.6	6.7	3.4
80	0.0	0.0	22.4	15.6	8.9	703.1	12.5	193.2	0.0	3.3	2.8
81	0.0	35.7	24.3	15.8	9.8	655.2	125.0	166.7	12.9	10.0	5.0
82	0.0	178.6	11.2	8.9	8.9	602.4	550.0	85.0	0.0	0.0	4.3
83	2.7	119.0	18.7	22.3	17.8	1189.7	525.0	160.0	21.6	0.0	5.6
84	0.0	17.9	26.1	8.9	7.1	362.1	37.5	125.0	4.3	6.7	5.0
85	5.4	190.4	9.3	13.4	7.1	534.5	200.0	77.5	0.0	0.0	5.9
86	0.0	422.6	27.8	11.2	4.5	689.7	287.5	226.2	0.0	0.0	5.3
87	0.0	148.8	9.3	22.3	7.1	517.2	250.0	60.0	12.9	0.0	5.0
88	0.0	142.9	7.5	29.0	7.1	344.8	215.5	22.5	4.3	0.0	5.3
89	12.2	41.7	41.0	22.3	53.0	568.9	125.0	166.7	12.9	6.7	5.9
90	0.0	0.0	14.9	15.6	7.1	551.7	25.0	75.0	8.6	3.3	4.3
91	2.7	65.5	16.8	26.8	13.4	2116.7	850.0	100.5	34.5	6.7	18.1
92	0.0	53.6	0.0	4.5	5.3	366.7	100.0	27.2	0.0	0.0	5.6
93	0.0	0.0	0.0	6.7	8.9	483.3	25.0	125.0	0.0	6.7	5.0
94	0.0	59.5	18.7	20.1	10.7	966.6	175.0	682.9	25.9	26.7	5.6
95	0.0	154.8	39.2	24.6	6.2	483.3	937.5	48.8	17.2	0.0	4.3
96.	0.0	11.9	22.4	15.6	9.8	333.3	25.0	111.4	0.0	6.7	4.3

SAMPLE No.	Ag Hx	Ca Cx	Co Hx	Cr Hx	Cu Hx	Fe Cx	Mg Cx	Mn Cx	Ni Hx	Pb Hx	Zn Cx
97	3.0	172.6	70.9	11.2	12.7	783.3	150.0	329.3	8.6	20.0	5.6
98	0.0	214.3	3.7	8.9	6.2	400.0	225.0	60.9	0.0	0.0	5.9
99	0.0	0.0	13.1	13.4	10.7	216.7	37.5	97.6	4.3	6.7	5.9
100	0.0	95.2	7.5	22.3	9.8	600.0	150.0	121.9	8.6	0.0	6.9
101	1.5	41.7	25.4	33.5	12.1	362.1	75.0	102.2	12.9	13.3	3.8
102	3.2	0.0	105.9	17.8	17.2	965.5	50.0	500.0	51.6	43.2	5.6
103	0.0	59.5	12.7	22.4	7.8	344.8	150.0	34.1	8.6	0.0	5.0
104	0.0	41.7	4.2	13.4	6.0	482.8	150.0	23.8	0.0	0.0	3.8
105	0.0	0.0	4.2	6.7	12.9	379.3	0.0	5.7	0.0	0.0	4.3
106	0.0	0.0	10.6	15.6	8.6	172.4	25.0	23.8	0.0	0.0	4.3
107	3.2	452.4	19.1	33.5	15.5	913.8	550.0	96.6	17.2	0.0	5.6
108	14.3	53.8	84.7	32.5	46.6	724.1	87.5	476.2	30.0	23.3	5.0
109	0.0	5.9	8.4	15.6	6.9	327.6	137.5	53.9	0.0	0.0	4.6
110	0.0	65.5	48.7	35.7	11.2	862.1	125.0	559.5	8.6	13.3	5.3
111	0.0	0.0	27.5	11.2	8.6	232.1	13.2	47.6	0.0	3.3	5.7
112	1.5	22.7	25.4	46.9	12.9	410.7	39.5	95.2	17.2	10.0	5.3
113	3.2	22.7	12.7	35.6	20.7	357.1	13.2	83.3	8.6	6.7	6.0
114	0.0	0.0	50.8	17.8	10.3	946.4	92.1	392.9	17.2	23.3	9.1
115	0.0	0.0	0.0	4.5	5.2	303.6	0.0	0.0	0.0	0.0	5.3
116	3.2	102.3	52.9	314.7	17.2	1017.9	894.7	119.0	193.9	0.0	5.3
117	3.2	56.8	50.8	37.9	15.5	171.4	157.9	47.6	12.9	23.3	6.8
118	0.0	45.5	80.5	40.2	13.8	625.0	157.9	178.6	17.2	20.0	6.0
119	0.0	56.8	12.7	20.1	12.9	714.3	197.4	59.5	4.3	0.0	6.0
120	0.0	22.8	12.7	22.3	8.6	267.9	197.4	47.6	2.9	0.0	4.9

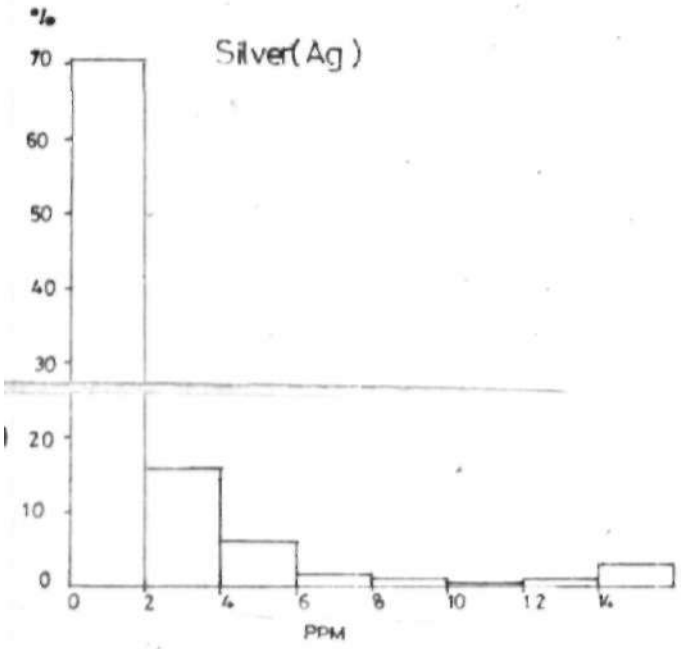
SAMPLE No.	Ag Hx	Ca Cx	Co Hx	Cr Hx	Cu Hx	Fe Cx	Mg Cx	Mn Cx	Ni Hx	Pb Hx	Zn Cx
121	3.2	96.6	34.1	29.0	16.1	250.0	421.1	57.6	52.4	3.4	6.6
122	3.2	22.8	22.7	33.5	13.4	166.7	26.4	23.3	24.2	6.7	3.9
123	7.9	228.0	13.6	37.9	27.7	833.3	421.1	49.0	64.5	6.7	7.2
124	9.5	166.7	131.8	37.9	32.1	900.0	144.7	430.2	40.3	37.2	5.9
125	3.2	178.6	29.5	252.2	17.9	120.0	1460.5	95.6	169.4	0.0	3.9
126	3.2	45.5	29.5	33.5	15.2	666.7	565.8	33.1	12.1	20.0	7.9
127	0.0	39.8	18.2	17.9	6.3	533.3	302.6	139.5	12.1	3.4	4.3
128	3.2	0.0	40.9	51.3	12.5	416.6	26.4	67.4	8.1	60.8	3.3
129	0.0	0.0	18.2	67.0	10.7	550.0	52.8	139.5	12.1	10.1	3.9
130	14.3	181.8	175.0	120.5	44.8	1516.7	421.1	860.5	116.9	50.7	5.6
131	4.8	0.0	27.3	51.3	20.6	576.9	26.4	186.0	16.2	64.2	3.7
132	0.0	96.6	13.6	15.6	10.7	692.3	236.8	68.6	12.1	0.0	4.1
133a	0.0	0.0	4.5	17.9	10.7	288.5	105.3	51.5	8.1	0.0	3.4
133b	0.0	26.7	38.6	58.0	11.6	2423.1	1289.5	162.8	40.3	0.0	15.5
134	0.0	56.8	13.6	8.9	7.2	538.5	144.7	313.9	4.0	0.0	4.1
*135	0.0	34.1	18.2	24.6	11.6	653.8	65.8	232.5	8.1	6.7	4.7
136	3.2	34.1	18.2	22.3	14.3	1000.0	631.6	40.4	8.1	13.3	10.8
137	4.8	102.2	86.4	22.3	21.5	1615.4	315.8	1093.0	40.3	40.0	4.7
138	0.0	0.0	13.6	24.6	9.0	903.8	39.5	104.7	12.1	10.1	4.7
139	0.0	51.1	72.7	75.9	9.0	807.7	736.8	279.1	326.6	0.0	5.4
140	0.0	272.0	22.7	22.5	14.3	461.5	197.4	197.7	12.1	3.7	4.1
141	0.0	386.4	4.7	8.9	3.3	685.2	710.5	10.0	12.5	6.7	4.4
142	0.0	96.6	18.9	17.8	8.3	481.5	289.5	125.0	16.2	3.4	4.4
143	1.5	198.9	9.5	17.8	13.3	740.7	381.6	62.5	16.2	0.0	4.7

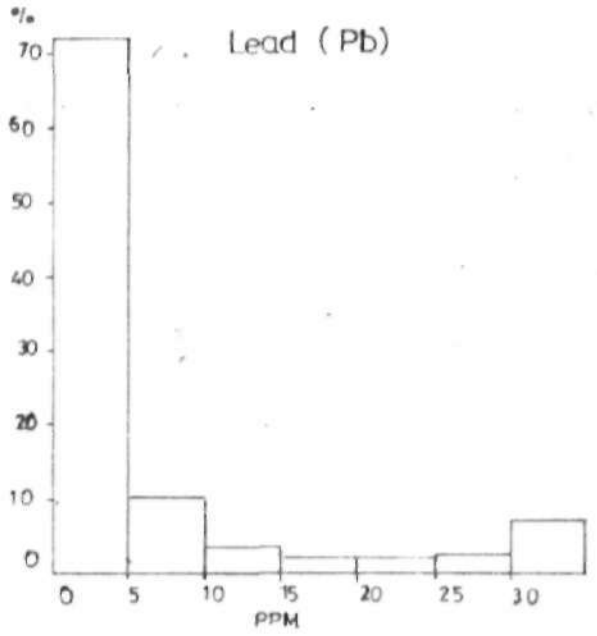
SAMPLE No.	Ag Hx	Ca Cx	Co Hx	Cr Hx	Cu Hx	Fe Cx	Mg Cx	Mn Cx	Ni Hx	Pb Hx	Zn Cx
144	0.0	28.4	16.5	17.8	10.0	1019.0	92.1	204.5	8.1	3.4	4.4
145	0.0	28.4	23.6	62.5	10.0	480.8	118.4	57.3	12.1	3.4	4.1
146	0.0	34.1	14.2	13.4	5.8	481.5	197.4	125.0	4.0	3.4	6.8
147	0.0	125.0	28.4	31.3	1.7	703.7	421.1	61.3	36.3	3.4	6.4
148	2.9	56.8	35.4	26.8	14.2	333.3	289.5	51.5	56.3	3.4	4.4
149	2.9	238.6	4.7	22.3	8.3	500.0	289.5	36.8	12.1	0.0	4.7
150	0.0	380.7	51.9	35.7	21.5	1203.0	486.8	34.1	36.3	0.0	5.7
151	0.0	28.4	18.9	17.8	9.2	156.3	26.4	68.8	8.1	0.0	3.5
152	0.0	22.7	51.9	22.3	13.4	1031.3	79.2	1011.4	32.4	78.8	4.8
153	0.0	107.9	0.0	8.9	6.7	359.4	210.5	35.0	4.0	0.0	4.5
154	2.9	332.9	35.4	11.2	12.5	609.4	539.5	193.2	20.2	6.7	6.3
155	0.0	301.1	18.9	26.8	15.8	1015.6	1026.3	90.0	40.3	0.0	7.3
156	0.0	79.5	11.8	26.8	14.2	562.5	631.5	100.0	20.2	0.0	3.5
157	0.0	187.5	16.5	17.8	13.4	453.0	250.0	78.8	8.1	0.0	3.1
158	5.0	232.9	21.2	51.3	24.2	718.8	263.2	96.3	12.1	0.0	4.2

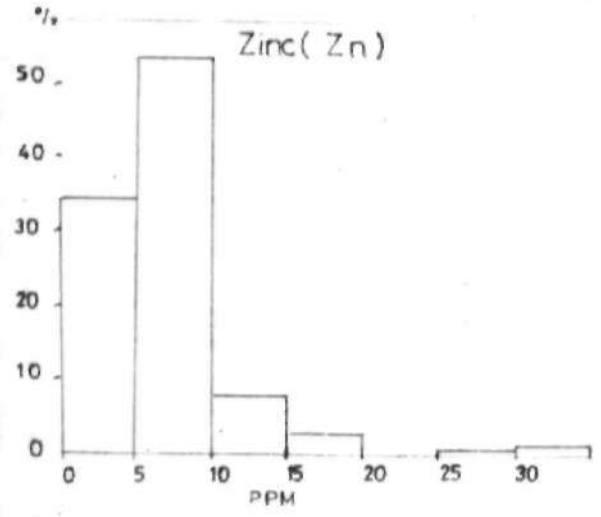
T = Samples taken along Tsareta/New Project road

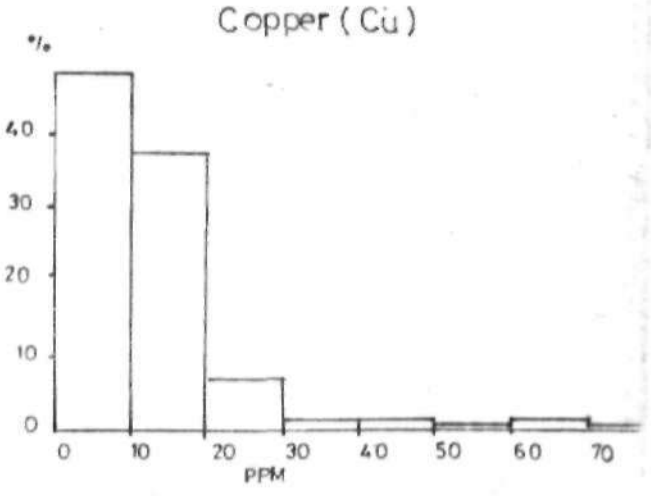
Z = Samples taken from Zurzurfa II

APPENDIX 2 HISTOGRAMS

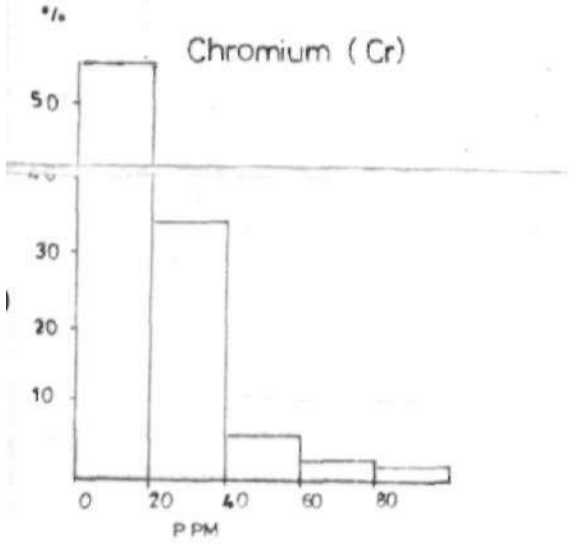


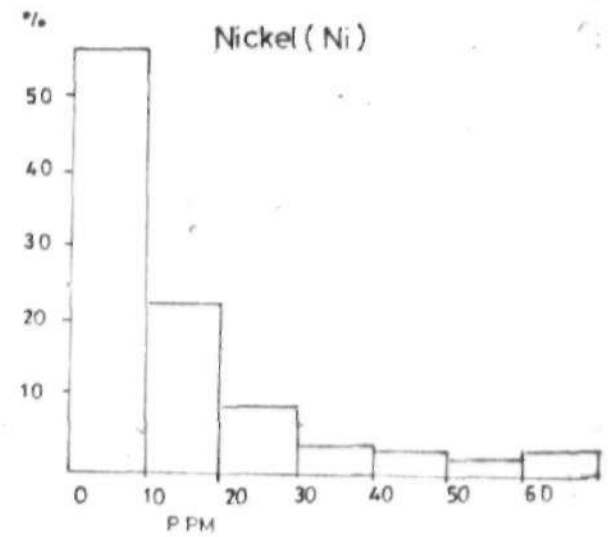


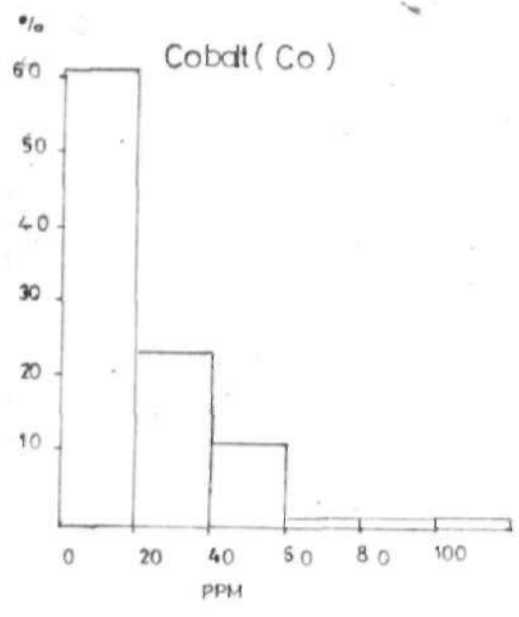


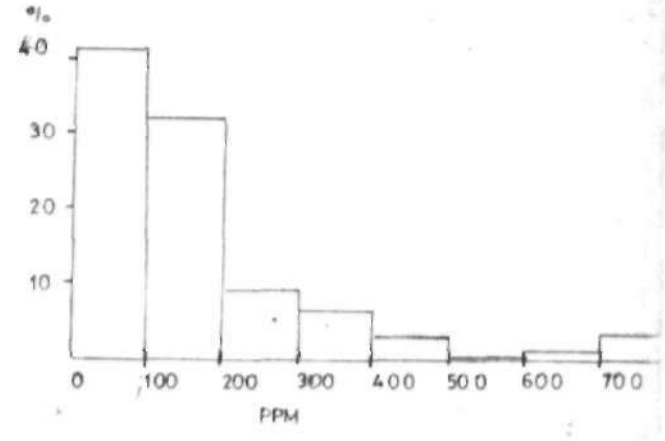


APPENDIX 2 HISTOGRAMS

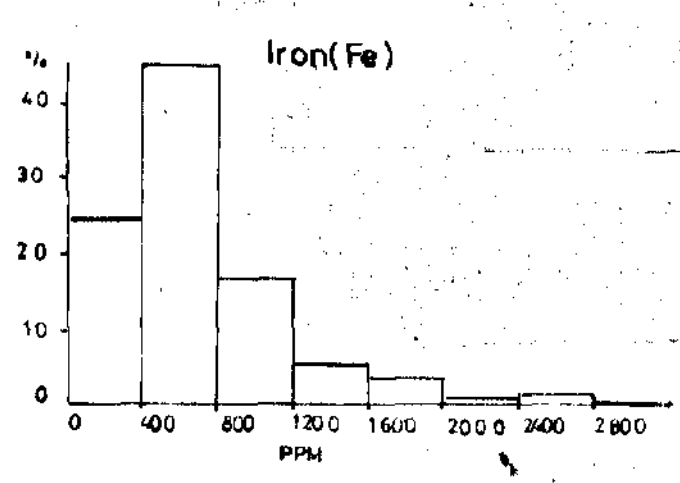


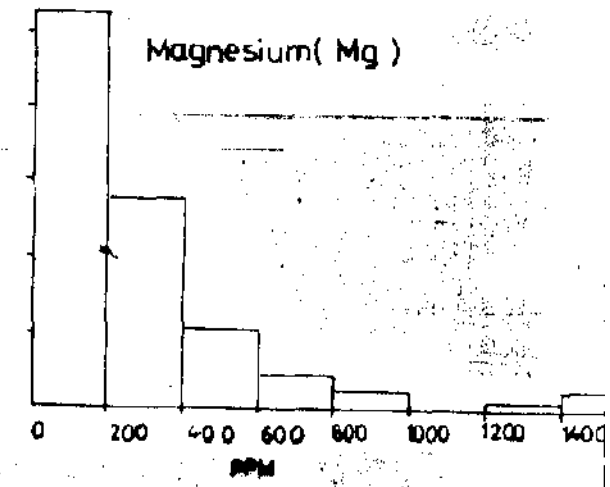


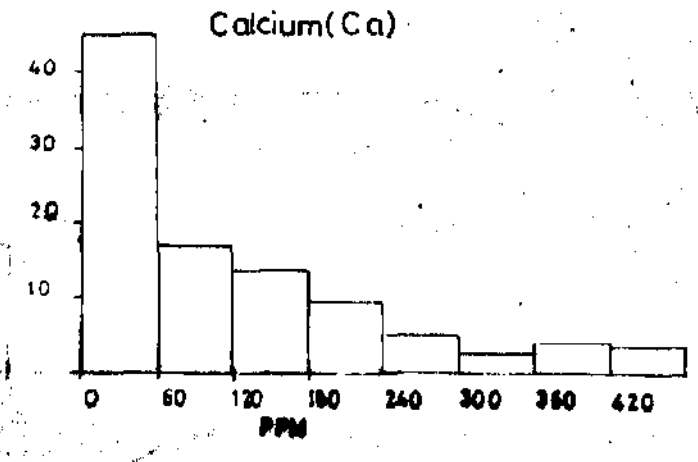




APPENDIX 2 HISTOGRAMS

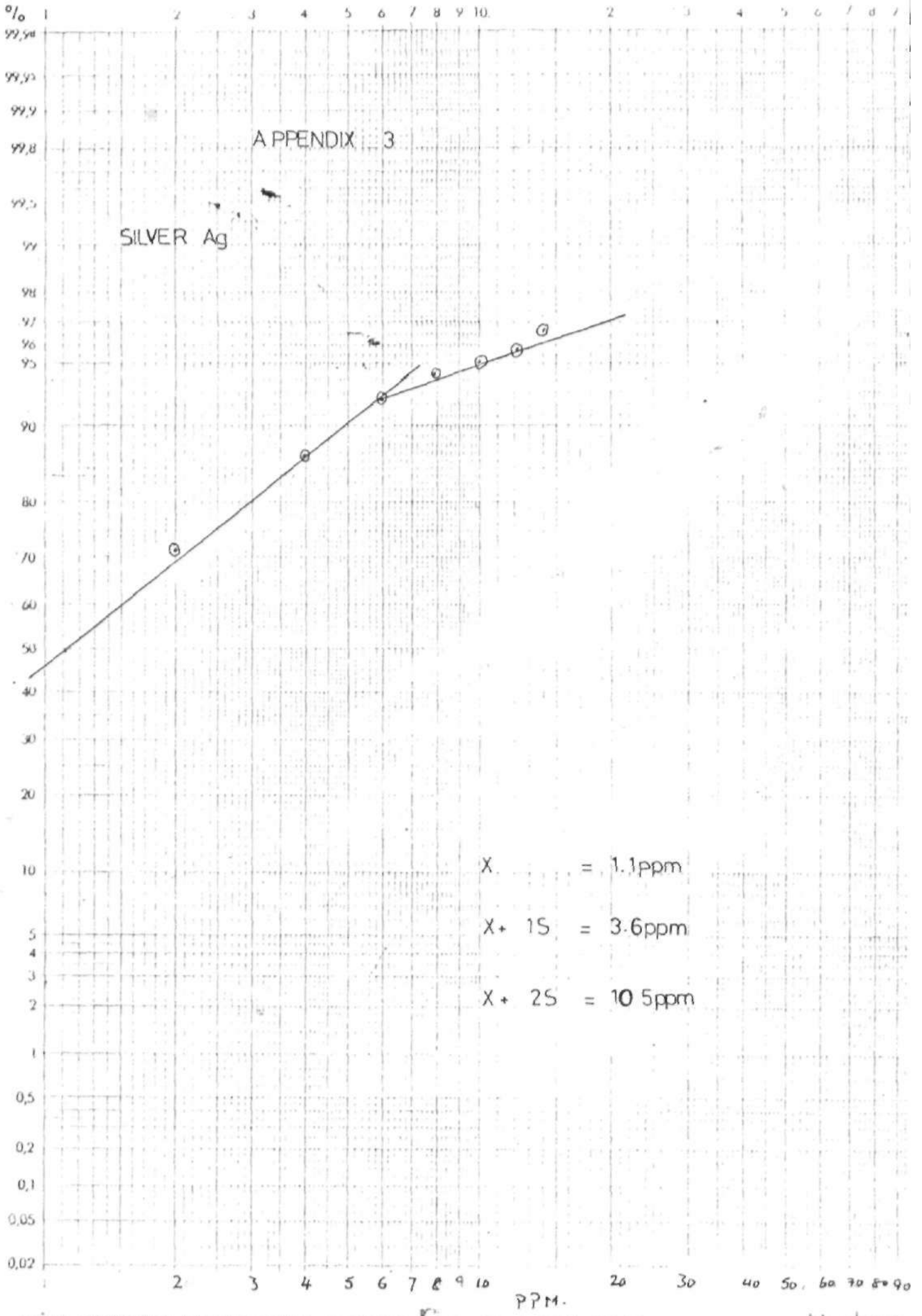






APPENDIX 3

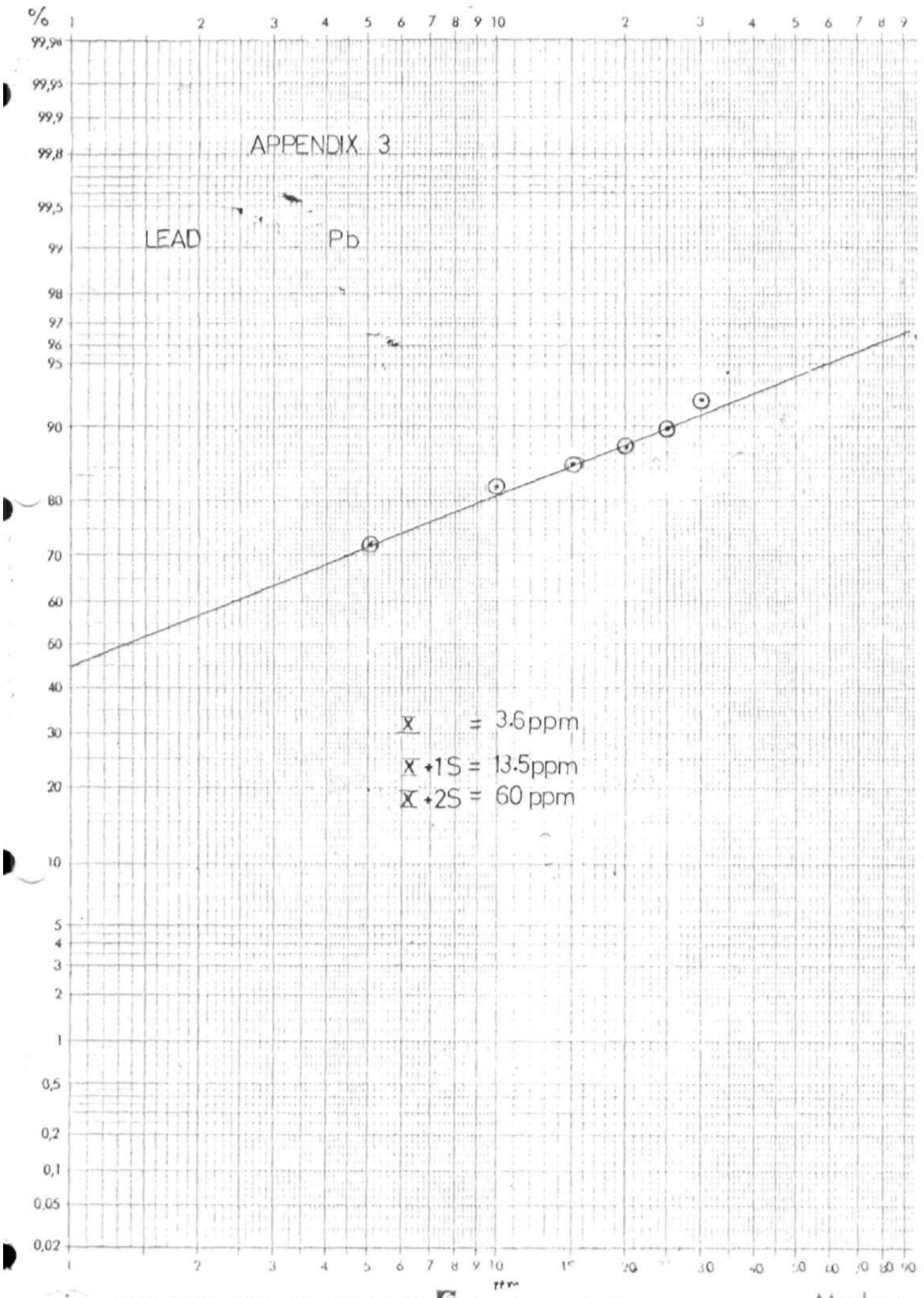
SILVER Ag



X = 1.1ppm

X + 1S = 3.6ppm

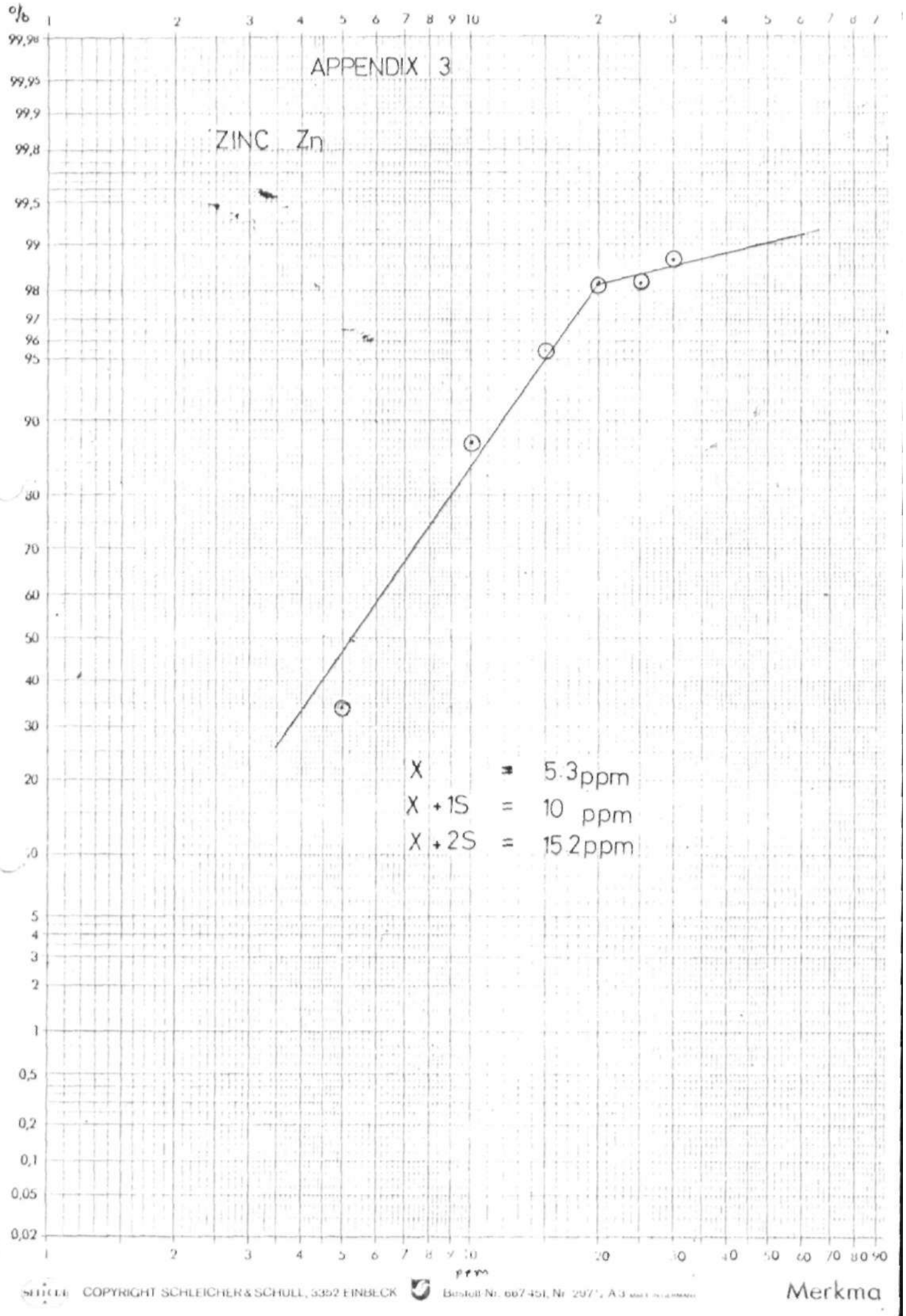
X + 2S = 10.5ppm



COPYRIGHT SCHLEICHER & SCHÜLL, 3352 EINBECK

Merkma

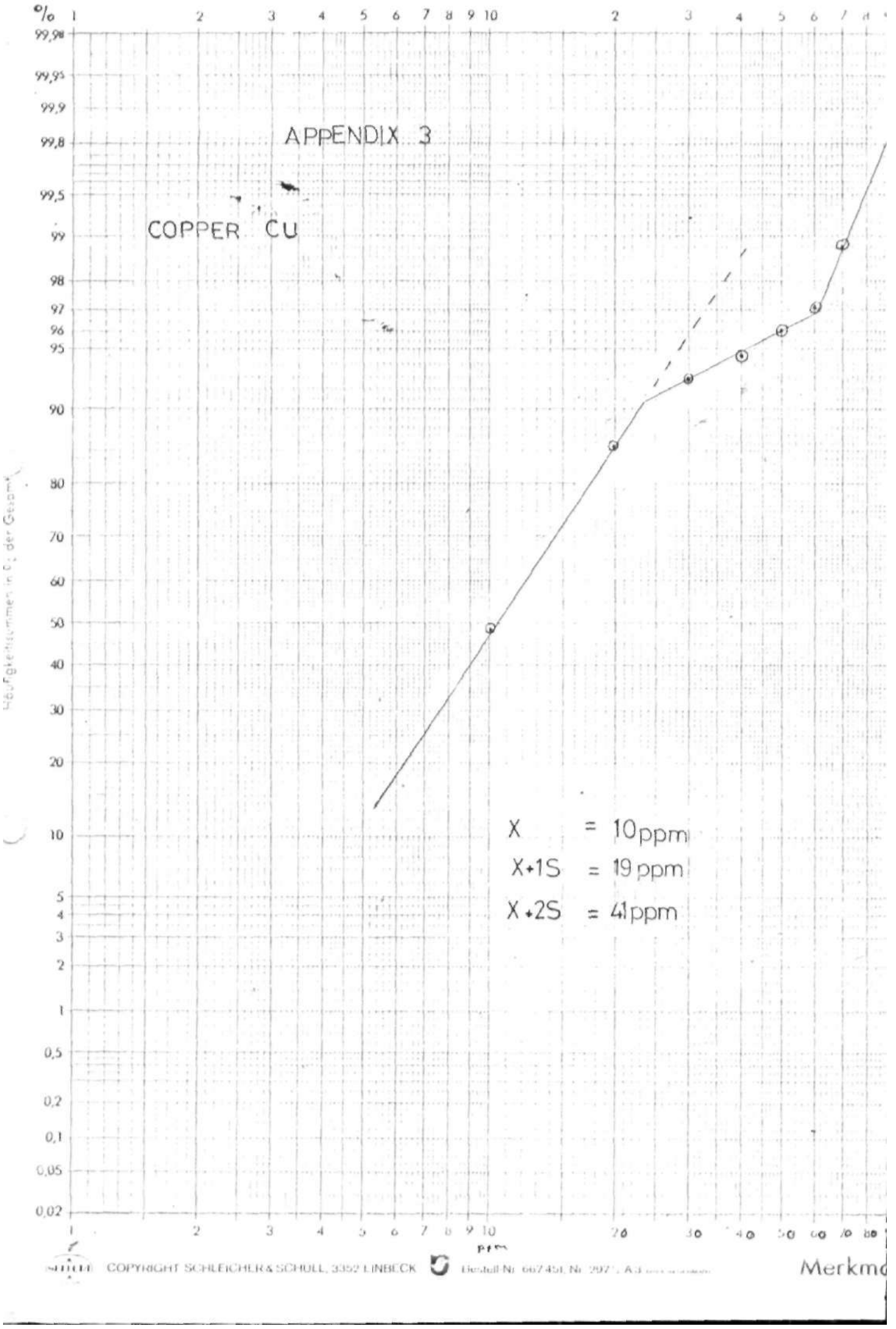
APPENDIX 3



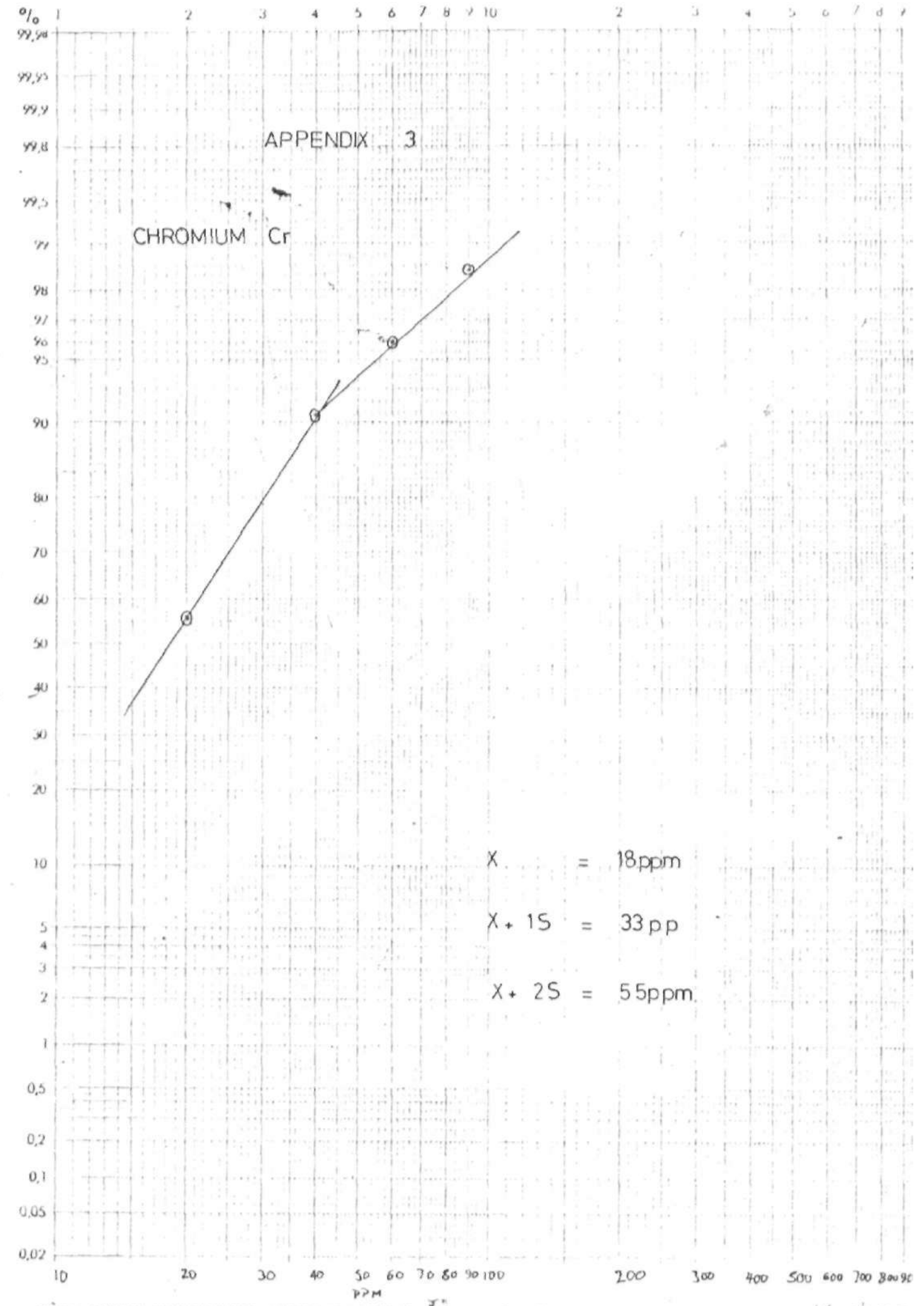
COPYRIGHT SCHLEICHER & SCHUELL, 3352 EINBECK

Merkma

APPENDIX 3


%
99,98
99,95
99,9
99,8
99,5
99
98
97
96
95
90
80
70
60
50
40
30
20
10
5
4
3
2
1
0,5
0,2
0,1
0,05
0,02
1 2 3 4 5 6 7 8 9 10 20 30 40 50 60 70 80
ppm
COPPER Cu
X = 10ppm
X+1S = 19 ppm
X+2S = 41ppm
COPYRIGHT SCHLEICHER & SCHUELL, 3352 EINBECK
Merkm

APPENDIX 3



X = 18ppm

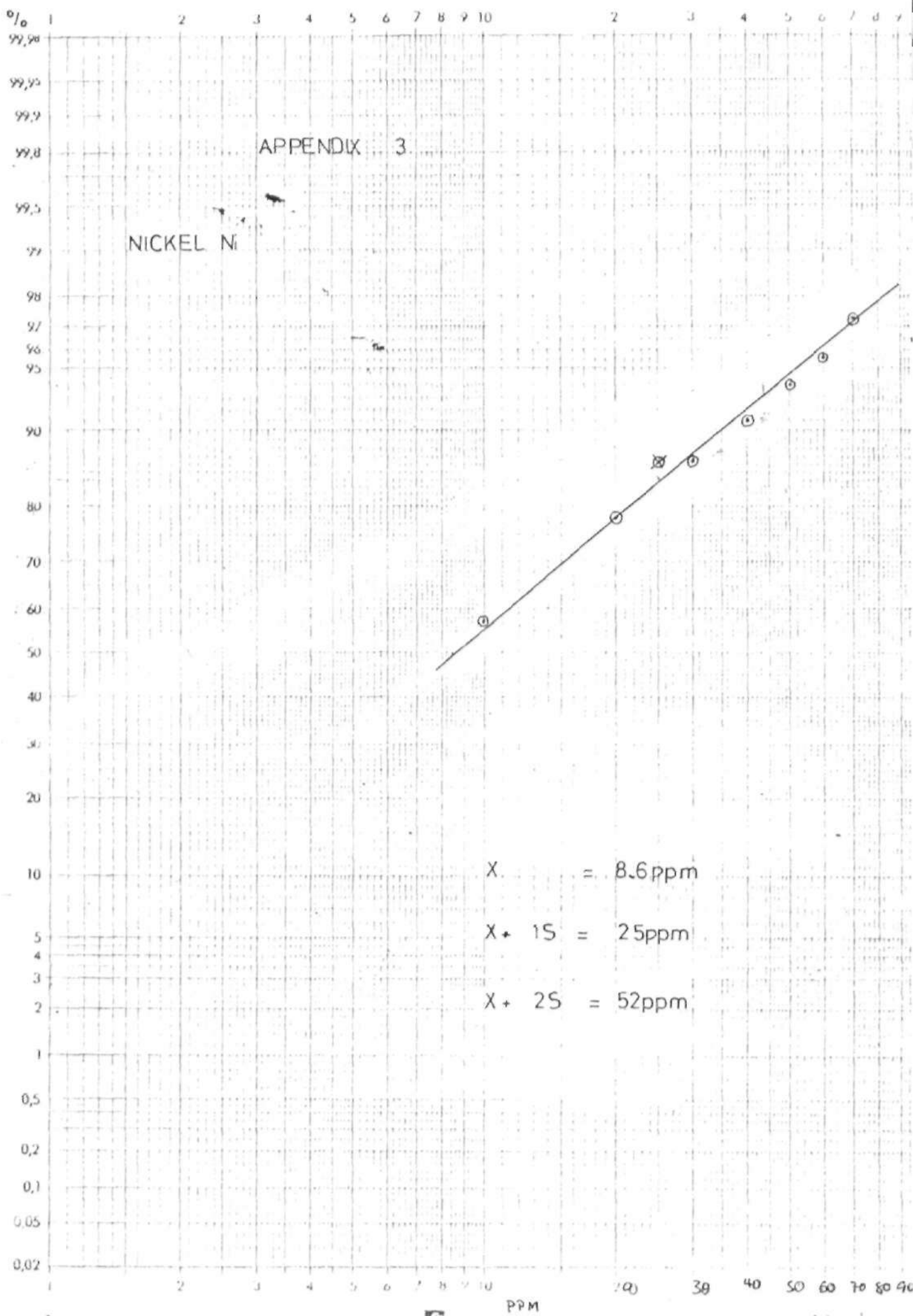
X + 1S = 33pp

X + 2S = 55ppm.

SCHLEICHER & SCHUELL, COPYRIGHT SCHLEICHER & SCHUELL, 3352 EINBECK

APPENDIX 3

NICKEL Ni



X = 8.6ppm

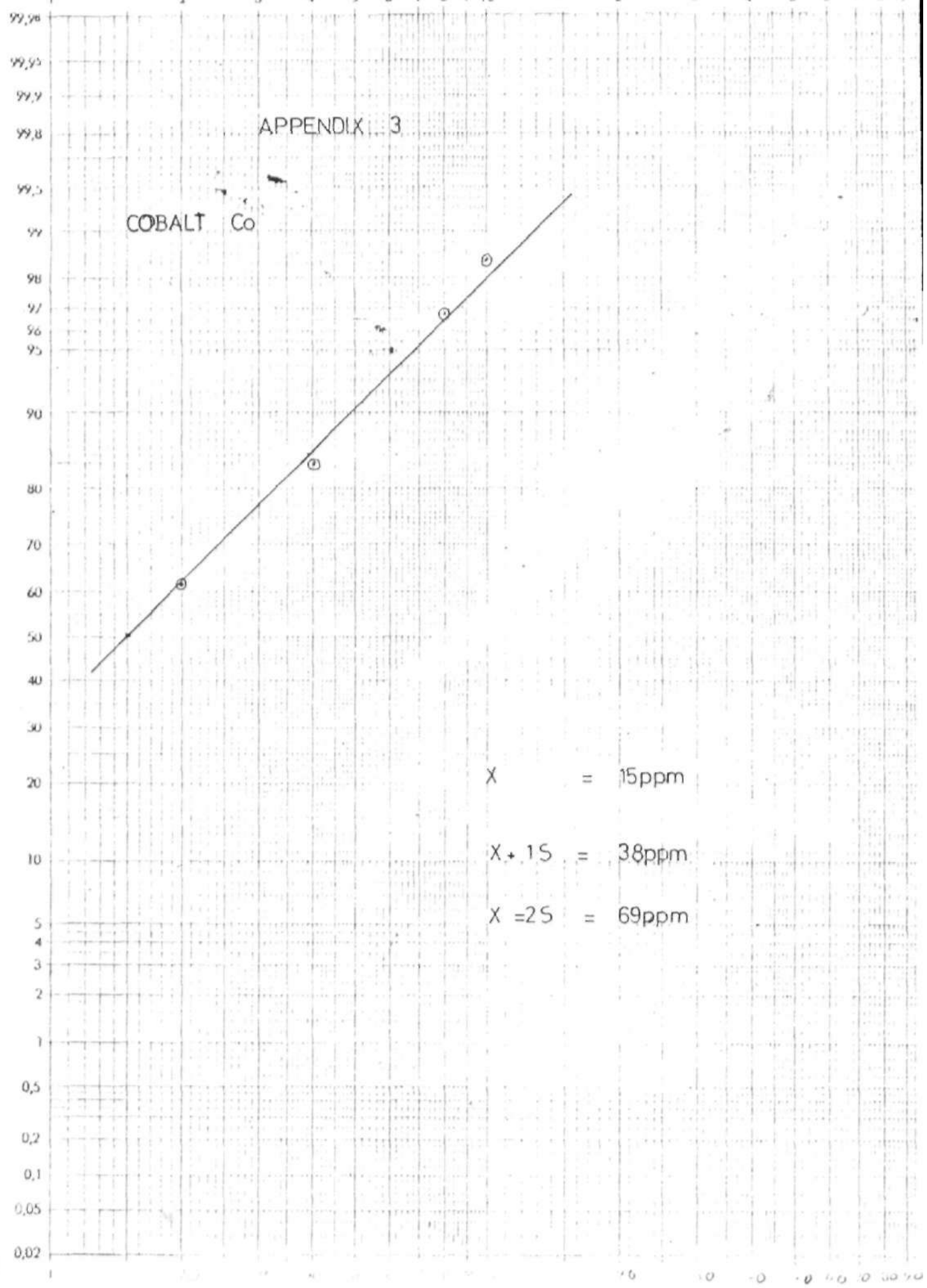
X + 1S = 25ppm

X + 2S = 52ppm

COPYRIGHT SCHLEICHER & SCHUELL, 3352 EINBECK Bestell Nr. 867451, Nr. 297

Merkma

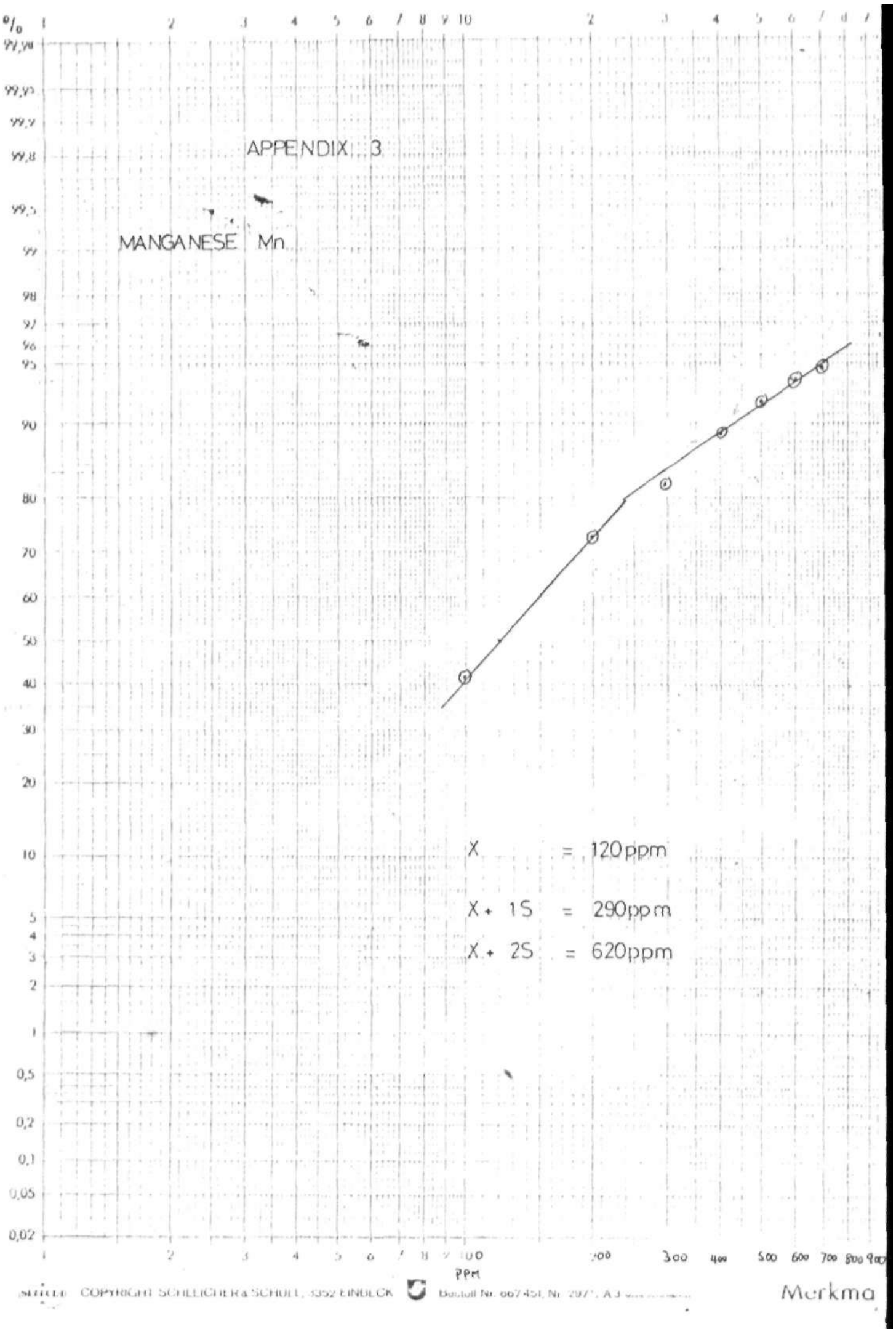
APPENDIX 3



COPYRIGHT SCHLEICHER & SCHUELL, 3352 EINBECK Bo.Stil Nr. 667451, Nr. 297 Merkma

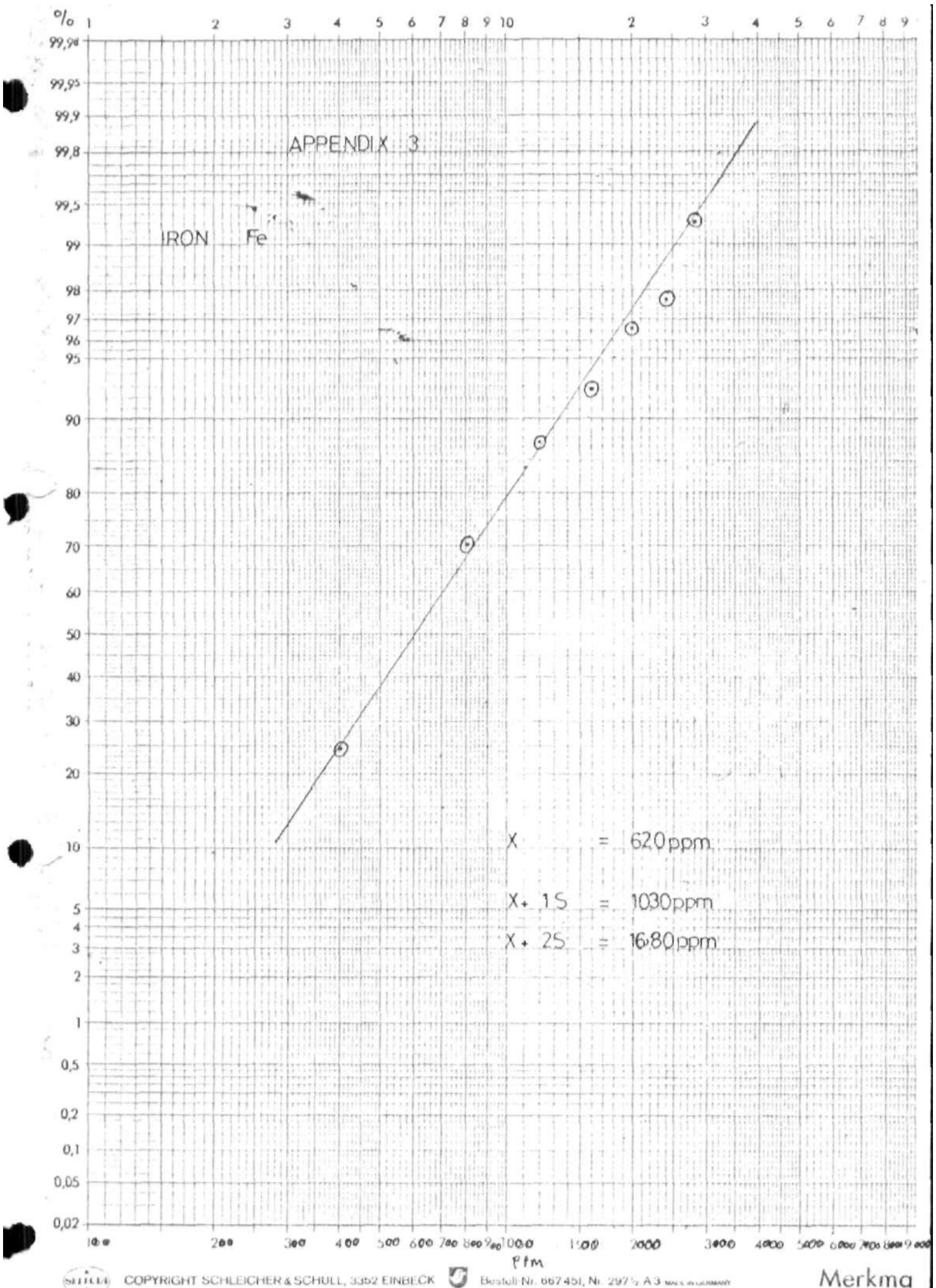
APPENDIX 3

MANGANESE Mn



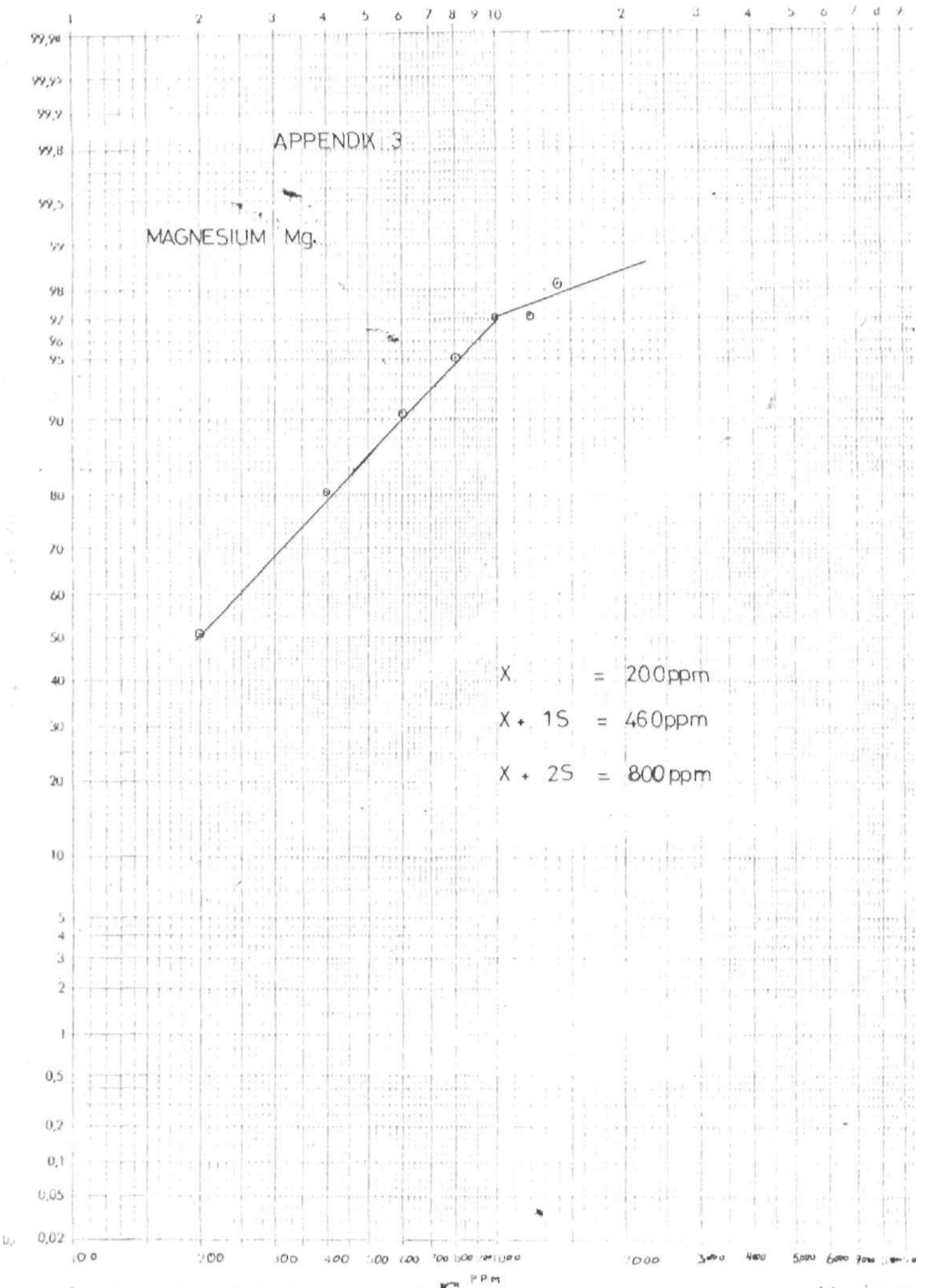
COPYRIGHT SCHLEICHER & SCHUELL, 3352 EINBECK

Merkma


%
99,98
99,95
99,9
99,8
99,5
99
98
97
96
95
90
80
70
60
50
40
30
20
10
5
4
3
2
1
0,5
0,2
0,1
0,05
0,02
APPENDIX 3
IRON Fe
X = 620ppm
X+ 1S = 1030ppm
X+ 2S = 1680ppm
ppm
COPYRIGHT SCHLEICHER & SCHULL, 3352 EINBECK
Merkma

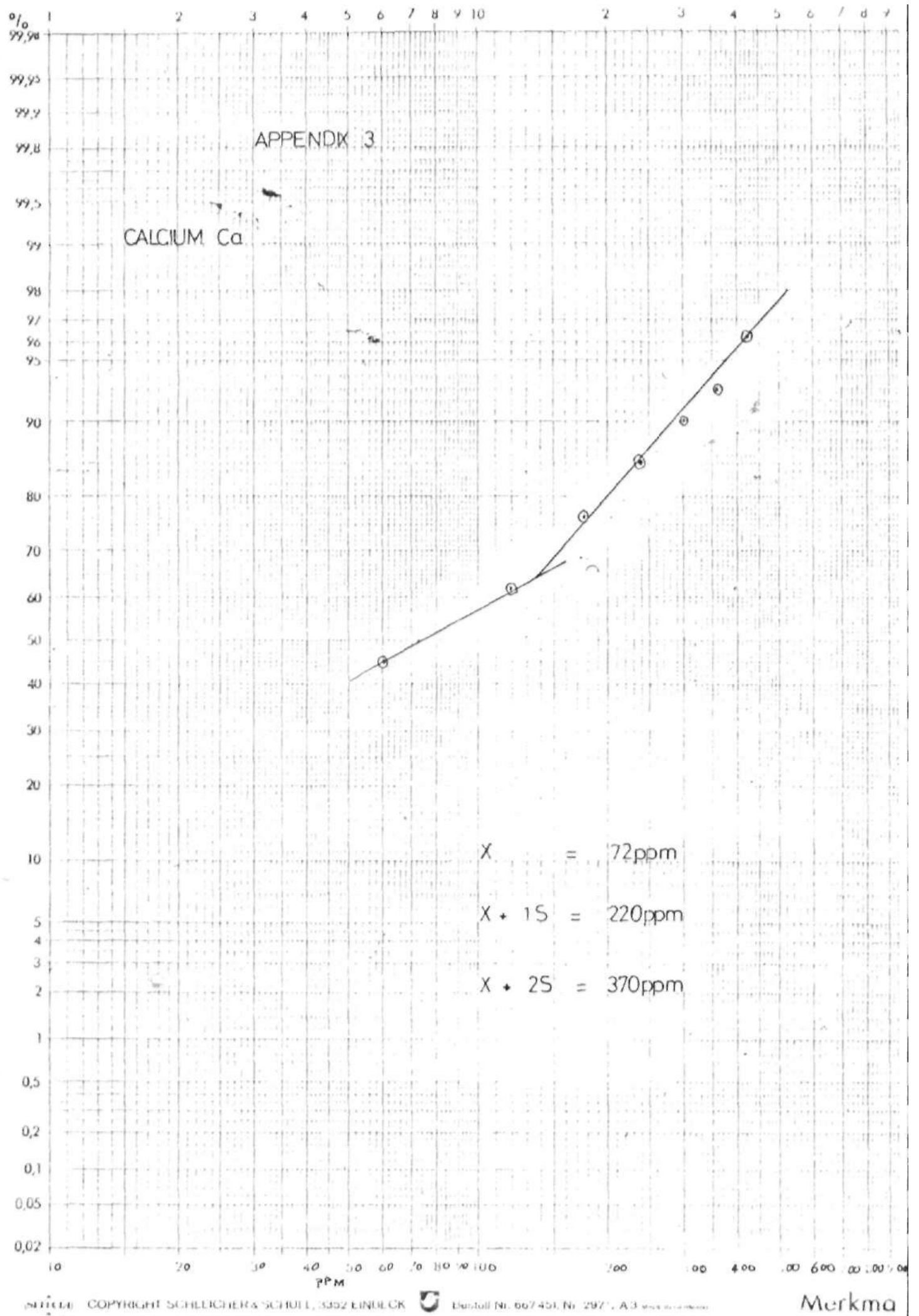
APPENDIX 3

MAGNESIUM Mg.



COPYRIGHT SCHLEICHER & SCHUELL, 3352 EINBECK Datoll Nr. 667451, Nr. 297 Merkma

APPENDIX 3



COPYRIGHT SCHLEICHER & SCHUELL, 3352 EINBECK

Merkma

APPENDIX 4

List of thin-sections

Thin section No	Rock Type	Locality
DB 51	Granite-gneiss	Tsareta ridge.
DB 7	Granite-gneiss/Biotite-granite contact rock	South-eastern end of Tsareta ridge.
DB 49	Biotite-granite	About 500 m north of northern end of Tsareta ridge.
Db 104	Biotite-granite	Biotite-granite outcrops west of Zurzurfa bridge.
DB 95	Phyllite	At a river confluence 2½ km WNW of Tungan-Kudaku village.
DB 122	Phyllite	2 km north-east of the Tsareta/New Project road junction.
DB 24	Metavolcanic rock	About 500 m north of DB 122.
DB 35	Metavolcanic rock	2½ km east of old road/New Project road crossing.
DB 124	Metavolcanic rock	500 m South-west of Tungan Kudaku/New Project road junction.
DB 13	Undeformed Diorite	Outcrops along Tungan Kudaku - New Project road.
DB 96	Trachyandesite	Outcrops along Tungan Kudaku/New Project road.
DB 107	Amphibolite (xenolith)	About 400 m west of Tungan Kudaku/New Project road junction.
DB 119	Amphibolite (xenolith)	In outcrops of serpentinite along New Project road.

Thin section No	Rock Type	Locality
DB 12	Serpentinite	Outcrops along Tungan-Kudaku/New Project road.
DB 12a	Serpentinite	"
DB 19	Epidote-quartz rock	About 6 km south west of Tsareta ridge.
DB 14	Hornblende-Lamprophyre	Within outcrops of serpentinite along New Project road.
DB 92	Quartz-Breccia	About 6 km south-west of Tsareta ridge.
DB 37	Banded-iron formation	About 1½ km north-east of Tungan Kudaku/New Project road junction.
DB 100	Banded-iron formation	About 1km ESE of the Tsareta/New Project road junction.
DB 106	Metaconglomerate	About 2 km east of Tungan Kudaku/New Project road junction.
DB 115	Amphibole rich rock	Within outcrops of serpentinite along the New Project road.